https://theses.gla.ac.uk/

Theses Digitisation:

https://www.gla.ac.uk/myglasgow/research/enlighten/theses/digitisation/

This is a digitised version of the original print thesis.

Copyright and moral rights for this work are retained by the author

A copy can be downloaded for personal non-commercial research or study, without prior permission or charge

This work cannot be reproduced or quoted extensively from without first obtaining permission in writing from the author

The content must not be changed in any way or sold commercially in any format or medium without the formal permission of the author

When referring to this work, full bibliographic details including the author, title, awarding institution and date of the thesis must be given

Enlighten: Theses
https://theses.gla.ac.uk/
research-enlighten@glasgow.ac.uk

AN ISOTOPIC AND MINERALOGICAL INVESTIGATION OF CONCRETE DECAY

A thesis submitted for the degree of
Doctor of Philosophy

by Gordon Macleod B.Sc (Hons)(Strathclyde)
Department of Geology and Applied Geology,
University of Glasgow.

June 1990

ProQuest Number: 11007610

All rights reserved

INFORMATION TO ALL USERS
The quality of this reproduction is dependent upon the quality of the copy submitted.

In the unlikely event that the author did not send a complete manuscript
and there are missing pages, these will be noted. Also, if material had to be removed,
a note will indicate the deletion.

ProQuest 11007610

Published by ProQuest LLC (2018). Copyright of the Dissertation is held by the Author.

All rights reserved.
This work is protected against unauthorized copying under Title 17, United States Code
Microform Edition © ProQuest LLC.

ProQuest LLC.
789 East Eisenhower Parkway
P.O. Box 1346
Ann Arbor, MI 48106 – 1346

ABSTRACT

Concrete is a man made rock composed of aggregate bound rigidly in a paste composed of hydrous cementitious minerals. It is a porous and permeable medium on both the macro and microscopic scales. This study has revealed that the phases present in cement pastes, in particular portlandite, can have random or preferred orientations at the cement paste to aggregate interface. The micro-mineralogy of the cement paste to aggregate bond interface in concretes is texturally complex and concrete mixing techniques can effect the phases present at the interface and the density of the interface. In a core of concrete from a road bridge undergoing active decay, pyrite and pyrrhotine were found to have oxidised by interaction with percolating rainwater. The sulphate released by the oxidised iron sulphides has been taken into solution and eventually precipitated in large spherical cavities in the cement paste, in the form of the mineral ettringite. Water flowing through the structure has possibly been more significant in leaching gypsum from the cement paste and depositing it in the cavities as ettringite. The ettringite has a whisker crystal habit, and has nucleated heterogenetically from solution on the walls of the spherical cavities. The whisker crystal habit is propagated by a screw dislocation in the crystal, the concentration of the elements required for growth being in the solution at low enough concentrations as to limit multi-directional nucleation. The fluid that has percolated through the structure oxidising the iron sulphides has become hyper-alkaline due to the leaching of

portlandite from the cement paste. This fluid has reacted with atmospheric carbon dioxide to produce a calcitic crust on the top of the road bridge and a stalactitic growth on the underside of the road bridge. Similar crusts and stalactites were collected from other concrete structures in the Midland Valley of Scotland, and analysed for $\partial^{13}C$ and $\partial^{18}O$ values. The $\partial^{13}C$ values are in the range of -18.8‰ to -28.9‰ PDB. The $\partial^{18}O$ values are in the range of +8.5‰ to +16.5‰ SMOW. The calcites formed by the interaction of the hyper-alkaline fluids that have percolated through the structures, with atmospheric carbon dioxide ($\partial^{13}C$ = -7‰ PDB, $\partial^{18}O$ = +41‰ SMOW). The stalactites have formed by the production of successive calcite layers, by the diffusion of carbon dioxide into the bulbs of hyper-alkaline solutions as they emerge on the underside of the structure. The computer codes EQ3NR/EQ6 predict that rainwater flowing through a structure will oxidise iron sulphides present in aggregate fragments, and precipitate ettringite. They also predict that the residual fluid that emerges from the structure has a pH in the range 12-13. It is this hyper-alkaline fluid that reacts with atmospheric carbon dioxide to produce the calcitic growths.

ACKNOWLEDGEMENTS

I wish to express my deepest gratitude to Dr. A. J. Hall, who instigated this project and supplied both enthusiasim and constructive guidance throughout its duration. I also wish to thank Allan for his unrelenting efforts to secure funding for the first, and for the final two years of the project. I also wish to thank Dr. A. E. Fallick (SURRC), for offering the services of SURRC and in particular for the provision of isotope analyses. His eagerness to supply analyses and to guide me in the interpretation of isotope data, coupled with stimulating conversations ensured that the isotope data was documented in a tangible form. Professor M. J. Russell with his enthusiasim, and philosophy on science was a source of comfort and inspiration when times were hard. Dr. B. Bell and Dr. G. Bowes are thanked for assisting me in matters geochemical and computational. I would also like to thank the following companies, institutions and individuals for either the provision of samples, information, analyses and site visits. Strathclyde Regional Council Roads Department, Tayside Regional Council Roads Department, Blue Circle plc, Blue Circle Works Dunbar, Blue Circle Works Weardale, Harry Stangers Ltd., and the IT Corporation of the USA in particular M. A. Givens. The Andersonian Bursary Committee of the University of Strathclyde are thanked for providing finance for the first year of the project and the SERC are thanked for funding the final two years of the project. All staff and technicians of the Department are thanked for their assistance and advice over the years and in particular I take this opportunity

to thank Dugie and Murdoch, two technicians who were integral in the completion of this project. Last but not least I thank my parents for their patience and for providing moral and financial assistance over the years, and my fellow postgraduate students who I thank for getting me addicted to rock climbing and with whom I had many constructive and some not so constructive conversations in the pub and curry house. In conclusion, I also wish to acknowledge the friendship of Mr. J. J. Hosick, who tragically died in a car accident in the latter part of 1989. John was my room mate in my undergraduate years, and a close companion from then onwards. I miss him greatly, and doubt if I would have completed this thesis had it not been for his friendship. I would finally, like to take this opportunity to thank Dr. W. J. French for his contributions to this thesis.

CONTENTS page no.

Chapter 1

1. INTRODUCTION

1.1 THESIS STRUCTURE

The format of this thesis consists of an introduction to the project, an outline of the project and an introduction to the basic mineralogy of concrete in Chapter 1. Chapter 1, also has a separate reference list. Chapters 2 to 6 are presented in "paper style" format each with their own introduction. Two of the papers have been accepted for publication, and are set out in the manner stipulated for each particular journal. The other three papers are set out in a standard paper format.

1.2 Outline of research and general objectives

This project is a study of the mineralogical aspects of concrete decay. The mineralogy of concretes themselves and their constituent components is complex. It is hoped that this project has elucidated on the mineralogy of concrete, and the methods with which these phases can be identified and studied. More importantly, I hope that by the combination of mineralogical and modern geochemical techniques I have shed light on the problem of concrete decay. It is hoped that the mechanisms of concrete decay and the symptomatic supergene mineral growth, will be of interest to other mineralogists, and more importantly, enable engineers and others with interests in concrete to understand the decay of this man-made rock. The objective of this project was to produce an interdisciplinary study of concrete decay. In particular the project was to concentrate on the mineralogical aspects of concrete decay, and

to make the results intelligible to all parties interested in concrete decay. The project was originally based on the mineralogy of cement powders, and Blue Circle cement works at Weardale and Dunbar were visited to obtain first hand information. From there I wished to apply mineralogical techniques to concrete, and in particular concrete decay.

1.3 Concrete mineralogy, a basic introductory description

From a mineralogical point of view, concrete may be considered as a man-made rock. Concrete is essentially composed of aggregate fragments bound in a matrix of cement paste, which is composed of a number of separate phases.

The aggregate found within concretes is variable in both its' composition and size. In general aggregate fragments usually have a heterogeneic mineralogy and are usually in the form of rock fragments. Fine-grained sand particles may also be added to the mix. There are numerous standards in both Britain and the USA governing the quality of aggregate used in the production of concrete. However, often in the problematic structures that are undergoing decay the degradation of the aggregate fragments plays a key role in the degradation mechanism. Iron sulphides in the form of pyrrhotine and pyrite may oxidise readily to produce sulphuric acid, clay minerals contained in aggregate fragments may also expand within the concrete environment causing fracturing. Certain varieties of quartz usually in the form of reactive flint, tridymite and chalcedony may interact with the alkalis in the pore waters of

the concrete to produce a gel that may cause fracturing.

It is thus important to note that the mineralogy of aggregate fragments is extremely variable and within this thesis where necessary the mineralogy of the aggregates hosted in the concrete being studied is discussed in more detail.

The mineralogy of cement pastes found in concrete is extremely variable, and depends upon the type of cement powder used in the preparation of the mix and the water to cement ratio of the mix (Lea, 1970). The phases encountered within the cement paste also depend on the age of the paste and whether the concrete has undergone any chemical alteration, either due to external or internal reactions.

To understand the mineralogical aspects of concrete decay it is necessary only to have a knowledge of the more common cement pastes and their bulk mineralogy, and to study in detail the mineralogy of pastes in concretes that have been subjected to decay investigation, as required.

The simplest cement paste to understand is a paste that has been produced from an Ordinary Portland Cement powder (OPC); the mineralogy of a cement paste produced from a High Alumina Cement powder will also be discussed in detail. Most other cement pastes encountered are similar in mineralogy or derivatives of these pastes.

The phase composition of OPC cement pastes has been investigated and debated by many workers. It has been suggested that the average OPC paste has a composition of: 70 %

C-S-H gel, 20% $Ca(OH)_2$, 7% aluminates and sulpho-aluminates and 3% unhydrated material (Diamond, 1976). A different composition of 50% C-S-H gel, 13% $Ca(OH)_2$, 12% aluminium sulphate and 25% pore space has been proposed for an OPC cement paste with a water to cement ratio of 0.5 (Jawed *et al.,* 1983). In general the difference in the C-S-H gel phase chemistry mineralogy and structure is greatest between the two suggestions. Much investigative work (Ramachandran *et al.,* 1981, Jawed *et al.,* 1983, Suzuki *et al.,* 1985), has been carried out on the C-S-H gel phase and this detailed research extends beyond the scope of this project. For this project it is necessary only to understand that the C-S-H gel phase is a poorly crystalline often amorphous material, composed of: Ca, Si, O, OH, and H_2O, the material having a high surface area. Previously the C-S-H gel phase has been likened to the naturally occurring mineral tobermorite ($Ca_5Si_6O_{17}.10.5H_2O$, 14 Å variety).

The description of C-S-H gel as a type of tobermorite (Grutzeck and Roy, 1981), has been succeeded by the characterisation of the C-S-H gel phase by its morphology or the Ca/Si ratio of the gel. When C-S-H gel is observed on a Scanning Electron Microscope it can be characterised by its morphology (Jawed *et al.,* 1983), type I C-S-H is in the form of needles radiating from clinker grains, type II is reticulated, type III has indefinite morphology and type IV is in the form of spherical agglomerates. Lea, 1970 suggested that C-S-H gel

could be simplistically divided into two types; C-S-H (I) and C-S-H (II), C-S-H (I) being poorly crystallised foils or platelets with a tobermorite type structure and a CaO/SiO_2 molar ratio of 0.8 to 1.5, and C-S-H (II) as having a fibrous structure with a molar ratio of 1.5 to 2. Further work (Lachowski *et al.,* 1981), suggests that it is possible to further subdivide and classify the C-S-H gel phase in terms of its Ca/Si ratio. This detailed work I feel is beyond the scope of this thesis. C-S-H gel as found in cement pastes can be said to have formed in the ternary system $CaO\text{-}SiO_2\text{-}H_2O$ (Glasser , 1986)(Fig 1a). The gel coupled with the portlandite ($Ca(OH)_2$), is thought to control the pH behaviour of cement pastes (Glasser and Macphee, 1987).

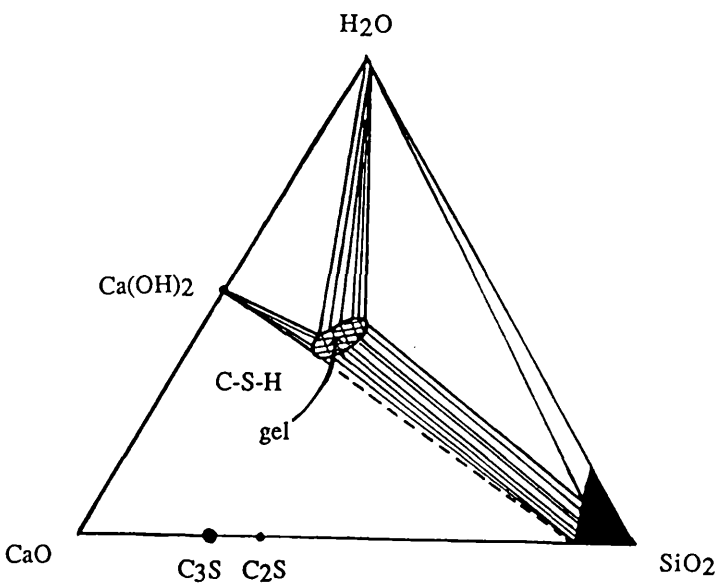

Fig. 1a. A simplified weight %, isothermal section (25°C), through the ternary system $Cao\text{-}SiO_2\text{-}H_2O$. Only condensed phases are shown (After Glasser, 1986).

As the chemistry and mineralogy of the C-S-H gel phase is contested, so to is the structure of C-S-H gel. A general appraisal of the work in this field suggests that the gel is a porous phase that contains micro-pores and connecting tubercles. The amount of porosity and its' exact form are discussed in detail in many texts such as (Neville and Brooks, 1985) and (Ramachandran *et al.,* 1988).

The other common hydrous phases found within a typical OPC paste are portlandite ($Ca(OH)_2$), hydrogarnet ($3CaO.Al_2O_3.6H_2O$) and the sulpho aluminate phases. Portlandite is a product of the hydration of the cement clinker minerals alite ($3CaO.SiO_2$), and belite ($2CaO.SiO_2$) (Neville and Brooks, 1985). Portlandite is usually a ubiquitous phase throughout the cement pastes and is also thought to concentrate in a complex double aureole around aggregate fragments (Hayakawa and Itoh, 1982), and at the surface of the structure. The portlandite is usually in the form of hexagonal crystal platelets the mineral being a member of the trigonal crystal system (Deer *et al.,* 1985).

The hydrogarnet phase is dispersed randomly throughout the cement paste and is often in the form of platelets (Lea, 1970). The sulpho-aluminate phases are thought to exist as three predominant discrete forms, mono-sulpho calcium aluminate, di-sulpho calcium aluminate and ettringite($Ca_6Al_2(SO_4)_3(OH)_{12}.26H_2O$) (Barnes, 1983).

The mineralogy of High Alumina Cement paste is more simple, as most of the phases produced at an early stage in the mix tend

to convert with time to the stable hydrogarnet (Lea, 1970). In fresh HAC cement pastes the mineral phases present include: $CaO.Al_2O_3.10H_2O$, $2CaO.Al_2O_3.8H_2O$, $3CaO.Al_2O_3.6H_2O$, Al_2O_3 hydroxy complexes and some C-S-H gel. The gel phase is produced by the hydration of $2CaO.SiO_2$, a contaminant in the original HAC clinker. A solid solution series exists between $3CaO.Al_2O_3$ and $4CaO.Al_2O_3.Fe_2O_3$ (pleochroite) and it is possible that a hydrogarnet of variable composition may be present.

Numerous admixtures, fibres and other mineralogical and chemical additives may be added to cement pastes. Pulverised fuel ash and industrial slags may also be blended into clinkers to produce various cement pastes with variable properties. To discuss the mineralogy and structure of all cement pastes would be an extremely difficult task; I have merely tried within this chapter to discuss the basic mineralogy of OPC and HAC cement pastes. I have only touched upon the debate on the structure and phase composition of such pastes. I hope that this chapter gives a basic understanding of the bulk mineralogy and chemistry of some of the commoner cement pastes, allowing an understanding of Chapters 2-6. If readers wish to further explore the mineralogy of cement pastes, I refer them to; Neville and Brooks (1987), Ramachandran *et al.,* (1981), Barnes (1983) and Lea (1970).

1.3 References

Barnes, P., Structure and performance of cements, Applied Science Publishers, (1983).

Deer, W. A., Howie, R. A., Zussman, An Introduction to the Rock Forming Minerals, Longman, 528 pp., (1985).

Diamond, S. Cement paste microstructure-an overview at several levels, Proc. Int. Conf. Hydraulic Cement Pastes, Their Structures and Properties, University of Sheffield, 2-30.

Glasser F. P. Chemical and geochemical basis for the immobilization of nuclear waste materials in cements, Fortschr Miner., 64, part 1, 19-35, (1986).

Glasser F. P., Macphee, D. E. and Lachowski, E. E. Solubility modelling of cements: implications for radioactive waste immobilisation, Mat. Res. Soc. Symp. Proc., Vol. 84, Materials Research Society, 331-341, (1987)

Grutzeck, M. W., Roy, D. M. Portland Cement Mineralogy, In The Encyclopedia of Mineralogy, (Frye Ed), Hutchison Ross, 412-417, (1981).

Hayakawa, M. and Itho, Y. Bond in Concrete, Applied Science Publishers, London, 282-288, (1982).

Jawed, I., Skalny J, Young, J. F. Hydration of Portland Cement, In Structure and Performance of Cements, (Barnes Ed.), Applied Science Publishers, 237-318, (1983).

Lachowski, E. E., Mohan, K., Taylor, H. F. W., Lawrence, C. D., Moore, A. E. J. Am. Ceram. Soc., 64, 319 (1981).

Lea, F. M. The Chemistry of Cement and Concrete, Edward Arnold,

London, 727 pp., (1970).

Neville, A. M. and Brooks, J. J. Concrete Technology, Longman Scientific and Technical, UK., 238 pp.,(1987).

Ramachandran, V. S., Feldman, R. F. and Beaudoin, J. J. Concrete Science, Heyden, London, 427 pp., (1981).

Suzuki, K., Nishikawa, T., Ito, S. Cement and Concrete Research, Vol. 15, 213-224, 1985.

Introduction and background

Chapter 2 (paper 1), is a paper concerned with a study of the mineralogy and micro-mineralogy of cement pastes, and in particular the cement paste to aggregate bond interface. The study deals with both conventionally and two-stage mixed concretes. This paper has been submitted for consideration for publication in the American journal, Cement and Concrete Research.

The study of the benefits of two-stage mixing of concrete has been carried out for some years. Dr. P. Ridgway of the Department of Civil Engineering, at Strathclyde University has been supervisor to numerous Ph.D research projects on the topic. Dr. A. Tamimi, carried out an investigation of two-stage mixed concrete for his Ph.D (Tamimi, 1990), supervised by Dr. Ridgway. Dr Tamimi's research included an investigation of the strength of two-stage mixed concretes and conventionally mixed concretes. He compared the compressive strength and paste to aggregate bond density of two-stage and conventionally mixed concretes produced with the same water/cement ratio, at ages from one day to twenty eight days. Two-stage mixed concrete is prepared by mixing all of the cement powder and aggregate with only half the required amount of water, this material is then mixed for 60 seconds and then the other half volume of water is added and the mixing continued. The portlandite would probably be precipitated before the second batch of water was added (French, pers. comm.).

Dr. Tamimi found during his research, that the two-stage mixed concrete, had a higher compressive strength at early ages than that

of the conventionally mixed concrete. The failures within the conventionally mixed concrete, when it was placed under compression appeared to nucleate from the cement paste to aggregate interface. He also found, by the use of Vickers Microhardeness testing, that the cement paste to aggregate interface in the two-stage mixed concrete was more dense than that of the conventionally mixed concrete. Dr. Tamimi used glass marbles as pseudo-aggregate within his prepared concretes, to keep his aggregate surfaces and composition a standard.

Dr. Ridgway and Dr. Tamimi assumed, that the failure at early ages in the conventionally mixed concrete was due to randomly oriented portlandite crystals at the paste to aggregate interface impinging upon one another and the aggregate (Fig. 2a). When the concrete was loaded the crystals fractured and the micro-fractures propagated outwards into larger more visible fractures. The two-stage mixed concrete, had portlandite crystals present with their *c*-axis perpendicular to the other portlandite crystals and the aggregate (Fig. 2b), thus did not fail as easily, giving a greater bond strength. Dr. Tamimi approached me and asked if it would be possible to determine the orientation of the portlandite crystals at the cement paste to aggregate interface and quantify the phases present using Powder X-ray diffraction spectrometry (XRD). A special holder was constructed by the Departmental technicians to hold the concrete specimens in the sample chamber of the XRD. This study was unsuccessful on two counts. The spherical sockets left in the cement paste where the glass marbles

were plucked out of the paste, were not suitable for orientation studies even if a reasonable amount of the scattered X-rays were detected. Secondly, the material bonded to the glass marbles themselves could not be studied as the sphericity of the marble did not allow a reliable study to be made.

A second suite of samples was prepared using glass microscope slides as pseudo-aggregate. The samples were cleaved open at the respective ages and an attempt was made to carry out an XRD study of the surfaces of both the cement paste and the glass slide it had been bonded to. Problems were encountered in retrieving the glass slides from the mix and often they were fractured or damaged as were the cement paste surfaces. Holding the samples in the sample chamber also proved difficult as they were all of irregular sizes.

A third suite of samples were prepared for analysis. These consisted of concrete samples that had small glass plates as pseudo-aggregate. The plates were previously cut to size to fit into a custom built sample holder for the XRD chamber. When the concrete specimens were due for analysis they were cut on a trim-saw allowing the glass plates and corresponding paste surfaces to be cleaved more easily and ensuring that the samples were of similar size and could be held in the custom built sample chamber. This proved successful and a full XRD study of the samples was carried out using computer stored diffractograms and programs for peak identification and quantification.

After the samples had been subjected to the XRD study, the same samples were studied by Dr. Tamimi and Dr. Ridgway on a Scanning

Electron Microscope equipped with an EDAX unit. By combining the SEM study and the XRD study it was possible to relate the strength differences at early ages between the two types of concrete to the micro mineralogy of the cement paste to aggregate interface. The following paper was the culmination of this work and is biased towards the engineering aspects of the two-stage concrete mixing. It does however, contain a lot of mineralogical study of the cement paste to aggregate interface and in particular portlandite orientation studies and phase textural relationships. Dr. Tamimi is the senior author, Dr. Ridgway and Dr. Hall assisted in the interpretation of the data. I was responsible for all mineralogical aspects of the paper including XRD, crystallography and some of the interpretation of the textures of the phases present. This project, occurred at an early stage in my own research and I found that this detailed study of the micro-mineralogy of the cement paste to aggregate interface gave me a good footing to continue my study of the mineralogical aspects of concrete decay.

I would like to acknowledge the work of other researchers who have attempted to study the aggregate to paste interface. These workers have carried out more detailed studies than I have, and have estimated the accuracy of their results. Work has recently been reported on the determination of the effect of silica-fume and other replacement materials on the orientation of the phases present at the interface(Bijen and Larbi, 1990). This study used the method of CH orientation determination developed by Grandet and Ollivier, 1980. Bijen and Larbi also determined the amount of

CH in the bulk cement paste, a calculation I did not attempt to make. Extensive studies of cement paste composition have been made, and the zone at the cement paste to aggregate interface is one of the most studied zones (Barnes, 1983). Following discussions with W. French (London), I would like to acknowledge the fact that we have possibly been erroneous in our study for three reasons. Firstly the use of silicate glass slides as pseudo-aggregate could have meant the interaction of the paste phases with the glass effected the study (Baker, 1972). Secondly we only carried out the study on one suite of samples and thus have no feel for the reproducability of the results. Thirdly, the cleaving of the slides from the paste at later stages could have fractured the paste at some distance from the aggregate. The result of this fracturing along planes of weakness, was that possibly the wrong part of the paste was analysed in the older samples. The beam size of the machine also limits the area of sample being analysed and could also cause erroneous results.

None-the-less, I feel that the work still merits reporting, as long as these problems are made clear.

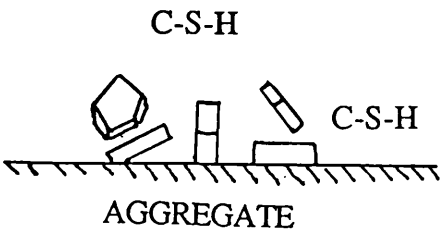

Figure 2a.

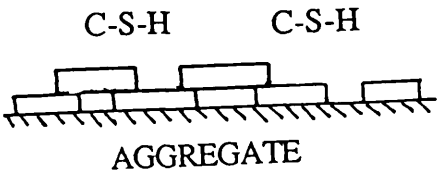

Figure 2b.

References

Baker, A.F., (1979) Petrological and physical aspects of alkali-silica reactivity in concretes, Ph.D thesis, Queen Mary College, Dept. of Geomaterials.

Barnes, P. (ed), (1983) Structure and performance of cements, Applied Science Publishers, London.

Bijen, J. and Larbi, J. (1990) Advanced seminar on alkali aggregate reaction, Queen Mary and Westfield College London, Sept. 1990.

2. MICROSTRUCTURAL INVESTIGATIONS OF THE INTERFACIAL ZONE OF TWO-STAGED MIXED CONCRETE.

(Draft May 1990)

(with minor additions in December 1990)

A. K. AL-Tamimi(1), G. Macleod(2), P. Ridgway(1) and A. J. Hall(2)

(1) Department of Civil Engineering, University of Strathclyde, Glasgow, Scotland, G4 0NG.

(2) Department of Geology and Applied Geology, University of Glasgow, Glasgow, Scotland, G12 8QQ.

2.1 Abstract

Samples of concrete with water/cement ratio of 0.65 have been produced using both a conventional and a two-stage mixing technique. In the two stage mixed samples the second batch of water was added 60 seconds after the first. Compressive strength testing was carried out at time intervals of 1,3,7,14 and 28 days. At ages up to 7 days it was noted that the samples produced by the two stage mixing technique gave compressive strengths that were up to 25% greater than then those of the similarily aged conventional mix blocks. An investigation of the micro-mineralogy of the interfacial zone confirmed a higher concentration of hydrated phases at early stages in the two-stage mix. The investigation showed that the two-stage mix produced a stronger dense bond between the paste and the aggregate, where small portlandite crystals grow with their *c*-axis perpendicular to the

aggregate. C-S-H gel is more abundant at the interfacial zone and voids are considerably less in the two-stage mix than in the conventional mix. Quantitative X-ray diffraction was used to identify and quantify the phases present and also to determine the crystallographic orientation of the portlandite crystals. Scanning electron microscopy (SEM) with Energy Dispersive X-Ray Analysis (EDXA), has been used to confirm the morphology of the phases and to analyse the phases in the interfacial zone.

2.2 Introduction

The merits of two-stage mixing and conventional mixing of concrete have been discussed and investigated by several workers (1,2,3). Much of the previous work has been inconclusive and the work reported here is an attempt to establish the effects of two-stage mixing. Two sets of concrete samples were prepared, one by conventional mixing and the other by two-stage mixing; both mixes were prepared with a water cement ratio of 0.65. Earlier work (4), has shown that the effects of two stage mixing, on both strength and bleeding, were greatest for concrete mixes of water/cement ratios in excess of 0.55 and the figure of 0.65 was chosen to maximise the differences between the two techniques.

2.3 Mineralogical study and sample preparation

In order to allow a detailed mineralogical study of the interface zone between the cement paste and aggregate by X-ray diffraction (XRD) and SEM, different samples were prepared. Glass microscope

slides that had been cut to size to fit in the XRD sample chamber, were added to mixes as pseudo-aggregate. One set of samples was prepared by the conventional mixing technique and the other by the two-stage mixing technique.

The samples were cured for 1, 3, 7, 14 and 28 days. At the respective ages the blocks were cracked open and the glass slides were cleaved from the cement paste. The surface of each glass slide and the corresponding paste contact surface which had been bonded to the glass, were subjected to a XRD study: This method differs from that of Grandet and Ollivier (5), in that glass plates and not polished rock surfaces are used to give a bond surface. For each sample the following procedure was carried out:- a diffractogram was plotted but the diffraction profile was also stored digitally on an ITT microcomputer in order to allow quantitative X-Ray diffraction (QXRD) to be carried out, to estimate the abundance of the phases present. The XRD analyses were undertaken on a Phillips machine using Fe filtered Co K alpha radiation. The machine has a standard fixed specimen and a scanning goniometer arrangement.

The method of preparation and analysis of the concrete specimens also differs from that of Detwiler et al. (6), in that the glass plates used were incorporated into the concrete mix as pseudo-aggregate. The orientation of the portlandite crystals in the interface zone was determined by the method used by Grandet and Ollivier (5). For portlandite crystals in a random arrangement (JCPDS 4-733), the XRD peak intensity ratio:-

$$R = I(001)/I(101) = Int(4.90\ \mathring{A})/Int(2.62\mathring{A})$$
$$= 74/100 = 0.74$$

Higher values than 0.74 were taken as indicating that the portlandite crystals were in a preferred orientation, having their *c*-axis perpendicular to the aggregate. This calculation was applied to the one day and twenty eight day old specimens only (Table. 1). This was done to give an estimate of the trend of orientation of portlandite crystals in the two different mixes, more detailed work was carried out to determine the amount of the phases present at the interface.

QXRD was carried out on the specimens to give the abundance of the phases:- portlandite (P), C-S-H gel (C), and alite and belite (A). The peaks selected for area measurement are listed in Table 2, and were selected on the basis that each peak was not overlapped or contributed to by another phase. The area under the specific peaks for each phase (Table 2), was calculated for the diffractograms of both the block and the glass slide for all the specimens. The area under the specific peaks was used as an estimated measure of the abundance of the phase, this did not take into account absorption factors of the phases and preferred orientation problems,but none-the less was felt to give a reasonable estimate of abundance. The broad background pattern in the diffraction traces, due to the effect of the glass slide, was taken into account by the computer program used to determine the peak intensities and areas.

Following the XRD studies the, the surfaces of the glass slides and blocks were studied using the SEM, to observe the morphology

of the phases present at the interface and to study the micro-structure of the cement paste in the interfacial zone. An energy dispersive X-ray analysis unit (EDXA), attached to the SEM was used to make elemental analyses of the phases present, and in particular for the determination of Ca/Si ratios.

2.4 Results

Diffractograms of the glass slides and blocks for the samples at one day (Figs. 1 and 2), are displayed for comparison. The contrast between the diffractogram of the glass slides from the conventional and two-stage mixes is clear. The diffractogram of the glass slide from the conventional mix (Fig. 1a), has a large broad spurious background that is similar to that of a diffractogram of amorphous silica as found in a clean glass slide with no material covering it. Thus it is reasonable to say that the slide does not have a considerable amount of hydration product bonded to it. The diffractogram from the two-stage mix concrete (Fig. 1b), has a considerably smaller effect from the glass, due to the fact that it has more hydration product bonded to it. The phases present in the thin film that is partially covering the glass slide from the conventional mix are portlandite (P), and some non-hydrated clinker particles of alite and belite (A). The only phase present in the film covering the glass slide from the two-stage mix is portlandite. The diffractogram of the block surface that had been bonded to the glass plate in the conventional mix (Fig. 2a), displays the presence of quartz (Q) (sand aggregate), portlandite (P), C-S-H gel (C), ettringite (E) and the calcium silicates; alite

and belite (A). Comparison of this diffractogram with that of the two stage mix block (Fig. 2b), indicates that the same phases are present. By comparing peak intensities it is clear that the two-stage block has less quartz and more portlandite then the conventionally mixed block.

At the stated ages, a similar study of each glass slide and block was carried out and mineralogical variations in the specimens noted; the film of hydration products on all the glass slides increased with age and as a result the effect of the glass on the diffractogram was reduced. This is effectively due to increase in the distance of the cleavage surface from the glass. The areas under the chosen peaks were measured for each diffractogram on the computer system and the quantity (as relative intensity), of each mineral present was plotted graphically against time (Figs. 3-8).

The graphs of portlandite abundance against time for the glass slides (Fig. 3), show that at early ages the amount of portlandite left on the glass slide from the conventional mix compared to the two stage mix was similar. However, at later stages the difference becomes considerable. When the graphs of the amount of portlandite left on the blocks are plotted (Fig. 4), it is clear that more portlandite is left on the conventional mix sample than on the two-stage mix sample. We suggest that the differences between the two types of mixes and the amounts of CH left on the slides and the block at later stages may be due to the fracturing of the conventionally mixed concrete from the slides at a greater distance from the aggregate, at the second zone of portlandite.

Thus there is an enrichment in portlandite in the block for the conventional mix. The two stage mix is cleaving from the glass behind the first zone of portlandite, and thus the block surface and the glass are apparently enriched with C-S-H. Thus the CH and C-S-H abundance in the older samples probably varies as a function of the position of cleavage between the glass and paste.

When the abundance of the C-S-H gel left on the glass is plotted against time, it can be seen that from three days onwards a greater amount of C-S-H gel has been left on the glass slide from the two-stage mix than the corresponding slide from the conventional mix as it appears in Fig. 5. The plot of C-S-H gel abundance on the block surfaces (Fig. 6), also indicates a greater amount of gel present in the two-stage mix. When the alite and belite abundances are plotted (Figs. 7 and 8), it is apparent that their presence on the slide and block is greater in the conventional mix than in the two-stage mix at early stages, but, at 28 days they are similar. The QXRD determination for ettringite abundance was considered to be unreliable for graphical interpretation as the relative abundance of ettringite compared to the other hydration products is small. However, the ettringite presence was verified by SEM. The different distance of fracturing through the paste from the slides on cleavage may influence the QXRD results and we acknowledge that plotting this against time data is tentative. We do however suggest that the graphical plots display an unusual difference in quantities with age and thus highlight the problem of obtaining identical surfaces to study.

SEM was applied to the samples to identify the phases present in the interface zone and to observe the morphology and micro-structure if the paste. Observation of a glass slide from the two-stage mix (Fig. 9), revealed the glass slide to be covered in a film of of small portlandite crystals with their *c*-axis perpendicular to the glass. Patches of C-S-H gel can also be found directly behind the portlandite crystals. The portlandite crystals are also overlying and overlapping one another. This visual evidence confirms the XRD results from the two-stage mix, in that portlandite crystals are abundant and have taken up a preferred orientation. The slide from the three day conventional mix has a poor covering of hydration products (Fig. 10). EDXA analysis of point (A), gave a Ca/Si ratio of 2.3 suggestive of the gel, and unhydrated clinker grains. Figure 11, is a photomicrograph of the block surface from the 28 day conventionally mixed specimen. A film of portlandite (B), can be seen and some acicular gel is present with a Ca/Si ratio of 3.16 suggesting type I (the Ca/Si ratios were estimated from EDXA analysis and cannot be taken as accurate as electron microprobe data.). Hadley shells (C), are prominent and in the same specimen the presence of large euhedral crystals of portlandite (Fig. 12), suggests that they had space to nucleate and grow and, more importantly, the presence of abundant voids in the interfacial zone, within the conventionally mixed concrete. The voids are produced by the excessively high water to cement ratio saturating the gel phase, and the remaining water is then gradually removed during curing leaving the voids. The voids allow large portlandite crystals to nucleate and grow with a

random orientation. The surface of the two-stage mix block (Fig. 13), has a mixed structure of C-S-H gel (type III), with a Ca/Si ratio of 2.16, intergrown with portlandite crystals. The portlandite crystals are growing with their c-axis perpendicular to the glass.

2.5 Conclusions

Several micro-structural changes were detected by XRD, QXRD, SEM and EDXA, and attempts were made to relate the observed micro-structural features and their subsequent effects on the strength behaviour of two-stage mixed concrete. The predominant feature in the interfacial film of the two-stage mix concrete was, a film of portlandite crystals on the surface of the aggregate. The portlandite in this film was almost perfectly oriented, with the crystal *c*-axis normal to the aggregate surface. A layer of C-S-H gel was subsequently deposited on the surface of the portlandite giving rise to a compound interfacial film. Needles of ettringite were developed and bridged the spaces between the hydrating grain particles. As a result, a dense, homogeneous microstructure was produced containing limited voids, thus enhancing the contact zone and increasing the bond strength. As evidence, larger quantities of the hydration products were observed firmly attached to the aggregate surface, and remained with it upon cleavage as seen in Fig. 11. In the conventional mixed concrete, the portlandite crystals are randomly oriented at the interface, and the crystals are large and well developed in the porous zone (Fig. 12). It engulfed some hydrating grains, reducing its potential for complete

hydration, thus producing a weak zone. SEM observations and QXRD analysis also showed that the two-stage mixed method has reduced dramatically the number of Hadley shells, alite and belite (unhydrated silicates), and hence increasing the gel/space ratio. The effects of these improvements would act to arrest the propagation of cracks from the contact zone to the mortar matrix, thus raising the stress level at failure. The experimental techniques used may possibly have produced some experimental error; in particular when the QXRD work is considered it should be noted that the cleaving of the glass slide from the specimens at variable distances from the sample may have produced some variation in the results.

2.6 Acknowledgements

Thanks are given to all fellow staff who contibuted assistance and ideas to this paper. Special thanks are due to the technicians in the X-ray diffraction laboratory, of the Dept of Geology and Applied Geology at the University of Glasgow, for their patience and innovative creativity.

2.7 References cited

1. M. Hayakawa and Y. Itoh. Bond in Concrete., p 282-288, Applied Science Publishers, London, 1982.

2. M. Ahmed. Effect of a Two-Stage Mixing Method on the properties of fresh and hardened concretes., M.Sc Thesis, Department of Civil Engineering, University of Strathclyde, 1983.

3. R. S. Gahir. Effects of a Two-Stage Mixing Method on the cement paste-aggregate bond., M.Sc Thesis, Department of Civil Engineering, University of Strathclyde, 1984.

4. A. K. Tamimi and P. Ridgway in preparation.

5. J. Grandet and J. P. Ollivier., 7th Congres International de la Chimie des Ciments, Paris, 1980, Vol. III, pp. VII-85-89.

6. R. J. Detwiler and J. Monteiro. Texture of Calcium Hydroxide near the Cement Paste-Aggregate Interface. Cement and Concrete Research, Vol. 18, pp. 823-829, 1988.

Reference in Introduction

Tamimi, A, The bond in two-stage mixed concrete, Ph.D thesis, Dept. of Civil Engineering, University of Strathclyde, 1990.

2.8 Figure captions

Fig. 1. X-ray diffractograms for the material remaining on the glass slide at one day, for conventional mix (a) and two-stage mix (b). Portlandite (P), quartz (Q) and ettringite (E).

Fig. 2. X-ray diffractograms for the cleaved block surfaces at one day, Conventional (a) and two-stage (b). Portlandite (P), quartz (Q), ettringite (E), C-S-H gel (C) and alite/belite (A).

Fig. 3. Amount of portlandite left on the glass slide.

Fig. 4. Amount of portlandite remaining on the block.

Fig. 5. Amount of C-S-H gel remaining on the glass slide.

Fig. 6. Amount of C-S-H gel remaining on the block.

Fig. 7. Amount of alite and belite remaining on the glass.

Fig. 8. Amount of alite and belite remaining on the block.

Fig. 9. SEM photomicrograph of cleaved glass plate surface from two-stage mixed concrete, three days old, scale markers = 100μm.

Fig. 10. SEM photomicrograph of cleaved glass plate surface from a conventional mix concrete, three days old, scale markers = 10μm.

Fig. 11. SEM photomicrograph of a cleaved block surface of a twenty-eight day old conventionally mixed concrete, scale markers = 100μm.

Fig. 12. SEM photomicrograph of cleaved block surface of a twenty-eight day old conventionally mixed concrete, scale markers = 100μm.

Fig. 13. SEM photomicrograph of cleaved block surface of a twenty-eight day old two stage mixed concrete block surface, scale markers = 10μm.

Table. 1. Orientation of portlandite crystals on the block and glass slide surfaces, of the one and twenty-eight day old samples.

Table. 2. Peaks used for QXRD analysis of the paste to aggregate interface.

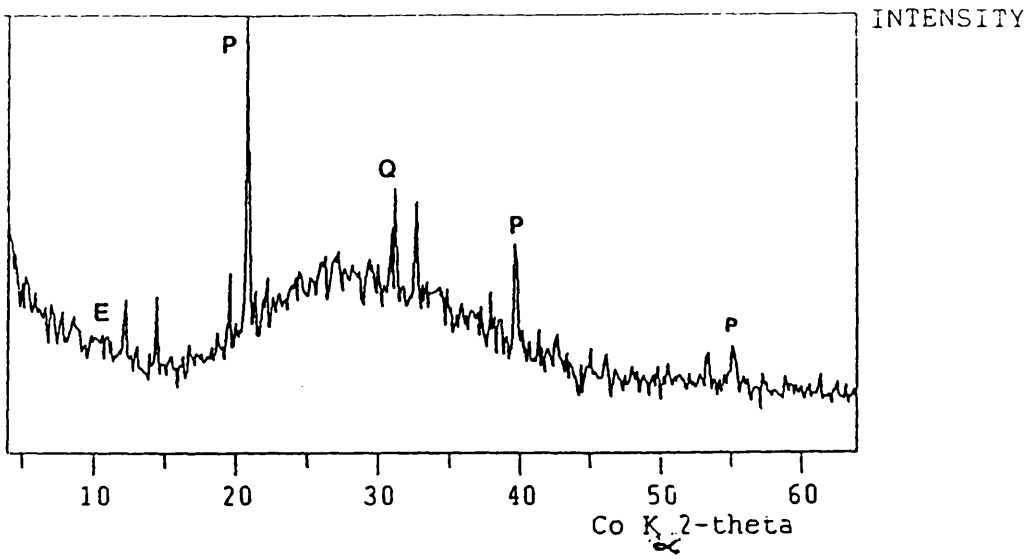

(a) Conventional Concrete at the Glass Slide (1-day)

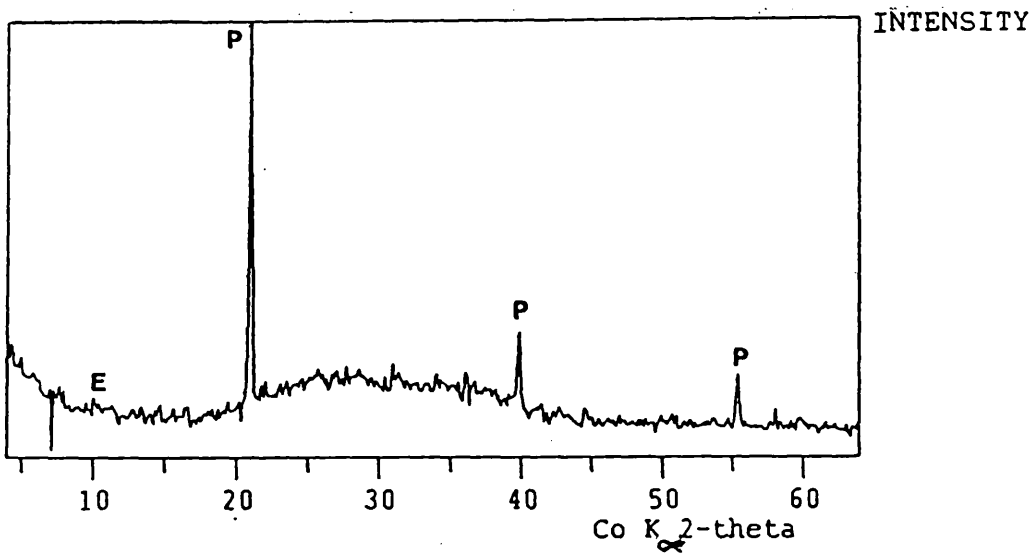

(b) Two-Stage Concrete at the Glass Slide (1-day)

Figure. 1.

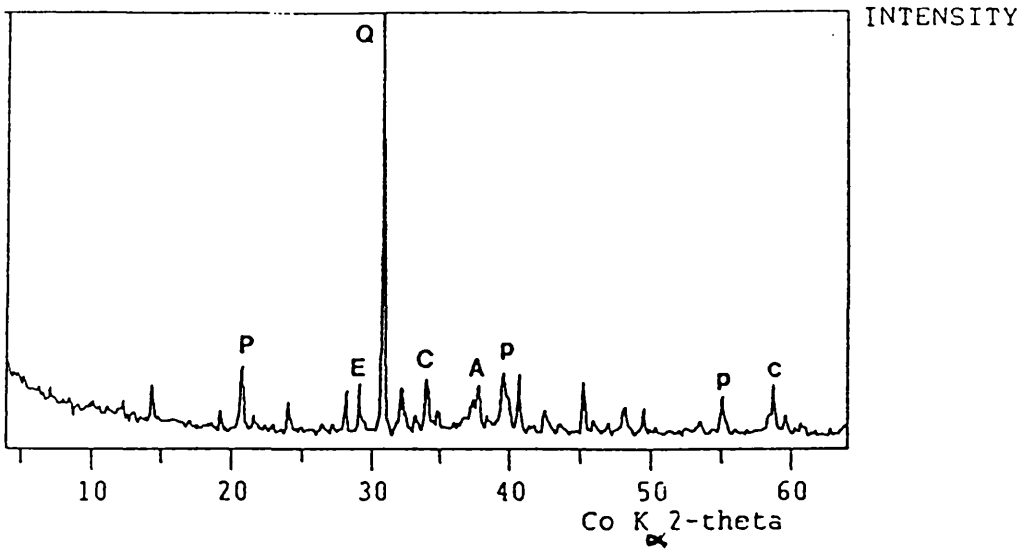

(a) Conventional Concrete at the Block Side (1-day)

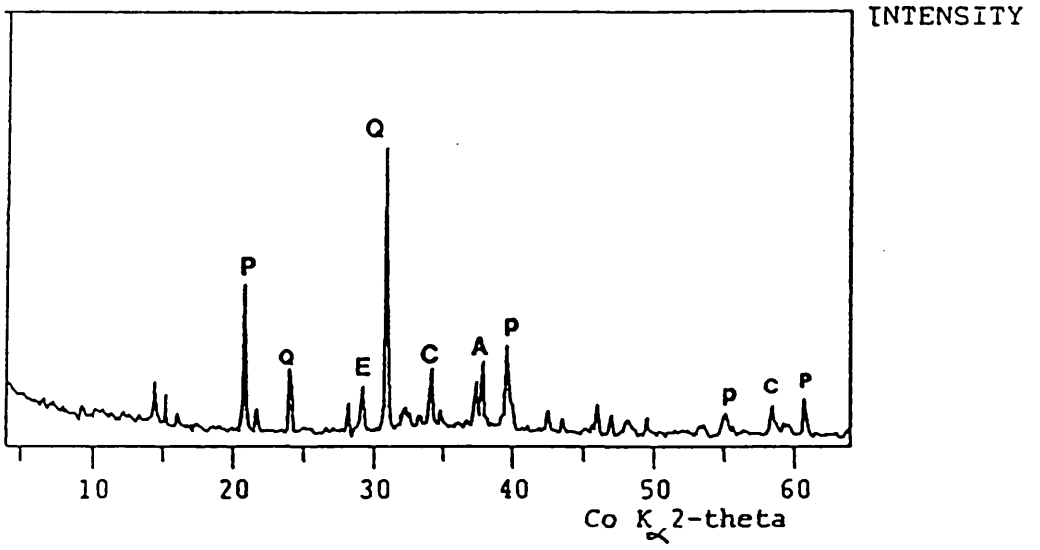

(b) Two-Stage Concrete at the Block Side (1-day)

Figure. 2.

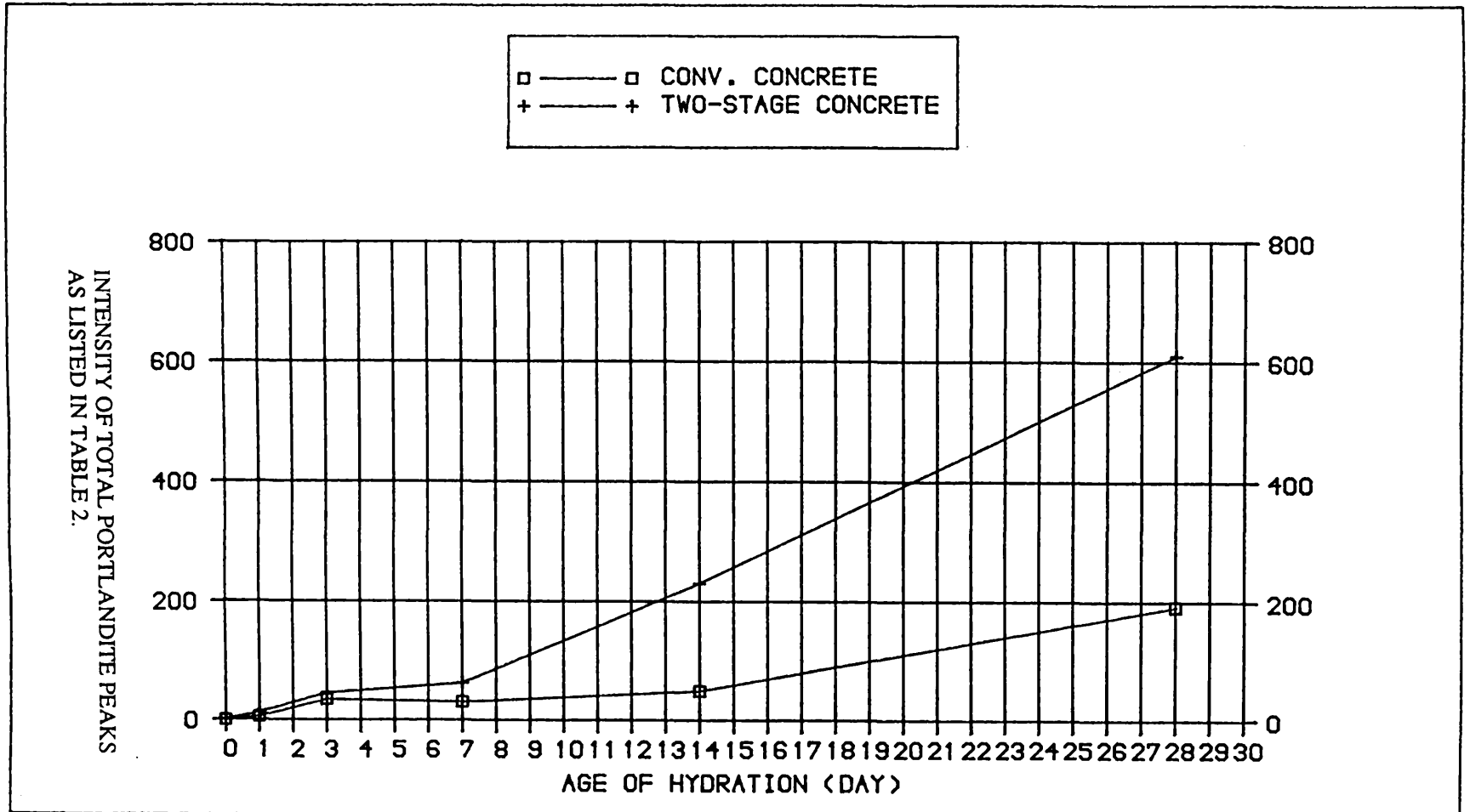

FIG 3 PORTLANDITE PRODUCTS COMPARISON ON THE GLASS SLIDE FOR BOTH MIXING TECHNIQUES

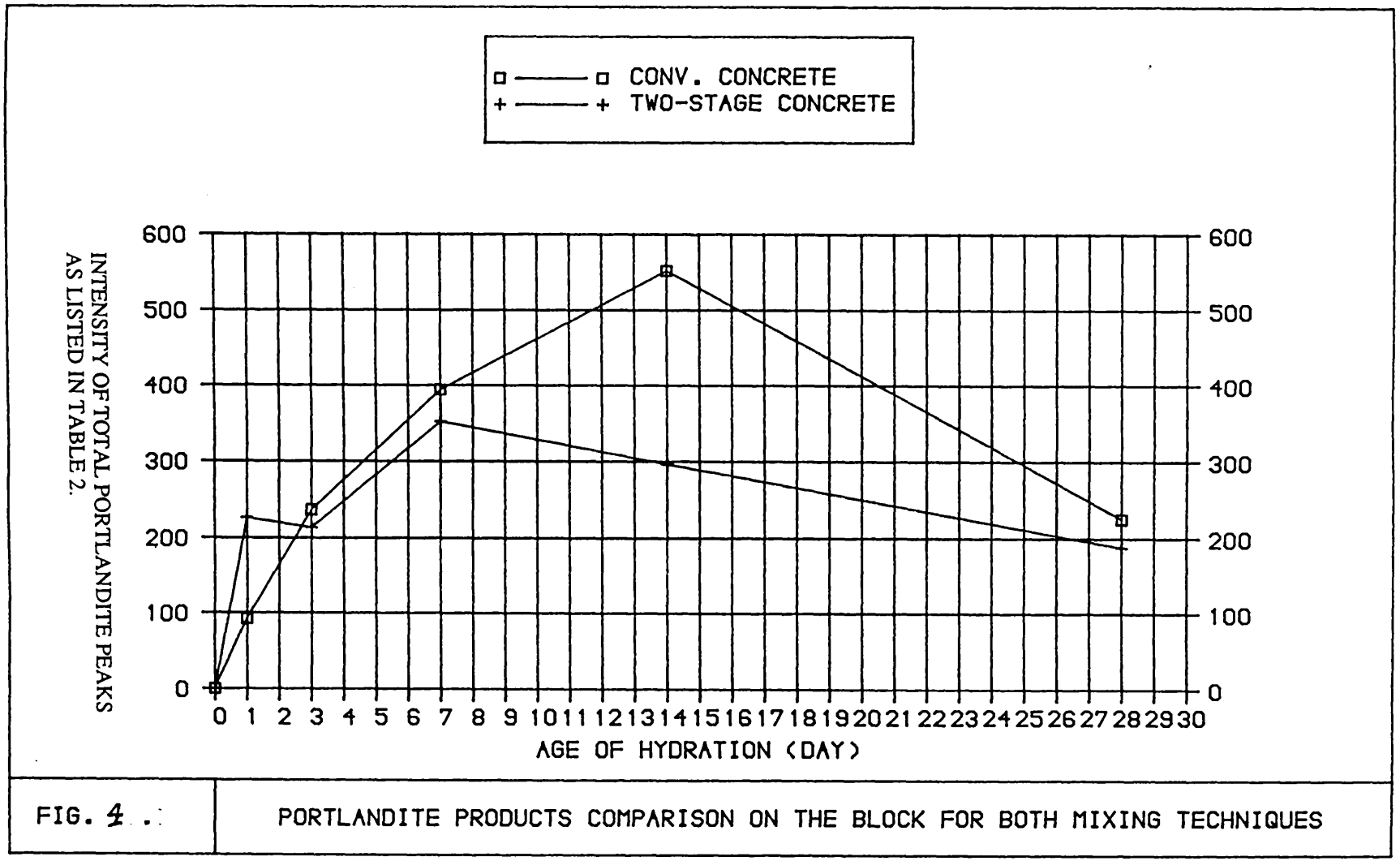

FIG. 4 . : PORTLANDITE PRODUCTS COMPARISON ON THE BLOCK FOR BOTH MIXING TECHNIQUES

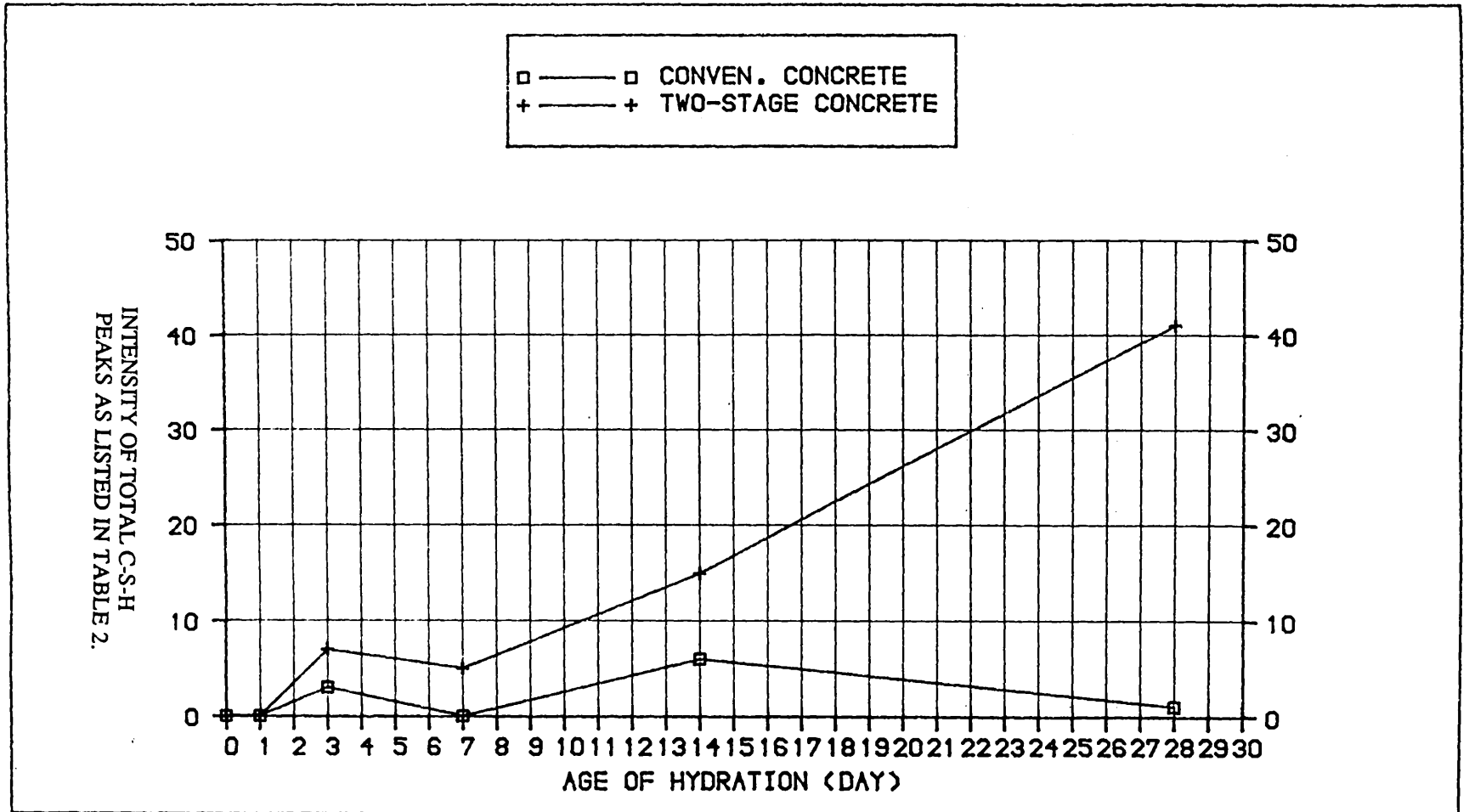

FIG. 5... CSH GEL PRODUCTS COMPARISON ON THE GLASS SLIDE FOR BOTH MIXING TECHNIQUES

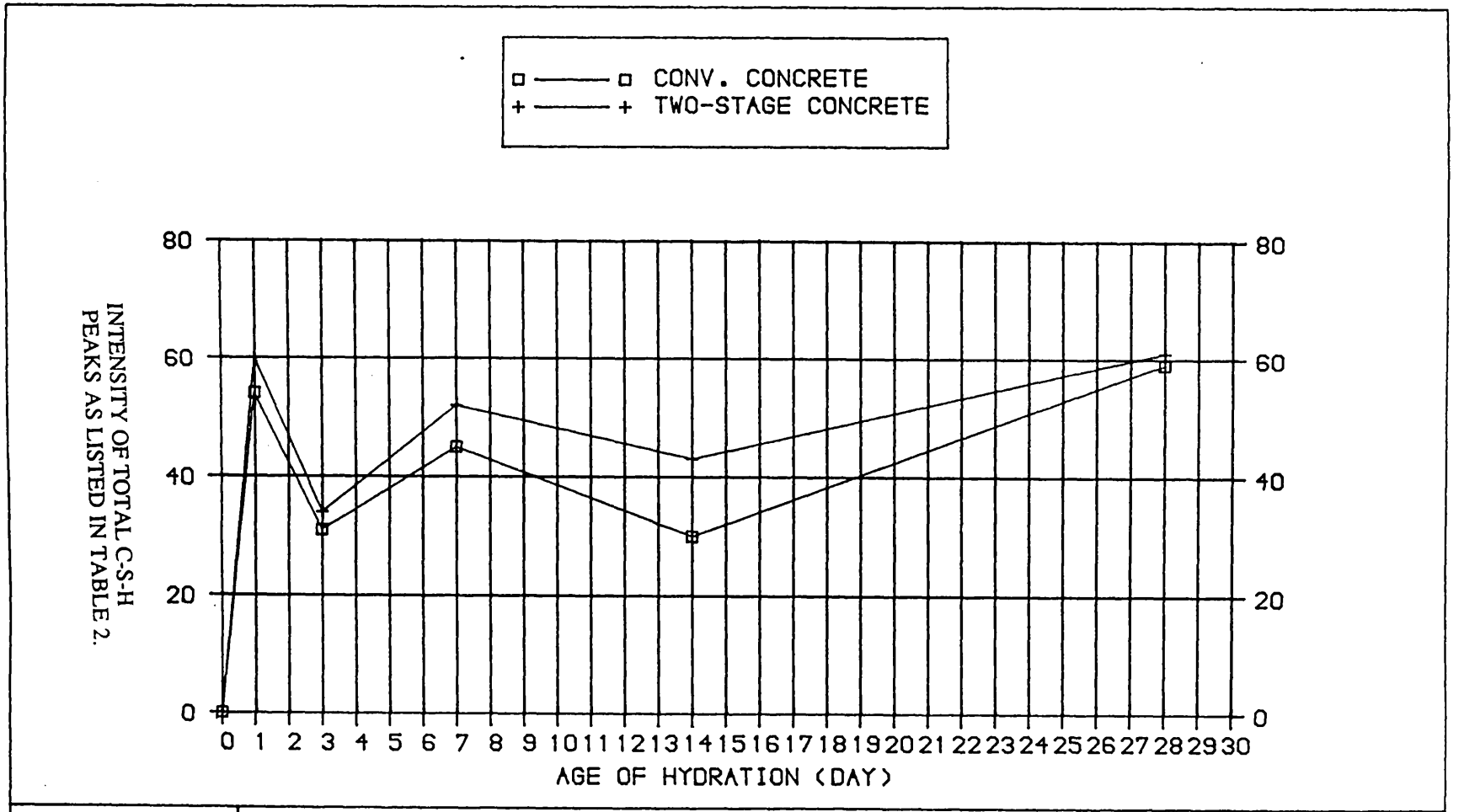

FIG. 6. CSH GEL PRODUCTS COMPARISON ON THE BLOCK FOR BOTH MIXING TECHNIQUES

02 USER: CHAR38 PLOTFILE: PLOTLIB ENTRY NO. 61410 QUEUED ON 21/12/89 AT 12:44 PLOTTED ON 22/12/89 AT 09:33

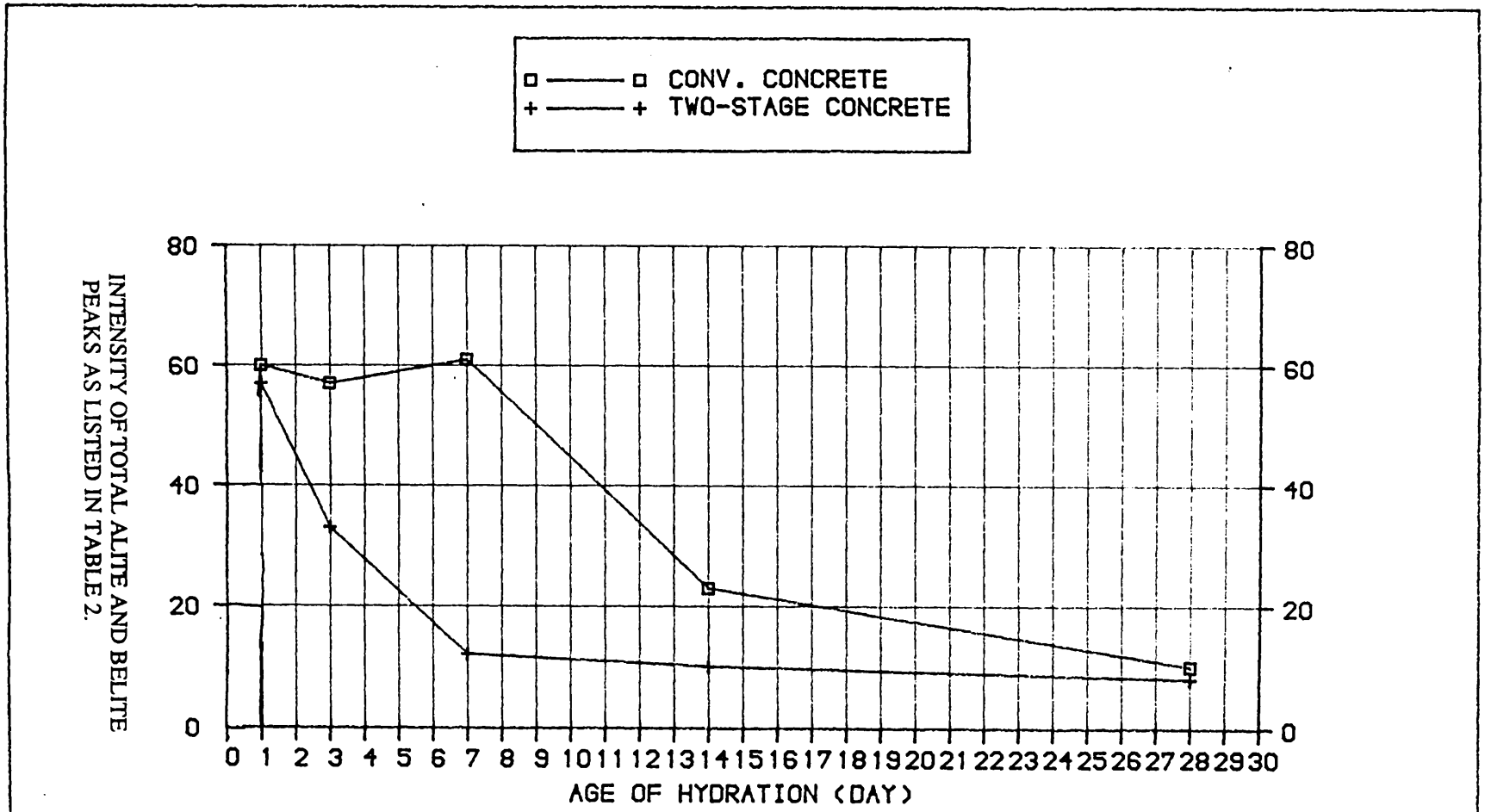

FIG. 7. ALITE AND BELITE PRODUCTS COMPARISON ON THE BLOCK FOR BOTH MIXING TECHNIQUES

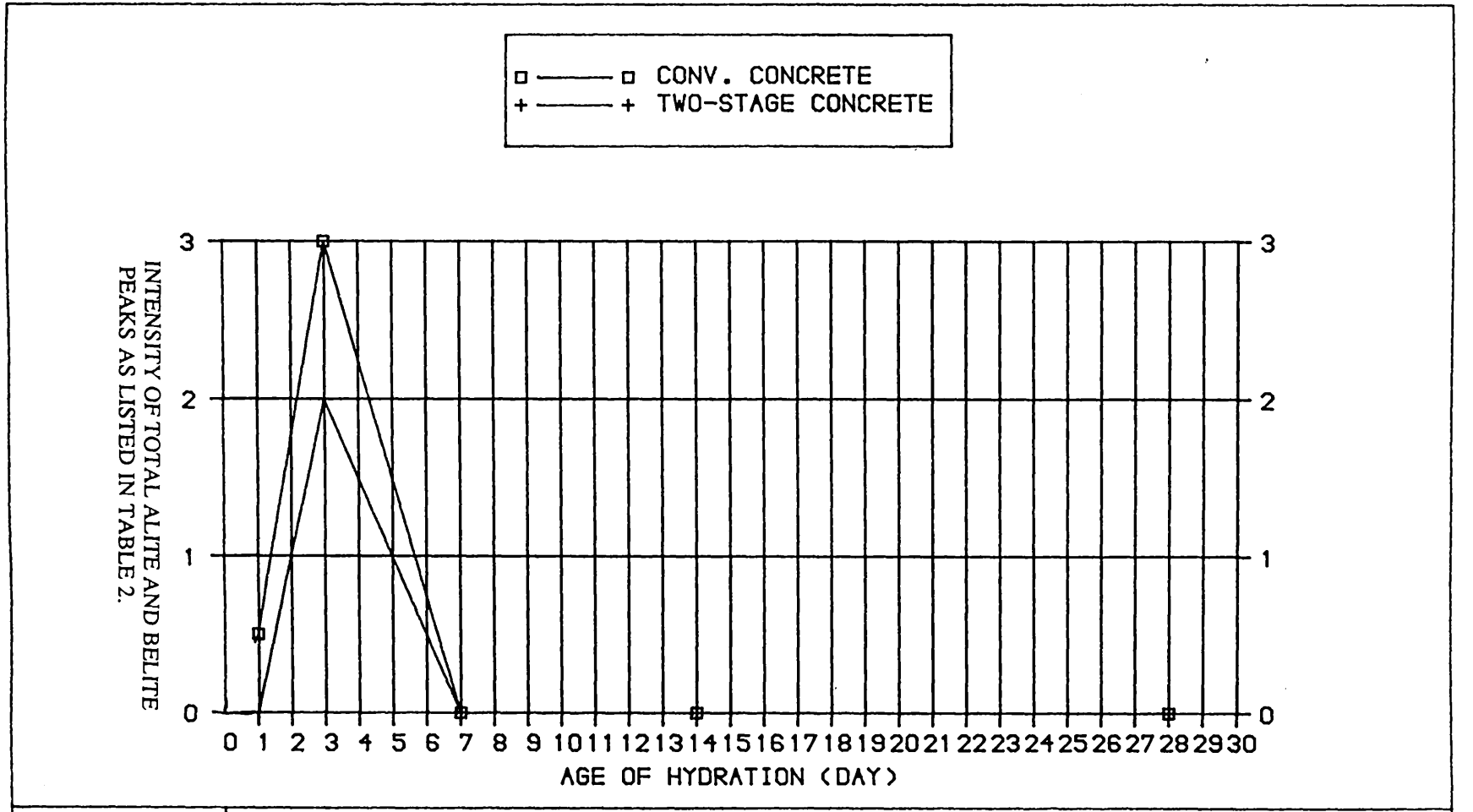

FIG. 8. ALITE AND BELITE PRODUCTS COMPARISON ON THE GLASS FOR BOTH MIXING TECHNIQUES

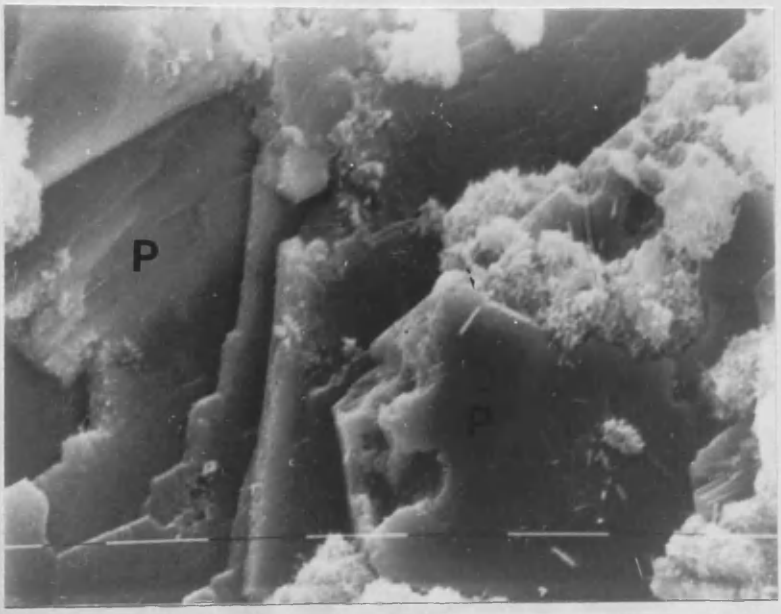

Figure 9.

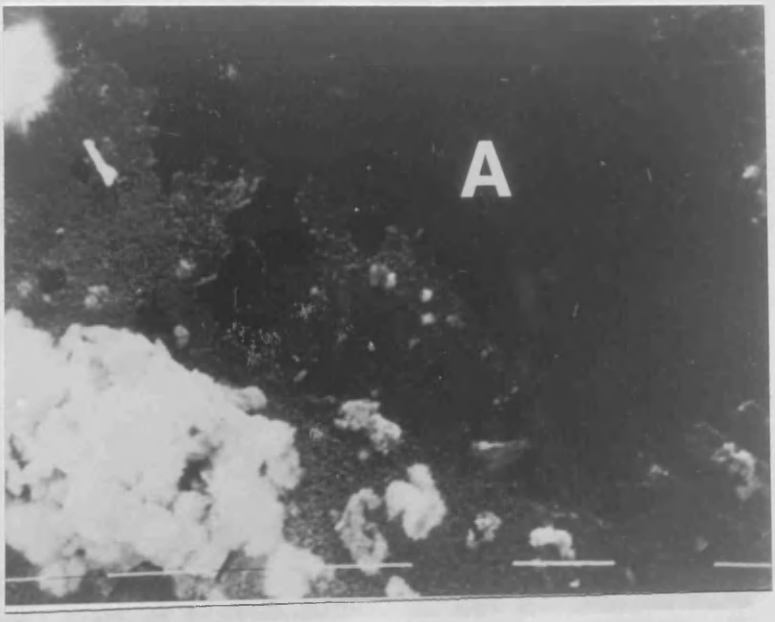

Figure 10.

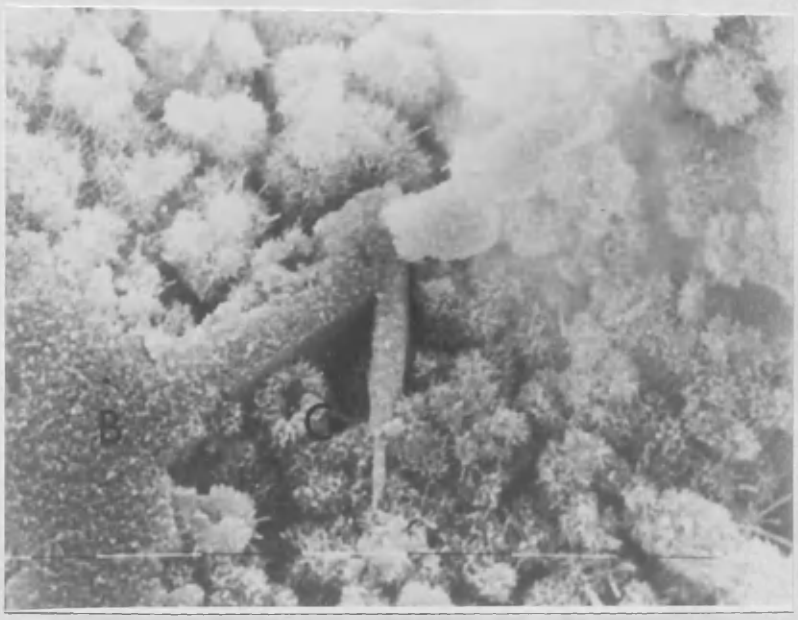

Figure 11.

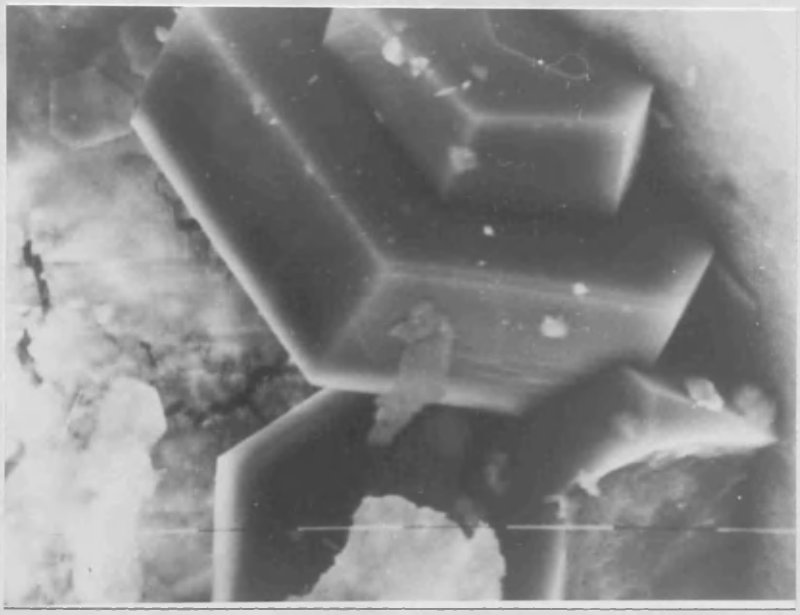

Figure 12.

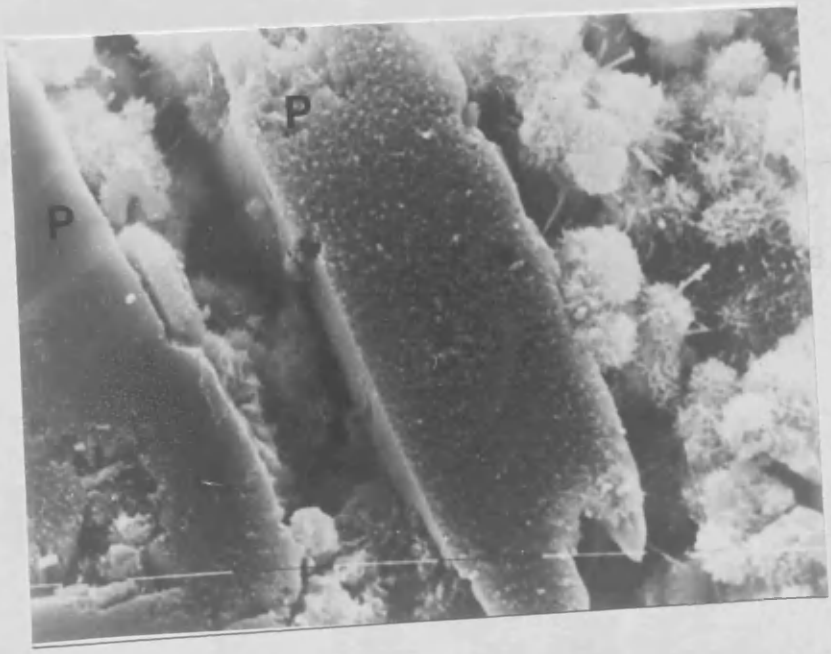

Figure 13.

Table 1.

RATIO (I(001)/I(101))

	TWO-STAGE		CONVENTIONAL	
	1 DAY	28 DAYS	1 DAY	28 DAYS
GLASS	3.28	1.80	2.09	0.78
BLOCK	1.80	7.20	1.13	3.28

Table 2.

PHASE	hkl	d-spacing Å	degrees 2θ, Co K-alpha
portlandite	001	4.90	21.05
portlandite	100	3.11	33.43
portlandite	101	2.62	39.83
portlandite	102	1.92	55.34
portlandite	110	1.79	59.82
C-S-H		3.06	34.02
C-S-H		1.82	59.82
ettringite		3.48	29.80
alite/belite		2.77	37.68
alite/belite		2.75	38.00

Chapter 3

Introduction and background

Chapter 3 (paper 2), is a paper dealing with a general mineralogical investigation of concrete decay. Standard techniques such as hand specimen analysis, X-ray diffraction, petrography and Scanning Electron Microscopy as well as stable isotope analyses, were applied to a core of concrete taken from a road bridge in the Midland Valley of Scotland, which is undergoing severe degradation. A study of the degradation was made and mineralogical mechanisms proposed. This paper has been accepted for publication in the British Mineralogical Magazine.

In the early stages of this research project I carried out an assessment of the usefulness of such mineralogical techniques as X-ray diffractometry (XRD), Scanning Electron Microscopy (SEM) and petrography in the study of concretes. I was already involved with XRD studies of cement pastes with colleagues from Civil Engineering at Strathclyde University. However, I wished to determine the general application of XRD studies to concrete. I started my assessment of XRD by first using XRD to study unhydrated cement powders. The crystalline minerals found in cement powders lend themselves to study by XRD. I loaded the JCPDS data for the more common of these crystalline minerals into the program XRDGRAPH, which was written by Dr. A. J. Hall, and is run on an Archimedes microcomputer. The program allows computer stored diffractograms to be studied on screen and JCPDS data of minerals to be displayed over the diffractogram. The program also allows peaks to be selected from the diffractogram

and a small data base of minerals to be searched for peak position identification. After studying the unhydrated crystalline cement powders, I began to hydrate cement powders and to try and study the hydrous cementitious minerals that may be encountered in a real concrete specimen. Unfortunately the lack of crystallinity of the C-S-H gel minerals and indeed a poor JCPDS data base for such minerals made identification difficult. Crystalline hydration products such as portlandite and to a lesser extent hydrogarnet and ettringite were identifiable, but exact identification of C-S-H gel peaks proved difficult and indeed their poor crystallinity causes the peaks of the crystalline compounds to be displaced. Similarily when I attempted to study concretes, that had been donated to the project by local materials testing companies, I found the identification of the cement paste phases even more complicated as fine grained aggregate, usually quartz was present and small rock fragments were also present in the pastes. Thus the diffractograms were extremely complex, and often had so many phase peaks overlapping that definite identification of the phases proved impossible. It was apparent that general XRD studies of concretes when both paste and aggregate are present are extremely difficult to interpret. However, if specimens of supergene alteration minerals or aggregate fragments or cement paste could be picked out or concentrated, then XRD would be invaluable in the identification of the phases involved.

SEM when applied to donated concrete specimens proved to be an extremely useful tool. I had already used SEM to observe the

texture of the phases present at the cement paste to aggregate interface, and I extended this experience to studying general concrete specimens. The micro-structure of cement pastes and aggregates was greatly enhanced by SEM studies and supergene alteration minerals could be identified easily and their textures and crystal habits studied. The analyser unit (EDAX), attached to the SEM was extremely useful in the identification of elements present in phases. I also endeavoured to apply Cathodoluminescence (CL), to concrete specimens, via the CL unit attached to the SEM. Unfortunately the elements present in the cement pastes and aggregates caused a general luminescence of the samples and very little textural interpretation could be made.

Standard petrography of concretes using petrological microscopes was found to be quite useful at high magnification, when standard transmitted light petrography was used. Petrography in transmitted light allowed aggregate petrologies to be determined, alteration of aggregates to be noted and porosity and fracturing of the cement paste to be studied. When thin sections were stained for porosity only fractures and large pores were highlighted; the microporosity of the cement pastes was not revealed. The constituent phases of the cement paste were generally revealed using optical microscopy. Reflected light microscopy allowed the identification of opaque phases in aggregates to be identified. It was apparent that neither XRD, SEM or petrography was an answer in itself to the study of concrete

decay, but a study involving all these techniques could prove fruitful.

At this stage in my research, I became aware after discussions with many industrial and academic parties interested in concrete decay, that there was scope for the development of a technique that could fingerprint the source of sulphur, carbon and oxygen involved in the growth of sulphate and carbonate minerals in and on the surface concrete. The reasons for such fingerprinting ranged from legal action for structure failure to a general interest in the mechanism of such mineral growth. If the source of sulphur for sulphate growth could be labelled as sewage source, groundwater source, road salt source or acid rain source, then the blame for structure failure could be aportioned. Similarily if the source of carbon and oxygen could be identified, then the carbonate mineral growth on concrete structures could be understood, and steps taken to rectify the problem in the future. Dr. Hall and I, felt that stable isotopes would lend themselves to such a study, and when a core of concrete from a major concrete road bridge in the Glasgow area (Fig. 3a), was made available for study by Strathclyde Roads Department. We decided to combine XRD, SEM, petrography and stable isotopes to the core of concrete and a stalactite from the underside of the bridge to try and piece together a model for the decay of the bridge. A report based on this study was sent to Strathclyde Regional Council. The ensuing paper is the final draft of the work carried out. I was senior author and Dr Hall and Dr. Fallick assisted in the preparation of the paper. Dr. Fallick gave

his permission for the carbon and oxygen stable isotope analyses to be carried out, and assisted greatly in their interpretation. I would like to point out that the basic carbonate mechanism proposed for the stalactite growth model in this paper has been more thoroughly studied and updated in Chapter 5. Cores of concrete have also been donated to this project by Tayside Regional Council; the cores from the Tay Bridge have been subjected to a preliminary study and the alteration found to be different than that discussed in this Chapter. Thus the work is not described within this thesis.

The solitary core studied within this chapter cannot be regarded as sufficient to definitely define the decay mechanisms for two reasons. Firstly the core only penetrated into the structure for 15cm and would only encounter the outer layered section of the concrete structure (French, 1990). Secondly, within a major structure such as this, up to fifteen deep penetrating cores would be necessary to provide a detailed investigation. Only small polished thin sections were prepared from the core and thus the resultant point counting analysis is probably slightly erroneous. A modal analysis of the point count data from two-thin sections gives values of 26% paste, 23% sand, 50.5% coarse aggregate and 0.5% voids. The coarse aggregate analysis is probably too high due to the small size of the sections. It should be in the region 40%. If this is taken into account and the other analysis proportionally scaled it is possible to calculate the "recipe" of the concrete (French, 1990). The paste probably had a w/c ratio of 0.5 (weight) and 1:3.2 (wt). Assuming the cement had some 5% gypsum and 2.5%

of sulphate as SO_3. This would yield some 13% by weight of cement in the cement paste (some 8% of ettringite by volume of paste). Thus of the 26% of paste about 2% could be ettringite. This value may explain the amount of ettringite produced on percolation of fluid through the structure as being caused by the remobilisation of sulphate in the cement paste.

Electron probe analysis of the cement paste revealed it to be enriched in magnesium and chlorine (Table. 1). Spot analysis of clinker grains hosted in the cement paste also revealed an enrichment in chloride ions and magnesium (Table. 2). Petrographical analysis of clinker grains in the cement paste revealed them as being converted to C-S-H gel by a secondary hydration after the original hydration of the cement paste (Fig. 3b). Portlandite was noted by petrographical means as being present in lower concentrations than usual (French, 1990). The assumption that can tentatively be made from this data is that fluid has percolated through the structure leaching portlandite, hydrating clinker particles and re-mobilising sulphate. The fact that chlorine and magnesium are enriched in the paste and in hydrated clinker particles suggests that the fluid percolating through the structure has been enriched by road-salts. The road salts being used in the area are evaporitic deposits, and thus have high magnesium contents.

Electron probe analysis of some of the needles in the voids in the cement paste revealed an enrichment of chloride (Table. 3). It is possible to suggest that a calcium-chloro-aluminate phase is

present in the paste and in the voids, where it is mixed with the ettringite , due to chloride ingression and the leaching of aluminium. Phases similar to the carbonate-bearing calcium sulpho-silicate thaumasite, were also found in voids in the carbonate zone. Ettringite is a common feature in voids in cement paste and can be related to moisture movement through the paste (French, 1991).

The upper section of the core has been extensively carbonated by diffusing carbon dioxide altering paste phases (Fig. 3c). This carbonation of the paste has also caused the conversion of the secondary alteration of ettringite to a thaumasite-ettringite phase (Table. 4). In the upper section of the core where the needles are connected to the void walls a silica enrichment has occurred (Table. 5). This may be due to the fluid percolating through the structure, or a feature of ASR. Ettringite is often found within the gel produced by ASR (French. 1991), and ASR is present in a small amount within the core Figure 3d.

With a limited amount of core and a limited penetration into the structure the models and mechanisms in the following paper can only be described as preliminary.

Figure 3a. Photograph of bridge from which the core was taken.

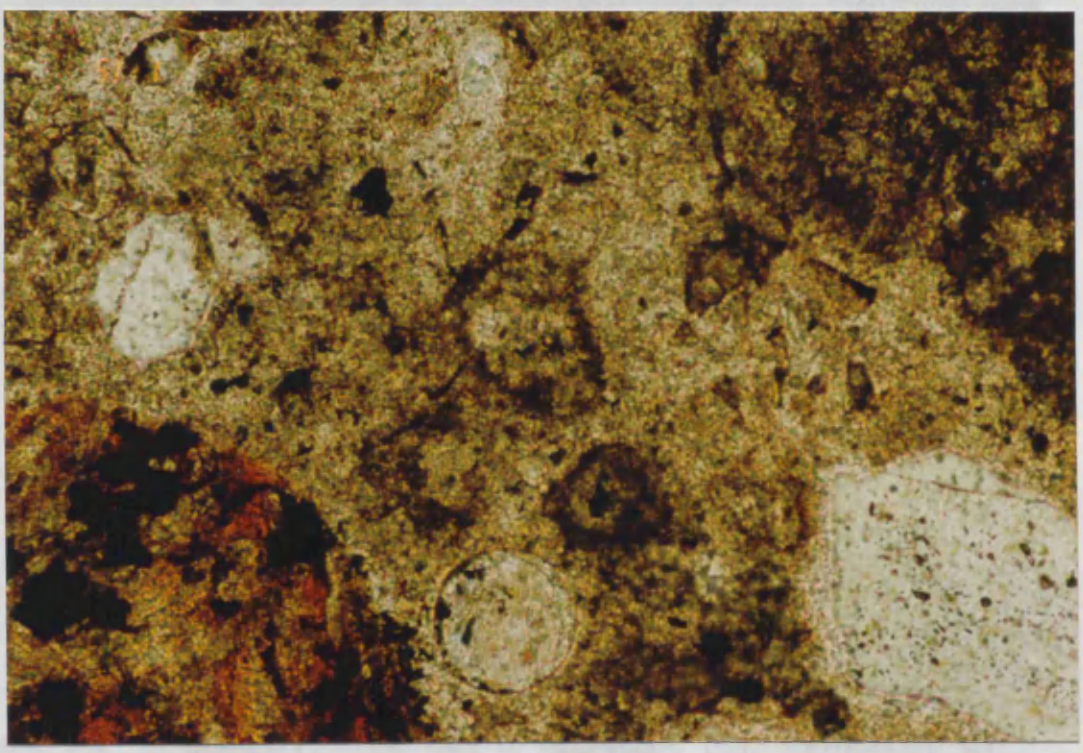

Figure 3b. C-S-H gel pseudomorphing a clinker grain in the paste after a secondary hydration reaction, field of view 0.5mm.

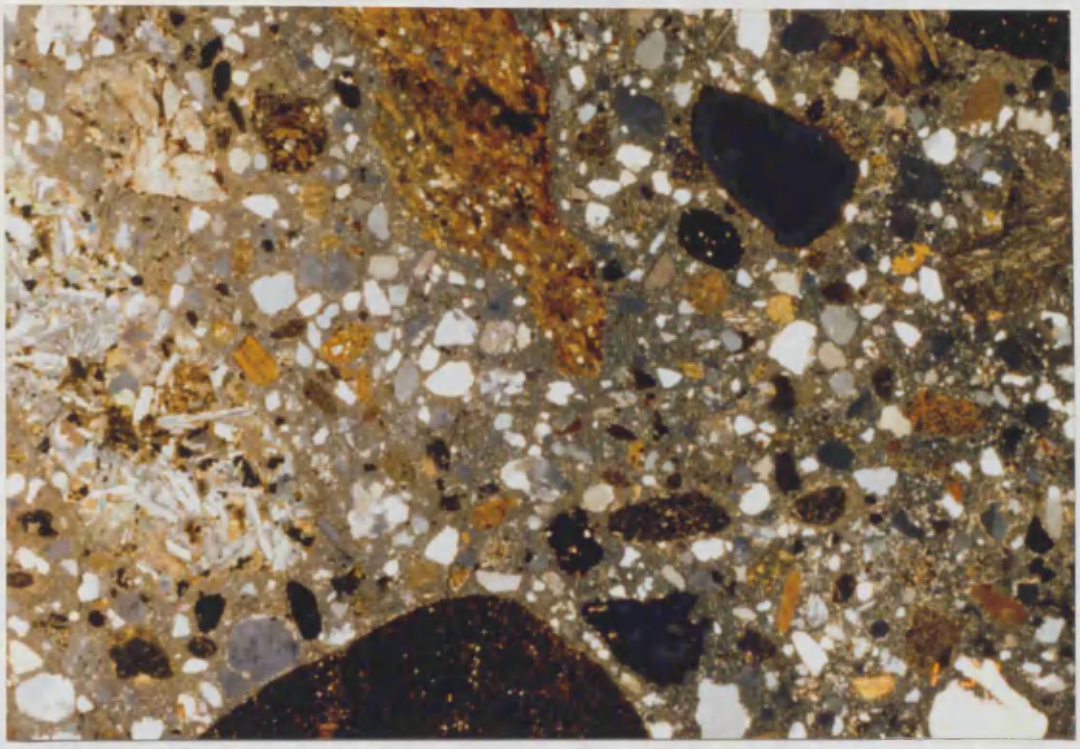

Figure 3c. Extensive carbonation of the cement paste, field of view 20 mm.

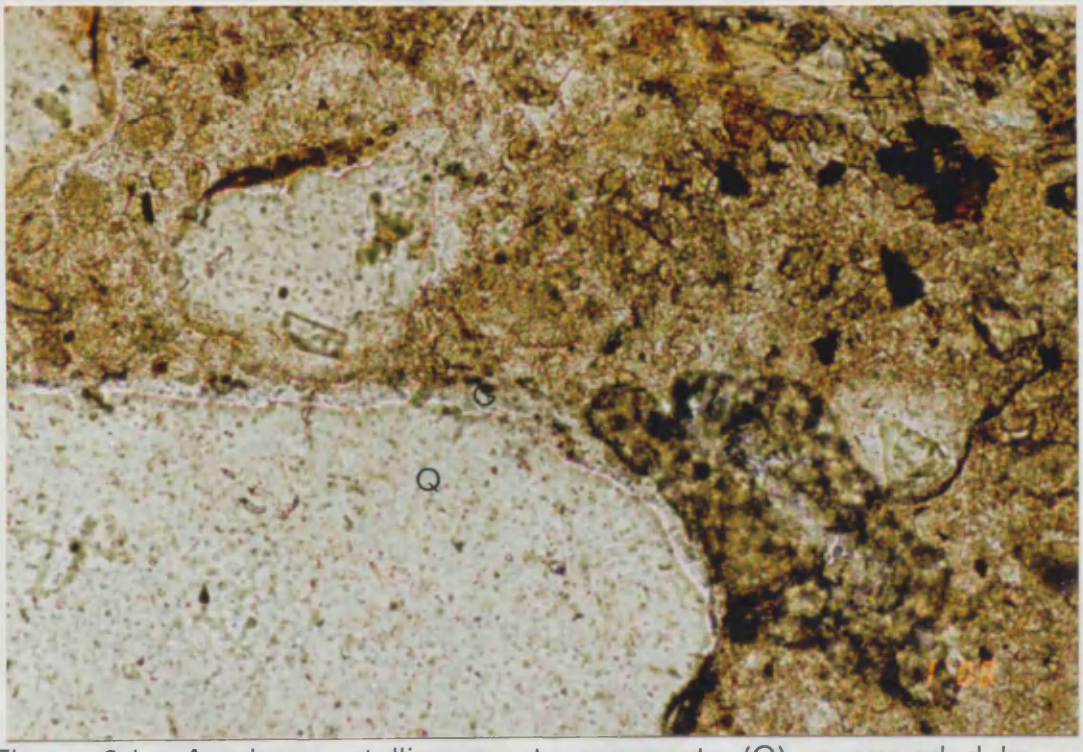

Figure 3d. A microcrystalline quartz aggregate (Q), surrounded by gel(G), produced by an ASR reaction, field of view 0.5 mm.

References

French, W. J. (1990). Personal communication.

French, W. J. (1991). Concrete petrography. Quarterly Journal of Geology, Vol. 24, (1)., pp 1-32.

Table. 1 Electron microprobe analysis of the bulk paste, showing chloride and magnesium enrichment.

No 7. BULK PASTE LIVETIME(spec.)= 100

ENERGY	RES	AREA
1.9	125.02	64907

TOTAL AREA= 188288
.....Si Ca Peaks used :
GF correction = - .020

FIT INDEX= .66

ELMT		APP.CONC	ERROR (WT%)
Si K	: 9	13.98	.18
Ti K	: 9	.18	.08
Al K	: 9	3.67	.24
Fe K	: 9	2.24	.17
Mn K	: 9	.10	.06* < 2 Sigma*
Mg K	: 9	.75	.33
Ca K	: 9	33.00	.25
Na K	: 9	.42	.40* < 2Sigma*
K K	: 9	.16	.09* < 2Sigma*
S K	: 9	.69	.08
Cl K	: 9	1.33	.10

...(3 ZAF'S)

20.00 kV TILT= .00 ELEV=30.00 AZIM= .00 COSINE=1

Spectrum: No. 7. BULK PASTE 2/10/90

Last elmt by STOICH., NORMALISED

ELMT	ZAF	%ELMT	ATOM%		%OXIDE	FORMULA
Si K : 9	1.00	15.00	12.87	Si 1O2	32.10	5.38
Ti K : 9	1.03	.190	.10	Ti 1O2	.32	.04
Al K : 9	1.03	3.84	3.43	Al 2O3	7.25	1.43
Fe K : 9	1.00	2.39	1.03	Fe 2O3	3.41	.43
Mn K : 9	.79	.14	.06	Mn 2O3	.20	.026
Mg K : 9	1.03	.77	.77	Mg 1O1	1.28	.32
Ca K : 9	.98	36.23	21.78	Ca 1O1	50.70	9.10
Na K : 9	.63	.72	.75	Na 2O1	.96	.31
K K : 9	.94	.19	.12	K 2O1	.23	.05
S K : 9	.95	.78	.58	S 1O3	1.94	.24
Cl K : 9	.90	1.60	1.09	Cl 1O0	1.60	.46
O K : 0	.00	38.15	57.44			24.00
TOTAL		100.00	100.00		100.00	17.79

Table. 2. Electron microprobe data for the analysis of an altered clinker grain, showing magnesium and chloride ion enrichment.

No 7. SPOT ANALYSIS CLINKER LIVETIME(spec.)= 100

ENERGY	RES	AREA
1.4	121.33	64786

TOTAL AREA= 115921
.....Si Ca Peaks used :
GF correction = - .028

FIT INDEX= .27

ELMT		APP.CONC	ERROR (WT%)
Si K	: 9	5.86	.13
Ti K	: 9	.13	.08* < 2 Sigma*
Al K	: 9	2.60	.19
Fe K	: 9	.92	.14
Mn K	: 9	-.01	.05* < 2 Sigma*
Mg K	: 9	2.66	.29
Ca K	: 9	15.98	.18
Na K	: 9	.30	.32* < 2Sigma*
K K	: 9	.10	.08* < 2Sigma*
S K	: 9	.27	.07
Cl K	: 9	1.58	.09

...(3 ZAF'S)

20.00 kV TILT= .00 ELEV=30.00 AZIM= .00 COSINE=1

Spectrum: No. 7. SPOT CLINKER ANALYSIS 2/10/90

Last elmt by STOICH., NORMALISED

ELMT	ZAF	%ELMT	ATOM%		%OXIDE	FORMULA
Si K : 9	.95	12.32	10.48	Si 1O2	26.36	4.52
Ti K : 9	1.03	.25	.13	Ti 1O2	.42	.06
Al K : 9	.98	5.29	4.68	Al 2O3	9.99	2.02
Fe K : 9	1.00	1.80	.77	Fe 2O3	2.59	.33
Mn K : 9	.79	.00	.00	Mn 2O3	.00	.00
Mg K : 9	1.07	4.96	4.87	Mg 1O1	8.22	2.10
Ca K : 9	.97	32.90	19.56	Ca 1O1	46.03	8.46
Na K : 9	.67	.92	.96	Na 2O1	1.24	.41
K K : 9	.92	.21	.13	K 2O1	.25	.06
S K : 9	.94	.55	.41	S 1O3	1.38	.18
Cl K : 9	.90	2.38	1.09	Cl 1O0	3.53	1.03
O K : 0	.00	37.27	55.61			24.00
TOTAL		99.99	100.00		99.99	19.16

Table. 3. Electron microprobe data for the analysis of an ettringite-type phase showing enhanced chlorine ion content.

No 7. SPOT ANALYSIS ETTRINGITE LIVETIME(spec.)= 100

ENERGY	RES	AREA
1.9	123.02	64657

TOTAL AREA= 181595
.....Si Ca Peaks used :
GF correction = - .019

FIT INDEX= .65

ELMT		APP.CONC	ERROR (WT%)
Si K	: 9	.84	.10
Ti K	: 9	.05	.07* < 2 Sigma*
Al K	: 9	11.81	.27
Fe K	: 9	.29	.13
Mn K	: 9	-.004	.05* < 2 Sigma*
Mg K	: 9	.44	.35* < 2 SIGMA*
Ca K	: 9	34.77	.25
Na K	: 9	.26	.41* < 2Sigma*
K K	: 9	-.08	.09* < 2Sigma*
S K	: 9	6.80	.13
Cl K	: 9	2.22	.11

...(3 ZAF'S)

20.00 kV TILT= .00 ELEV=30.00 AZIM= .00 COSINE=1

Spectrum: No. 7. SPOT ANALYSIS ETTRINGITE 2/10/90

Last elmt by STOICH., NORMALISED

ELMT	ZAF	%ELMT	ATOM%		%OXIDE	FORMULA
Si K : 9	.91	.99	.85	Si 1O2	2.11	.35
Ti K : 9	1.02	.05	.03	Ti 1O2	.09	.01
Al K : 9	1.05	11.95	10.68	Al 2O3	22.59	4.47
Fe K : 9	1.00	.30	.13	Fe 2O3	.43	.06
Mn K : 9	.79	.00	.00	Mn 2O3	.00	.00
Mg K : 9	1.06	.44	.44	Mg 1O1	.73	.18
Ca K : 9	.97	38.03	22.88	Ca 1O1	53.21	9.56
Na K : 9	.65	.43	.45	Na 2O1	.57	.19
K K : 9	.94	.00	.00	K 2O1	.00	.00
S K : 9	1.03	7.06	5.31	S 1O3	17.63	2.22
Cl K : 9	.89	2.65	1.80	Cl 1O0	2.65	.75
O K : 0	.00	38.11	57.44			24.00
TOTAL		100.00	100.00		100.00	17.78

Table. 4. Electron microprobe data for the analysis of an ettringite-thaumasite phase, closely approaching ettringite in composition.

No 7. SPOT ANALYSIS ETTRINGITE LIVETIME(spec.)= 100

ENERGY	RES	AREA
2.1	121.10	64251

TOTAL AREA= 190367
.....Si Ca Peaks used :
GF correction = .003

FIT INDEX= 1.29

ELMT		APP.CONC	ERROR (WT%)
Si K	: 9	.95	.11
Ti K	: 9	.08	.07* < 2Sigma*
Al K	: 9	10.18	.27
Fe K	: 9	.17	.12* < 2Sigma
Mn K	: 9	.01	.05* < 2Sigma*
Mg K	: 9	.03	.38* < 2SIGMA*
Ca K	: 9	33.06	.25
Na K	: 9	.19	.47* < 2Sigma*
K K	: 9	-.05	.09* < 2Sigma*
S K	: 9	12.02	.16
Cl K	: 9	.13	.09

...(3 ZAF'S)

20.00 kV TILT= .00 ELEV=30.00 AZIM= .00 COSINE=1

Spectrum: No. 7. SPOT ANALYSIS ETTRINGITE 2/10/90

Last elmt by STOICH., NORMALISED

ELMT	ZAF	%ELMT	ATOM%		%OXIDE	FORMULA
Si K : 9	.94	1.29	.86	Si 1O2	2.20	.34
Ti K : 9	1.02	.08	.04	Ti 1O2	.14	.02
Al K : 9	1.05	9.83	8.53	Al 2O3	18.57	3.35
Fe K : 9	1.00	.17	.07	Fe 2O3	.24	.03
Mn K : 9	.79	.02	.01	Mn 2O3	.02	.01
Mg K : 9	1.06	.03	.03	Mg 1O1	.04	.01
Ca K : 9	.97	34.86	20.37	Ca 1O1	48.78	8.00
Na K : 9	.65	.30	.30	Na 2O1	.40	.12
K K : 9	.93	.00	.00	K 2O1	.00	.00
S K : 9	1.04	11.80	8.61	S 1O3	29.45	3.38
Cl K : 9	.86	.15	.10	Cl 1O0	.15	.04
O K : 0	.00	41.75	61.09			24.00
TOTAL		100.00	100.00		100.00	15.29

Table. 5. Electron microprobe data for the analysis of an ettringite- Ca-chloroaluminate phase enriched in chlorine. This could be a mixture of the two phases or a solid solution produced by alteration effected by percolating water.

No 7. SPOT ANALYSIS ETTRINGITE LIVETIME(spec.)= 100

ENERGY	RES	AREA
2.3	124.40	64476

TOTAL AREA= 225462
.....Si Ca Peaks used :
GF correction = .032

FIT INDEX= .75

ELMT			APP.CONC	ERROR (WT%)
Si K	:	9	.58	.11
Ti K	:	9	.03	.08* < 2Sigma*
Al K	:	9	21.20	.34
Fe K	:	9	.39	.13
Mn K	:	9	.01	.06* < 2Sigma*
Mg K	:	9	.03	.44* < 2SIGMA*
Ca K	:	9	41.98	.28
Na K	:	9	.12	.50* < 2Sigma*
K K	:	9	-.12	.09* < 2Sigma*
S K	:	9	5.69	.13
Cl K	:	9	5.27	.14

...(3 ZAF'S)

20.00 kV TILT= .00 ELEV=30.00 AZIM= .00 COSINE=1

Spectrum: No. 7. SPOT ANALYSIS ETTRINGITE 2/10/90

Last elmt by STOICH., NORMALISED

ELMT	ZAF	%ELMT	ATOM%		%OXIDE	FORMULA
Si K : 9	.87	.55	.47	Si 1O2	1.17	.20
Ti K : 9	1.02	.02	.01	Ti 1O2	.04	.01
Al K : 9	1.08	16.32	14.64	Al 2O3	30.85	6.30
Fe K : 9	1.01	.32	.14	Fe 2O3	.45	.06
Mn K : 9	.79	.00	.00	Mn 2O3	.00	.00
Mg K : 9	1.09	.02	.02	Mg 1O1	.04	.01
Ca K : 9	.97	36.02	21.75	Ca 1O1	50.40	9.37
Na K : 9	.67	.35	.36	Na 2O1	.47	.16
K K : 9	.92	.00	.00	K 2O1	.00	.00
S K : 9	1.01	4.70	3.55	S 1O3	11.73	1.53
Cl K : 9	.90	4.86	3.32	Cl 1O0	4.86	1.43
O K : 0	.00	36.84	55.73			24.00
TOTAL		100.00	100.00		100.00	19.06

---

3. An applied mineralogical investigation of concrete degradation in a major concrete road bridge.

(Draft September 1990)

G. Macleod, A. J., Hall and A. E. Fallick*

Dept. of Geology & Applied Geology, University of Glasgow, Glasgow G12 8QQ.

* Scottish Universities Research and Reactor Centre, East Kilbride, Glasgow G75 0QU.

3.1 Abstract

A core of concrete taken from a major road bridge in Strathclyde Region, Scotland has been subjected to an applied mineralogical investigation, which involved stable isotope analysis, petrography, X-ray diffraction and scanning electron microscopy.

The structure is actively undergoing severe degradation due to mineral growth which is related to chemical reactions between the concrete and pore fluids. The physical growth of minerals causes disfigurement and structural weakening. Water flowing through the structure has leached sulphur from the sulphur bearing phases in the cement paste and deposited the sulphur as sulphate, in ettringite in spherical cavities in the cement paste (French, W. J., pers. comm.). Pyrite and pyrrhotine hosted by dolerite aggregate appear to have been oxidised, probably providing additional sulphate for the deposition of ettringite and minor gypsum, within the spheroidal cavities within the cement paste. The rainwater which passes through the structure leaching sulphur species and

possibly oxidising the iron sulphides, is also involved in the further leaching of elements from the cement paste and in the deposition of calcite. The isotopic values of calcites forming a crust on the concrete and a stalactite under the bridge are similar with $\partial^{13}C$=-19‰ PDB and $\partial^{18}O$=+16‰ SMOW. We suggest that atmospheric carbon dioxide was the carbon source. The carbon isotopic fractionation of -12‰ from atmospheric carbon dioxide of $\partial^{13}C$ = -7‰ (O'Neil and Barnes, 1971) can best be explained as due to a kinetic fractionation related to the hyper-basicity of the pore water. The equilibrium formation temperature of about 45 °C calculated from the oxygen isotope values, assuming a $\partial^{18}O$ value of meteoric water of -8‰ SMOW, is considered unreasonable. The exceptionally low $\partial^{18}O$ values are attributed mainly to reaction kinetics and the calcite inheriting its oxygen, two-thirds from atmospheric carbon dioxide and one third from the meteoric formation water (O'Neil and Barnes, 1971). A $\partial^{18}O$ value of atmospheric carbon dioxide of +41‰ SMOW and a $\partial^{18}O$ value of meteoric water of -8‰ lead to a calculated $\partial^{18}O$ value for the calcites of +10‰ SMOW. The calcites analysed have a value of +16‰ and this may be due to partial re-equilibration towards a calculated value of +21‰ for calcite in equilibrium with the meteoric water at 20 °C.

KEYWORDS; concrete deterioration, petrography, ettringite, calcite, stable isotopes.

3.2 Introduction

Concrete degradation is an endemic problem in the British Isles and throughout the world. The problem of concrete and building stone decay has been investigated by many workers, but they have often been unable to establish exact mechanisms for the decay reaction processes (Smith *et al.,* 1988). Common causes of concrete decay in Scotland are sulphate mineral growth (sulphate attack), carbonate mineral growth (carbonation), and chloride attack due to the use of road salt. Samples of a road bridge were made available by Strathclyde Region Roads Department. This structure had previously been classified in unpublished reports as having undergone carbonation.

Carbonate mineral growth in concrete structures is a major cause of decay; carbonate mineral growth reduces the alkalinity of the structure, allowing encased steel support bars to oxidise and corrode (Minoru, 1968). The structure may also suffer shrinkage related to carbonate mineral growth (Lea, 1970). The carbonate mineral growth in concrete is thought to be mainly related to the reaction of the paste phases with diffusing atmospheric carbon dioxide (Lea, 1970). Surface carbonate mineral growth (efflorescence), may also disfigure decorative structures and stalactitic growths are not uncommon. The carbonate minerals themselves are susceptible to leaching by aggressive acidic waters and this leaching leads to further structural damage and decorative disfigurement (Smith *et al.,* 1988).

The predominant carbonate mineral found growing in concrete is calcite ($CaCO_3$), but other less common carbonates have been reported, trona ($Na_3H(CO_3)_2.2H_2O$) and thermonatrite ($Na_2CO_3.2H_2O$) (Charola and Lewin, 1979). Often these occur as efflorescent growths on the external surface of the structure. Sulphate minerals are produced by various mechanisms, the most common being the invasion of the structure by groundwaters enriched in sulphate. Water flowing through the structure may also leach sulphur components from the paste and deposit them as sulphate phases. Common sulphate minerals deposited in concrete are gypsum ($CaSO_4.2H_2O$), ettringite ($Ca_6Al_2(SO_4)_3(OH)_{12}.26H_20$) and thaumasite ($Ca_6Si_2(SO_4)_2(CO_3)_2(OH)_{12}.24H_2O$), the complex sulphocarbonate.

To our knowledge, no detailed mineralogical study, involving carbon and oxygen stable isotopes has been reported on a concrete structure that is undergoing active degradation. There appears to be a missing link between chemical and engineering studies, and applied geochemical studies of concrete deterioration. The road bridge investigated has a dual carriageway passing on top and a double railway track passing below. A core of concrete was obtained from below the tar surface perpendicular to the bridge deck (see Fig. 1). The technique of stable isotope analyses was employed to aid in the identification of sources of carbon and of depositional processes. The core was also subjected to mineralogical investigation, using established techniques such as petrography, scanning electron microscopy and X-ray diffraction spectrometry.

3.3 Mineralogical Composition of Concrete

Concrete is composed of two materials, cement paste and aggregate. The paste is produced by hydrating cement powder which, in an exothermic reaction, produces hydrous cementitious minerals. The aggregate consists of sand-sized particles grading into rock fragments and may be monomineralic, but more commonly aggregate consists of rock fragments. The types of minerals and their abundance vary with each batch and type of concrete. The cement paste studied in the structure is a paste produced from an Ordinary Portland Cement. The mineral composition of Ordinary Portland Cement paste is thought to be 70% C-S-H gels, 20% portlandite ($Ca(OH)_2$), 7% aluminates and sulpho-aluminates and 3% unhydrated material (Diamond, 1976).

The portlandite present in cement paste is in the form of hexagonal platelets that concentrate at the paste-to-aggregate interface in a complex double aureole. It is portlandite that is thought to provide the bond strength in concrete (Lea, 1970). The mineralogy of the C-S-H gels is complex; they have a morphology similar to the phyllosilicates and both their crystal structure and chemistry is variable. Examples of these so-called gel minerals are tobermorite, gyrolite and reyerite (Komarneni and Guggenheim, 1988 Merlino, 1988a,b). The hydrated alumina minerals present are most usually in the form of hydrogarnet ($3CaO.Al_2O_3.6H_2O$) which is randomly dispersed through the paste along with a small amount of the mineral ettringite ($Ca_6Al_2(SO_4)_3(OH)_{12}.26H_2O$). The microstructure of the C-S-H gel consists of microscopic pores of diameters in the range of 2 nm, linked by similarily minute

tubercles (Neville and Brooks, 1987). For a more detailed study of the structure of cement paste readers are referred to Ramachandran *et al.,* 1981.

3.4 Hand Specimen Analysis

Examination of the core by naked eye and below a binocular microscope revealed three zones in the core. The first zone occurs on the outermost surface of the core closest to the tar surface of the road. It consists of a cream coloured precipitate with patches of brown staining; the concrete itself is pitted and friable. This zone extended to half a centimetre in depth from the top of the core. The second zone extended from 0.5cm to 2cm depth in the core and consisted of cement paste and aggregate; the paste has a cream colouration and is pitted. The third zone extended from the base of the second zone to the base of the core, a distance of 15cm. This zone consisted of reasonably fresh concrete with unaltered aggregate.

Observation of the core below a binocular microscope revealed the ubiquitous presence of white spheres in the cement paste; the spheres were present in all three zones and ranged in diameter from 1mm to 4mm. Similar-sized spherical cavities could also be seen throughout the cement paste. It was apparent that the white material had preferentially grown within the spherical cavities. Observation of the aggregate in the concrete indicated that some of the aggregate fragments had undergone alteration in the cement paste. Staining of fragments and occasional brown haloes around aggregate fragments could be noted by the naked eye.

3.5 X-ray Diffraction Studies

Material from the two upper zones was found by powder X-ray diffractometry to be composed of calcite, quartz and C-S-H gel. The cream colouration of the top of the core is undoubtedly due to calcite growth. Quartz was present in the form of sand grains added as fine aggregate to the cement paste. The cementitious minerals of the C-S-H gel type. All the samples analysed from the upper two zones of the concrete were depleted in the mineral portlandite ($Ca(OH)_2$). One of the white spheres was picked out and found to consist of ettringite with a minor presence of gypsum. Non-carbonated cement paste revealed a depletion in the hydration mineral hydrogarnet ($3CaO.Al_2O_3.6H_2O$). Similarily, portlandite is in lower concentrations than would be expected. The hydrous cementitious minerals found in cement paste give poor diffractograms at best due to their lack of crystallinity. However, in the non-carbonated cement paste it appeared that these minerals were less crystalline than would be expected. The lack of crystallinity of the components and the depletion of hydrogarnet suggests that water may have passed through the paste leaching chemical species and altering minerals.

3.6 Petrography

A suite of polished thin sections was prepared from the core. The cementitious minerals found in the cement paste are usually to fine grained to be observed under a normal light microscope, except at high magnification, but it is occasionally possible to identify

portlandite grains (Powers and Hammersley, 1978), and to observe unhydrated clinker grains. Within the cement paste studied it was difficult to observe any cementitious minerals. Phases that were identifiable had obviously reacted with water in a secondary reaction after the initial hydration of the cement paste. Throughout the paste there are unusually abundant spherical cavities ranging in diameter from < 1mm to 6mm. The cavities are occasionally empty, but are commonly filled with acicular needle-like growths that radiate into the pore space, presumably having nucleated on the side of the pores (Fig. 2).

The mineral grains are extremely fine (<4μm), and almost whisker like and were identified by powder X-ray diffraction as ettringite (Fig. 3). Isolated ettringite needles can also be seen in the cement paste and it is presumed that they are original ettringite produced as the cement powder hydrated. It is obvious that the ettringite found growing in the abundant cavities is a secondary alteration product. The filling of air cavities with ettringite has been noted previously (Powers and Hammersley, 1978), and is noted in the American Society for Testing and Materials standard for concrete petrography (ASTM C856). It is apparent that the ettringite filling the cavities in this cement paste, has been produced by the percolation of water through the structure, mobilising sulphate to be deposited as ettringite in the cavities.

The most common aggregate is dolerite, but gabbro, lava, sandstone and schist fragments are also present. Exotic aggregate included wood fragments, coal particles, rose quartz, mudstone and

limestone. None of these aggregate fragments had obviously reacted with the cement paste; however, surrounding a solitary limestone fragment is a yellow reaction rim which may be due to reaction with the cement paste or fluids percolating through the structure.

In transmitted light the dolerite aggregate fragments (1cm to 10cm), can be seen to contain an abundance of opaque minerals. The grains, when studied in reflected light, were revealed as the iron sulphides pyrite and pyrrhotine (Fig. 4), as well as the iron-titanium oxide phases, ilmenite and magnetite. In the chemical environment found in concrete, iron-titanium oxides are not potentially reactive but pyrite and pyrrhotine are undesirable as they may oxidise easily to produce sulphuric acid (Shayan, 1988).

A dolerite aggregate that had been observed by the naked eye as having iron staining was picked out, and a polished thin section prepared (Fig. 5). In thin section it could be seen that in the iron-stained area of the fragment pyrrhotine and pyrite were absent and in the unstained area they were present. The iron staining is probably due to the oxidation of pyrrhotine and pyrite producing sulphuric acid (Shayan, 1988), and leaving a residual iron hydroxide (Eqns. 1 and 2). Water and oxygen are required for the oxidation of pyrite and pyrrhotine and the oxidation staining observable in numerous aggregate fragments indicates that fluids have percolated through the structure. It is probable that oxidising iron-sulphides may have made a minor contribution of sulphur to the secondary ettringite growth.

Eqn.1 $4FeS+6H_2O+9O_2 \longrightarrow 4FeO.OH+4H_2SO_4$

pyrrhotine

Eqn.2 $4FeS_2+10H_2O+15O_2 \longrightarrow 4FeO.OH+8H_2SO_4$

pyrite

3.7 Scanning Electron Microscopy

Samples of paste and aggregate were picked out from the core and observed by SEM equipped with energy dispersive X-ray analysis. Paste from the top 0.5cm of the core was rich in calcite distributed as fine-grained material throughout the paste. Microfractures in the paste are lined with a white gel-type material that was rich in silicon, aluminium, potassium and sulphur. The material was similar in morphology to a gel and it is possible that it is a symptom of alkali silica reaction (Lea, 1970). SEM observation of the cement paste allowed the spherical cavities to be studied in greater detail. The often perfect sphericity of the cavities suggests that they are air bubbles that have been trapped in the cement paste as it cured and their abundance indicates that the concrete may have been a poorly prepared concrete. The cavities are often filled with spherical masses of acicular needles of ettringite. The needles radiate outwards apparently nucleating on the side of the cavity. Gypsum crystals nestle within the needles along with crystals of an unidentified chlorine-rich phase (Fig. 6). The phase may be a calcium-chloro-aluminate phase, the chlorine being introduced to the system by dissolved road salts in the percolating waters.

3.8 Stable isotopes

We are not aware of previously published carbon and oxygen stable isotope studies on minerals produced during the degradation of concrete. Two samples of calcite were analysed for $\partial^{13}C$ PDB and $\partial^{18}O$ SMOW in the standard manner (McCrea, 1950). The results are listed in Table 1, along with the formation temperatures of the calcites calculated using an assumed meteoric water $\partial^{18}O$ value of -8‰ SMOW. The first sample was taken from the calcitic crust from the top of the core and the second from a stalactite, one of several growing on the underside of the bridge deck (Fig. 1). Both samples have very similar $\partial^{13}C$ and $\partial^{18}O$ values.

In order to make an intelligible interpretation of the results a comparison had to be made with a similar natural process. The pore fluids of concrete are extremely alkaline and often attain pH values of 12 or more (Glasser, 1986). Carbon dioxide reacts rapidly with alkaline water possibly due to an affinity of OH^- for the carbon dioxide molecule. The formation of travertine deposits by the deposition of calcite scums in highly alkaline fresh water pools is analogous to the concrete growth system in chemical terms. During the deposition of such calcites the $\partial^{13}C$ value is fractionated by at least -10‰ (O'Neil and Barnes, 1971). This value coincides approximately with fractionation expected from a kinetic process with an inverse square root of mass dependence (e.g. diffusion velocity). Similarily a kinetic fractionation of the oxygen isotope value of the carbon dioxide would be -22‰ but the $\partial^{18}O$ value for the calcite is thought to be obtained by a mixture of

one third oxygen from the meteoric formation water and two-thirds from the atmospheric carbon dioxide involved in the reaction Eqn. 3 (O'Neil and Barnes, 1971).

Eqn. 3	$H_2O(l)$	+	$CO_2(g)$	$\longrightarrow$	$H_2CO_3(l)$
$\partial^{18}O$	-8‰		(+41‰ -22‰)	$\longrightarrow$	+10‰

Assuming the carbon dioxide involved in the calcite growth in the concrete is atmospheric ($\partial^{13}C$ = -7‰), then the expected ∂13C values for the samples are at least -18‰ PDB. The $\partial^{13}C$ values (Table 1) are slightly lighter than expected and this could be related to the high pH of the water. The precipitation of the calcitic scums studied by O'Neil and Barnes (1971) is extremely rapid and as a result the calcites are out of oxygen isotopic equilibrium. The calcites found within this concrete may not have been so rapidly deposited, but they are certainly not in isotopic equilibrium as the calculated formation temperature of approximately 45°C is too high (Fig. 7). Reasonable temperatures for the calcite to have formed at are around 20°C and if they formed in equilibrium with the formation water (-8‰), they would be expected to have a $\partial^{18}O$ SMOW value of +21‰. Also, the $\partial^{18}O$ value of the formation water may be different to that of local meteoric water, oxygen being contributed to the system from other minerals such as portlandite (see Eqn. 4) perhaps by isotope exchange.

The $\partial^{13}C$ and $\partial^{18}O$ values of the two samples are very close and this suggests that they were formed by one fluid with a similar isotopic composition and a similar reaction process.

3.9 Proposed model for mineral deposition

A calcitic crust occurs on the upper side of the bridge deck below the tar surface. Stalactitic growths composed of calcite are abundant on the underside of the bridge deck. Within the concrete structure there is no calcite growth, except as occasional fine grained fracture linings. Most of the calcite growth is due to water percolation through the structure. The mineral portlandite ($Ca(OH)_2$) is concentrated in concrete structures at the surface of the structure and at the interface between the cement paste and aggregate fragments (Lea, 1970). Undoubtedly the portlandite at the surface of the bridge deck reacted immediately with atmospheric carbon dioxide to produce calcite (Eqn. 4). It is highly likely that the reaction at the concrete surfaces took place as it cured.

Eqn. 4 $$Ca(OH)_2\ (s) + CO_2\ (g) \longrightarrow CaCO_3\ (s) + H_2O\ (l)$$

This initial reaction must have left a fine coating of calcite on the surface of the concrete. The fine grained coating of calcite would act as a nucleus for the growth of calcite from the predominantly aqueous system. Rainwater with hydrated carbon dioxide and various dissolved carbon species has flowed along the roads on either side of the bridge below the tar surface, and

collected on the bridge deck. The bridge is topographically lower than the roads on either side. As the water flows it physically corrodes the concrete and leaches calcium hydroxide from the cement paste. The water may attain a pH of 12 and the dominant carbonate species is the carbonate ion CO_3^{2-} (Pourbaix, 1974). With a solid carbonate coating already present and with water rich in leached calcium ions and carbonate ions a calcitic crust is produced on the upper side of the deck.

The deck itself is composed of large concrete blocks joined together by vertical mortar-sealed joints. The blocks are also fractured and intricate patterns of fractures cross-cut the blocks. The pools of water collecting on the upper side of the bridge deck percolate downwards through the joints and fractures (Fig. 1), the driving mechanism for the water flow being surface tension and gravitational forces. As the water passes through the deck at a fairly rapid rate it interacts with the mortar and cement paste leaching calcium hydroxide. As time passed the available calcium hydroxide will have been gradually leached from the cement paste, and as a result the pH of the water would have fallen. At pH values of 6 to 10, the dominant carbon species is the HCO_3^- ion (Pourbaix, 1974).. As water emerges on the underside of the bridge deck stalactites may possibly be formed in the classic degassing fashion (Eqn. 5).

Eqn. 5 $2HCO_3^-(aq) + Ca^{2+}(aq) \longrightarrow CaCO_3(s) + H_2O(l) + CO_2(g)$

It is more probable that as the fluid is at a high pH, the stalactites

may be produced by the reaction of carbonate and calcium ions in the solution forming calcite (Eqn. 6). This reaction is the most dominant in the formation of stalactites on the bridge.

Eqn. 6 Ca^{2+} (aq) + CO_3^{2-} (aq) $\longrightarrow$ $CaCO_3$ (s)

At very high pH (>12) the very rapid reaction of carbon dioxide and alkaline solution could take place according to Eqn. 7.

Eqn. 7 Ca^{2+} (aq) + $2OH^-$ (aq) + CO_2 (g) $\longrightarrow$ $CaCO_3$ (s) + H_2O (l)

The stable isotope analyses of the calcite crust and stalactite supports the theory that atmospheric carbon dioxide is the source of the carbon for the calcite, and that the calcites have been deposited from hyper-basic solutions.

The hyper-basic solution that has percolated through the concrete depositing the calcite has permeated into the cement paste itself. Surface tension and capillary forces combine to pull the fluid into the micro-pores and tubercles in the cement paste. The fluid is continually reacting with minerals and aggregate fragments in the cement paste. The fluid may leach aluminium from hydrogarnet in the cement paste and sulphur from sulphur bearing phases, such as gypsum. It possibly plays a role in the minor oxidation of pyrite and pyrrhotine in doleritic aggregate fragmnets. Thus the fluid becomes enriched in dissolved sulphur species. Calcium will aslo be leached from the tobermorite-type

minerals present and calcium enrichment will occur as portlandite, concentrated around aggregate fragments, is taken into solution.

The pH of of the fluid passing through the micro-porous system is unlike the carbonate depositing fluids, in the sense that it probably has a fixed pH of around 12. At such a pH the dominant species are Ca^{2+}, Al^{3+}, SO_4^{2-} and (OH^-) (aq) (Pourbaix, 1974).

Within the micropores in the cement paste the capillary forces pulling the fluid through the minute tubercles ensure that the fluid is under a slight pressure. It is possible that as the fluid passes through the micropores it flows into the spherical cavities in the cement paste. As the fluid emerges into the spherical cavities from the micro-porous system ettringite nucleates and grows. With time, as fluid flows towards and through the spherical cavities, the whisker-like grains of ettringite are propagated. It is feasible that once ettringite has nucleated in a cavity, diffusion will take place. Calcium, aluminium and sulphate ions could migrate through the micropores in the cement paste towards an ettringite growth point. Some ions diffuse into the cavity, and other ions diffuse out of the cavity and eventually out of the underside of the bridge deck in solution.

To confirm the proposed mechanism, an attempt was made to compare the $\partial^{34}S$ isotope value of gypsum added to unhydrated cement powder, the pyrtite, pyrrhotine and the ettringite. Unfortunately a suitable amount of ettringite could not be collected to allow for a reliable sulphur isotope analysis. With the only other possible sources of sulphate being acid rain or environmental input such as groundwaters, it is possible to

attribute the major sulphate input as being internally discharged to the system by percolating waters leaching sulphur bearing phases in from the cement paste. A very loose estimate of voids in the cement paste, based on optical examination and estimation, suggests a value of 9%, if all these voids were originally filled with ettringite then gypsum leaching could theoretically have supplied the necessary sulphate. A minor contribution may be made by the oxidation of iron sulphides. Microscopic observation of the pyrite and pyrrhotine in dolerite fragments tends also to suggest that minor oxidation has taken place.

The presence of gypsum crystals amongst the ettringite needles suggests that the system may be running out of aluminium or that the aluminium content of the fluid varies. The lack of aluminium discourages the deposition of ettringite, and gypsum grows. A lack of hydrogarnet, the aluminium bearing mineral found in cement paste, has been confirmed by X-ray diffraction.

Thus, by studying this concrete core, it has been proved that stable isotope analyses coupled with mineralogy can contribute significantly to understanding the deterioration of a concrete structure. The intricate relationships between the mineral depositional systems and the chemical corrosion of the concrete can be more readily explained by a combination of geochemistry and mineralogy.

3.10 Acknowledgements

This research forms part of a Ph.D. project funded by the SERC. Strathclyde Region Roads Department are thanked for providing the core sample. The Isotope Geology Unit at SURRC is suported by NERC and the Scottish Universities; the staff are thanked for their assistance. This paper has been improved greatly following discussions with Dr. W. J. French.

3.11 References Cited

ASTM. (1988) Recommended Practice for Petrographic Examination of Hardened Concrete, ASTM Standard Practice Report C 856-88, ASTM Philadelphia USA.

Charola, A. E., Lewin, S. Z. (1979) Scanning Electron Microscopy, 1, 379-386.

Diamond, S. (1976) Cement paste microstructure-an overview at several levels, Proc, Conf Hydraulic Cement Pastes, Their Structures and Properties, University of Sheffield, 2-30.

Glasser, F. P. (1986) Fortschritte der Mineralogie, 64, 19-35.

Komarneni, S., Guggenheim, S. (1988) Mineralogical Magazine, 52 (3), 371-375.

Lea, F.M. (1970) The Chemistry of Cement and Concrete, Edward Arnold Ltd.

McCrea, J. M. (1950) Journal of Chemical Physics, 18, 849-857.

Merlino, S. (1988a) Mineralogical Magazine, 52 (2), 247-255.

Merlino, S. (1988b) Mineralogical Magazine, 52 (3), 377-387.

Minoru, H. (1986) Neutralisation of concrete and corrosion of reinforcing steel, Proc. 5th Int Symp, The Chemistry of Concrete, Part 3, Tokyo, The Cement Association of Japan.

Neville, A. M., Brooks, J. J. (1987) Concrete Technology, Longman Scientific and Technical U.K..

O'Neil, J. R., Barnes, I. (1971) Geochimica et Cosmochimica Acta, Vol 35, 687-697.

Pourbaix, M. (1974) Atlas of electrochemical equilibria in aqueous solutions, Pergammon Press.

Powers, T. C., Hammersley, G. P. (1978) Concrete, 12 (8), 27-31.

Ramachandran, V. S., Feldman, R. F., Beaudoin, J. J. (1981) Concrete Science, Heyden.

Smith, B., Whalley, B., Fassina, F. (1988) New Scientist, 2nd June, 49-53.

Shayan, A. (1988) Cement and Concrete Research, 18 (5), 723-730.

3.12 Figure Captions

Fig. 1 A schematic diagram to display the proposed environmental and chemical system that has deposited the calcite and ettringite, causing the concrete deterioration.

Fig. 2 Transmitted light photomicrograph (ppl) of cement paste, showing a spherical cavity filled with ettringite. Note also the fracture passing through the paste. Scale bar = 800 μm.

Fig. 3 A transmitted light photomicrograph (ppl) showing more detail of one of the spherical cavities. Note the ettringite whiskers nucleating on the side of the cavity. Scale bar = 600 μm.

Fig. 4 A reflected light photomicrograph showing a large pyrrhotine grain in an aggregate. Scale bar = 1,250 μm.

Fig. 5 Transmitted light photomicrograph (ppl) showing iron staining around feldspar grains, and in fractures in the grains in a dolerite aggregate due to iron sulphide oxidation. Scale bar = 500 μm.

Fig. 6 Scanning electron photomicrograph of a spherical mass of ettringite. Note the gypsum crystals (gy) and the chlorine rich phase (cl) nestling in the ettringite whiskers.

Fig. 7 Plot of temperature against $\partial^{18}O$ SMOW, the calcite-water equilibrium curve has been plotted to allow equilibrium formation temperatures to be noted. The more realistic formation temperature of 20°C has been marked for reference.

Table 1. Isotope analyses and calculated formation temperatures.

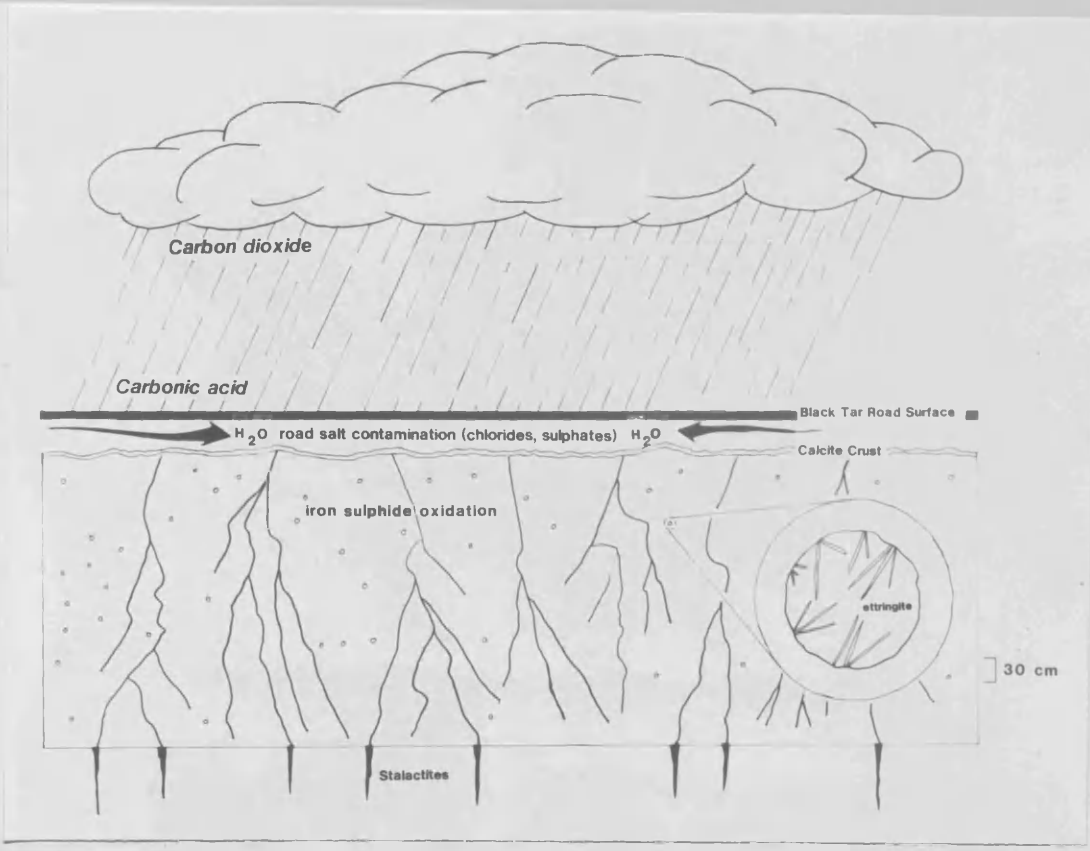

Figure 1.

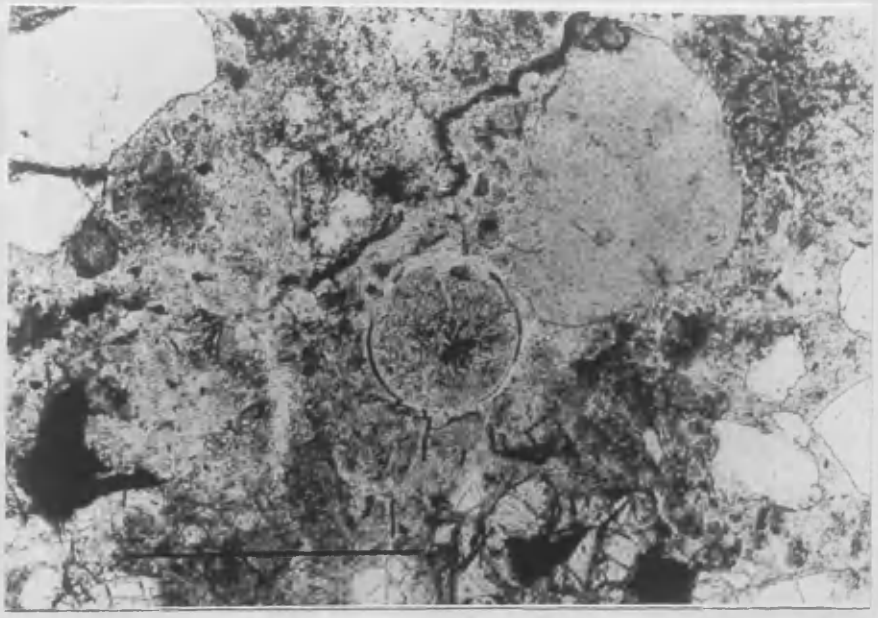

Figure 2.

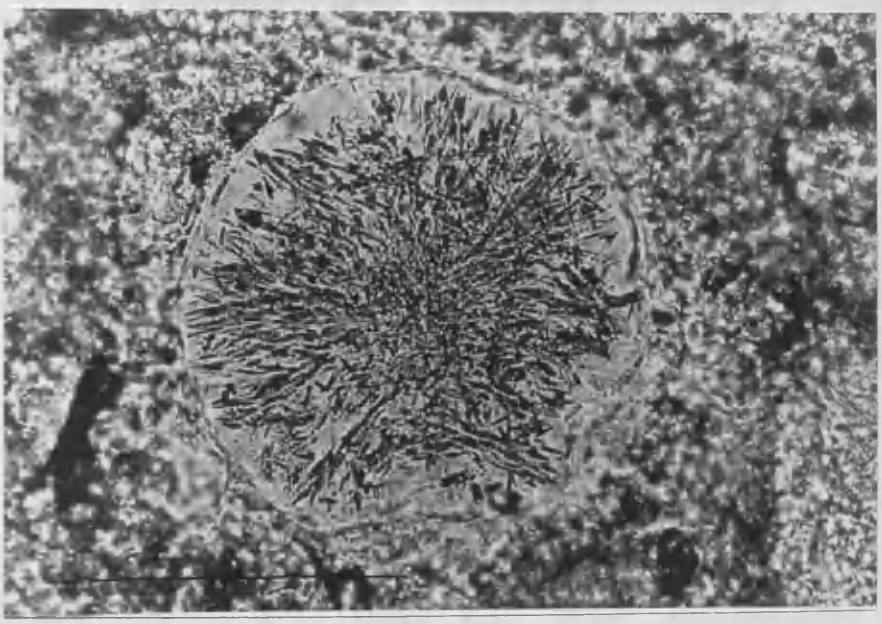

Figure 3.

Figure 4.

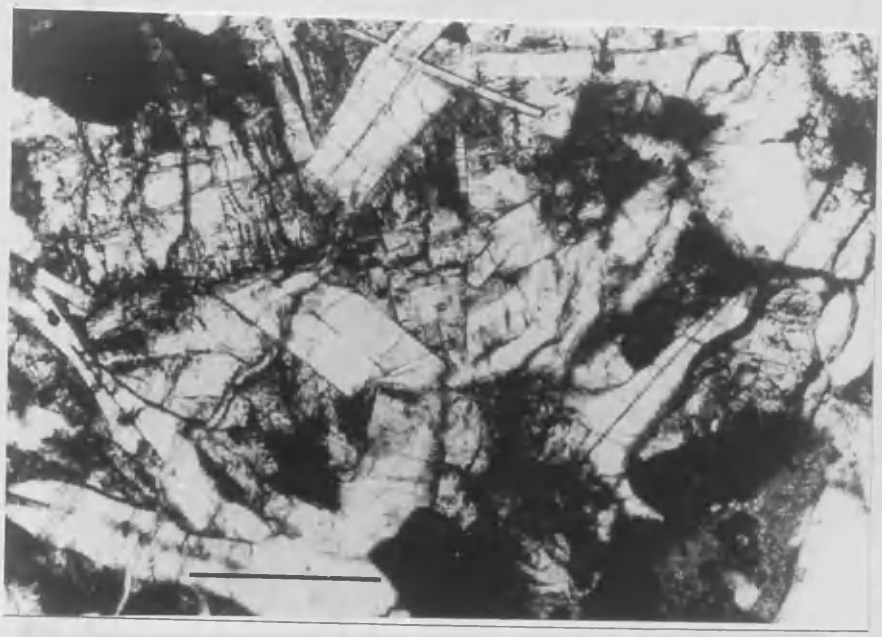

Figure 5.

Figure 6.

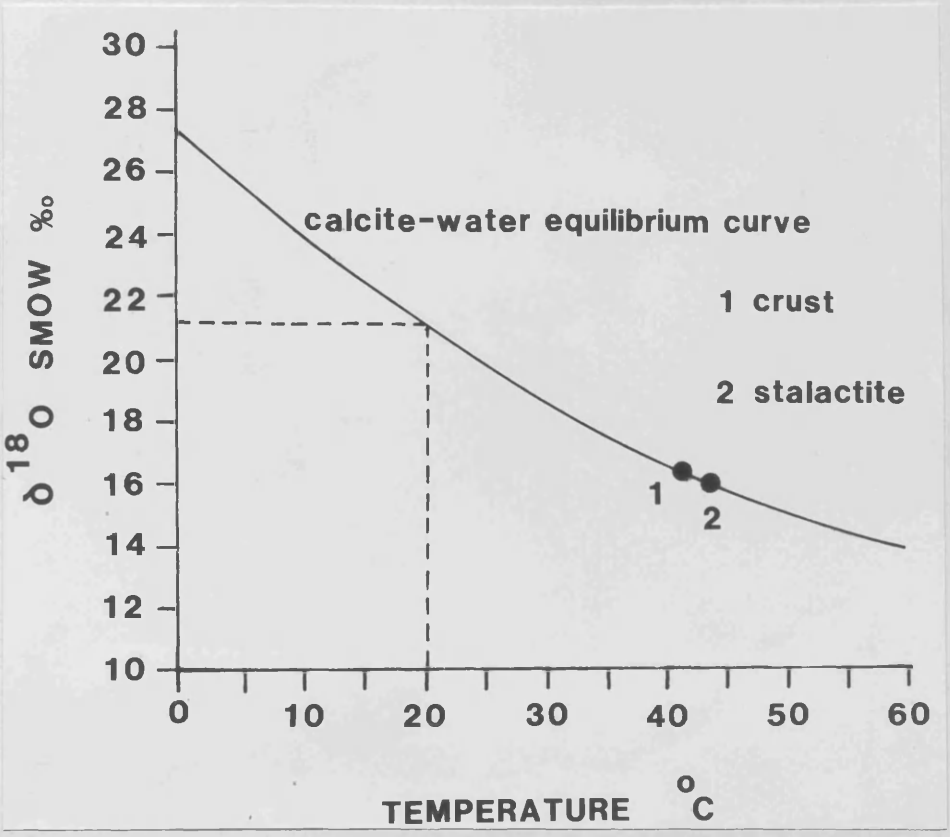
30
28
26
24
22
20
18
16
14
12
10
δ18O SMOW ‰
calcite-water equilibrium curve
1 crust
2 stalactite
1
2
0
10
20
30
40
50
60
TEMPERATURE °C

Figure 7.

Table 1.

SAMPLE	$\partial^{13}C$ PDB ‰	$\partial^{18}O$ SMOW ‰	FORMATION TEMP.
crust	-18.5‰	+16.6‰	45°C
stalactite	-19.2‰	+16.4‰	46°C

Chapter 4

Introduction and background

Chapter 4 (paper 3), is in the form of a short communication accepted for publication in the Journal of Mineralogy and Petrology. It is concerned with a study of the whisker crystal habit of the supergene mineral ettringite found growing in spherical cavities in the core of concrete studied in Chapter 3. The whisker growth is attributed to heterogenous nucleation on the negatively charged cavity walls, a screw dislocation in the crystal and the concentration of the elements required for growth being present in the solution at low enough concentrations to disqualify multi-directional crystal growth.

The whisker crystal habit of the supergene ettringite found in the concrete studied in Chapter 3 merited further investigation. The previous study of the ettringite indicated that the XRD profile of the whiskers was almost identical to that of the published JCPDS data for ettringite. However, I felt that due to the extraordinary whisker habit of the supergene concrete-hosted ettringite, I should investigate the unit cell dimensions of the whiskers to determine any differences with those published for naturally occurring ettringite. Some natural ettringite from the N'Chwanning mine, South Africa, was obtained from a dealer to allow a control study to be carried out. Unfortunately it proved extremely difficult to obtain X-ray powder photographs (Debye-Scherrer camera), of either the whiskers or natural ettringite. On each film the back reflections were of a poor quality, and unit cell dimension calculations could not be made. The exposure time and

type of film used in the camera were varied but a quality result could not be achieved. Some of the ettringite samples were sent to the Natural History museum in London; the crystallography unit at the museum could not obtain back reflections either. To obtain back reflections would have taken a great deal of time and effort on behalf of the museum staff and I felt the data did not justify the effort.

Similarily I had hoped to analyse the whiskers for a $\partial^{34}S$ value. Unfortunately, I could not collect a large enough quantity of the whiskers as to allow for a reliable $\partial^{34}S$ analysis.

I then endeavoured to explain the whisker habit of the concrete hosted ettringite by carrying out oil immersion microscopical studies of the whiskers, SEM studies of the whiskers and by carrying out a literature review on the phenomenon of whisker crystal habit. The results of these studies are combined in the following short communication. The fact that whisker growth is thought to occur most frequently in solution gave validity to my theory that fluid had percolated through the structure causing the concrete alteration. I was senior author and Dr. Hall assisted in the research and preparation of the paper.

4. Whisker crystals of the mineral ettringite.

(As published)

G. MACLEOD

AND

A. J. HALL

Department of Geology & Applied Geology, University of Glasgow, Glasgow, G12 8QQ.

With 5 Figures.

4.1 Communication

The mineral ettringite has been encountered growing in spherical cavities in the cement paste of a concrete road bridge located in the Midland Valley of Scotland. The bridge is known to have undergone alteration by percolating fluids. The spherical cavities are apparently relics of air bubbles that have been trapped in the cement paste. The diameter of the cavities varies from <1mm to 6mm. Throughout the cement paste the cavities are filled with masses of colourless acicular crystals, the crystals apparently having nucleated on the sides of the cavities (Fig. 1). Observation of the spheres by scanning electron microscopy revealed them as being composed of growths of filamental whiskers of ettringite (Fig. 2), and as such merited reporting. It is of importance as this habit is rare and it may be possible that natural ettringite may be encountered with such a habit. It may

also be possible that other members of the ettringite group and in particular thaumasite may also take up the whisker-like form. Minerals outwith the ettringite series have also been reported as having a whisker habit. Epsomite was reported in Dana's Textbook of Mineralogy (Ford, 1932), as efflorescent growths composed of fragile fibres. These growths were found in mine galleries at several locations in Europe and the United States. Halotrichite and alunogen have also been reported as existing as efflorescent masses of hair-like crystals, and were described as 'hair salt' in Dana's System of Mineralogy (Palache *et al.,* 1951). The proposed formation mechanism of the ettringite whiskers is discussed at the end of the communication.

Some of the whiskers were picked out and subjected to oil immersion microscopy and powder X-ray diffractometry. The optical properties of the ettringite whiskers are listed in Table 1, along with the published optical properties for naturally occurring ettringite (Phillips and Griffen, 1981). The refractive indices of the whiskers are different from published values for natural ettringite. Analysis of the whiskers did not indicate the presence of substituted cations, and we suggest that water molecules and hydroxyl ions are in different bond positions than those determined by Moore and Taylor, 1970; the crystal structure of ettringite is such that it is possible to consider slight variations in the positions of the hydrous units. Powder X-ray diffraction studies of the whiskers yielded d-spacings that were almost identical to those of ettringite JCPDS card 9 - 414. As may be expected because of preferred orientation effects, the

peak intensities of the diffraction pattern differed from the published data. In particular the 110 peak was enhanced.

Ettringite $Ca_6Al_2(SO_4)_3(OH)_{12}.26H_2O$ is the most common member of the ettringite group that occurs naturally, and was reported as early as 1874 by Lehmann. The paper reported prismatic ettringite growing in cavities in metamorphosed limestone fragments in a leucite-nepheline-tephrite. The group consists of the commoner member minerals ettringite and thaumasite $Ca_6Si_2(SO_4)_2(CO_3)_2(OH)_{12}.24H_2O$, and the less common minerals bentorite $Ca_6(Cr,Al)_2(SO_4)_3(OH)_{12}.26H_2O$, sturmanite $Ca_6(Fe^{3+}Al)_2(SO_4)_2(B(OH)_4)(OH)_{12}.26H_2O$, charlesite $Ca_6(Al,Si)_2(SO_4)_2(B(OH)_4)(OH)_{12}.26H_2O$, and jouravskite $Ca_6Mn_2(SO_4)_2(CO_3)_2(OH)_{12}.24H_2O$ (Dunn *et al.,* 1983).

The study (Dunn *et al.,* 1983) greatly clarified the situation by relating the various members of the ettringite group. Most of the members of the group have been encountered at various levels in the Crestmore Quarry California and Franklin New Jersey (Murdoch and Chalmers, 1958; Hurlbut and Baum, 1960), sturmanite in South Africa (Peacor *et al.,* 1983), ettringite at Scawt Hill Northern Ireland (Moore and Taylor, 1970) and charlesite from Franklin New Jersey (Dunn *et al.,* 1983). Thaumasite has also been reported at Brenk in East Germany (Kollmann and Strubel, 1981). The present authors have been unable to obtain any samples of natural ettringite found at the type locality at Ettringen, the Rheinland Germany. The British Museum (Natural History) has specimens; however it appears they have reacted with the atmosphere and been altered. One important fact that should be noted is that ettringite

has been found growing in conjunction with calcite ($CaCO_3$), afwillite ($3CaO.SiO_2.H_2O$), xonotlite ($Ca_6Si_6O_{16}(OH)_4$) and datolite ($CaB(SiO_4)(OH)$). At Scawt Hill Northern Ireland ettringite is found in conjunction with portlandite ($Ca(OH)_2$), afwillite and hydrocalumite (Moore and Taylor, 1970). Afwillite and xonotlite are naturally occuring minerals that are similar to the so called C-S-H gel minerals that are the major components of cement paste (Neville and Brooks, 1987), and portlandite is also a major constituent of cement paste. Thus it is not surprising that when sulphate charged waters flow through concrete, ettringite is formed in any available cavity. Ettringite is present in cement paste as soon as it is formed as a hydration product (Lea, 1970), and this may act as a nucleus for the growth of harmful ettringite. What is surprising about this ettringite occurrence is the whisker habit of the mineral. Ettringite is a member of the hexagonal crystal system having a prismatic crystal habit that occasionally has been described as elongate.

As water flows through the structure it has become rich in aluminium and calcium by interacting with the cement paste and leaching out the ions. Sulphate is provided by the leaching of sulphur species from components in the cement paste, and possibly a minor contribution is made by the oxidation of iron sulphides within aggregate fragments. The chemical reactions involved in the degradation of concrete are complex (Neville and Brooks, 1987). As the charged water flows through the cement paste it permeates into the abundant spherical cavities and ettringite nucleates. As the whiskers of ettringite grow the side

faces parallel to the c-axis act as low energy planes. Ions come out of solution and are pulled to the side of the crystal where they cannot be combined in the crystal as there is no defect in the lattice. It is probable that the only defect in the lattice is found at the tip of the whisker where a screw dislocation is present (Pamplin, 1975). Providing the supersaturation of the solution is low enough, two-way nucleation cannot take place and ions have to diffuse up the side of the whisker to the top where they are incorporated at the screw tip. Thus the filamental whisker crystals are produced (Pamplin, 1975). A scanning electron photomicrograph (Fig 3), of some ettringite whiskers beginning to nucleate in a cavity shows the perfect side faces of the whiskers and the tapered tip which may be the growth point of the crystal, and suggests that the ettringite whiskers are growing in a manner typical of whisker crystal propagation (Pamplin, 1975).

4.2 ACKNOWLEDGEMENTS

The authors wish to acknowledge the Science and Engineering Research Council of Great Britain who funded the project. Strathclyde Regional Roads Department are thanked for providing the core sample.

Authors' address: G. Macleod and Dr. A. J. Hall, Department of Geology & Applied Geology, University of Glasgow, Lilybank Gardens, Glasgow, G12 8QQ, Scotland, United Kingdom.

4.3 REFERENCES CITED

Dunn, P. J. Peacor, D. R., Leavens, P. B., and Baum J. L. (1983) Charlesite, a new mineral of the ettringite group, from Franklin, New Jersey. Amer Mineral 68:1033-1037.

Ford, W. E. (Ed)(1932) Dana's Textbook of Mineralogy. John Wiley & Sons, Boston, 851pp.

Hurlbut, C. S., Jnr., and Baum, J. L. (1960) Ettringite from Franklin, New Jersey. Amer Mineral 45: 1137-1143.

Kollmann, Von H., and Strubel, G. (1981) Ettringite-thaumasite mixed crystals of Brenk. Chem Erde 40: 110-120.

Lea, F. M. (1970) The Chemistry of Cement and Concrete. Edward Arnold Ltd, London, 727pp.

Lehmann, J., (1874) Uber den Ettringit, ein neues Mineral in Kalkeinschlussen der lava von ettringen. N.Jb. Miner. Abh. 6: 273-275.

Moore, A. E., and Taylor, H. F. W. (1970) Crystal structure of ettringite. Acta Crystallogr B26: 386-393.

Murdoch, J., and Chalmers, R. A. (1958) Woodfordite, a new mineral from Crestmore, California. Bull. of Geol. Soc. of Am. 69: 1620-1621.

Neville, A. M., and Brooks, J. J. (1987) Concrete Technology. Longman, Essex, England, 438 pp.

Palache, C., Berman, H., and Frendel, C.(Eds)(1951) Dana's System of Mineralogy (7th Edtn.,Vol. II). John Wiley & Sons, United States of America, 1124pp.

Pamplin, B. R. (1975) Crystal Growth. Pergammon, New York, 672 pp.

Peacor, D. R., Dunn, P. J., and Duggan, M. (1983) Sturmanite, a ferric iron, boron analogue of ettringite. Can MIneralogist 21: 705-709.

Phillips, W.R., and Griffen, D.T. (1981) The Nonopaque Minerals. Freeman and Company, San Francisco, 677pp.

4.4 Figure captions

Fig. 1. A transmitted light photomicrograph (ppl) showing one of the spherical cavities. Note the ettringite whiskers nucleating on the side of the cavity. Scale bar = 600 microns.

Fig. 2. A scanning electron photomicrograph of a spherical mass of filamental whiskers of ettringite.

Fig. 3. A scanning electron photomicrograph of a spherical cavity with ettringite whiskers at an early stage in growth. Note the ends of the whiskers tapering to a point.

Table. 1. Optical properties of ettringite whiskers and natural ettringite, determined in white light.

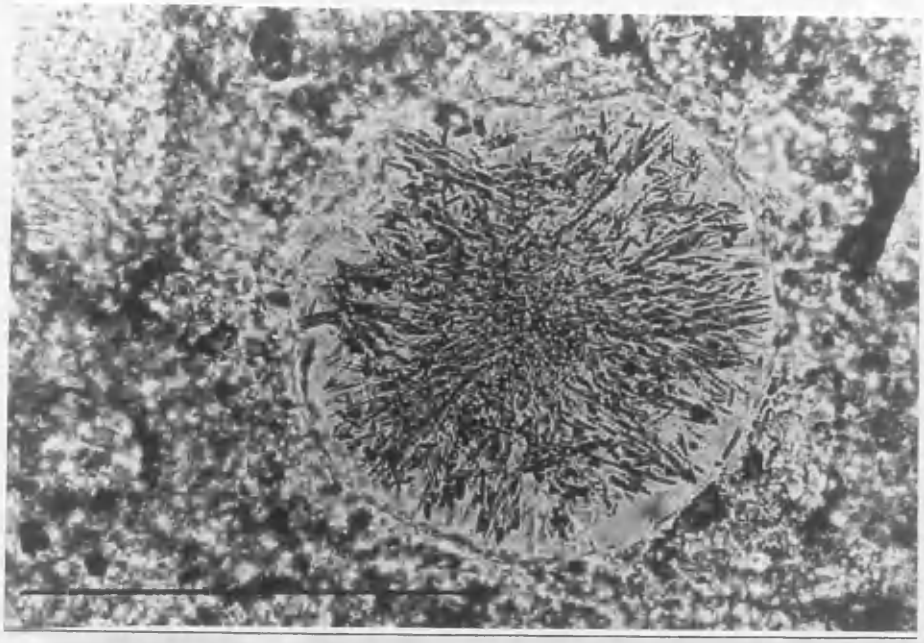

Figure. 1.

Figure. 2.

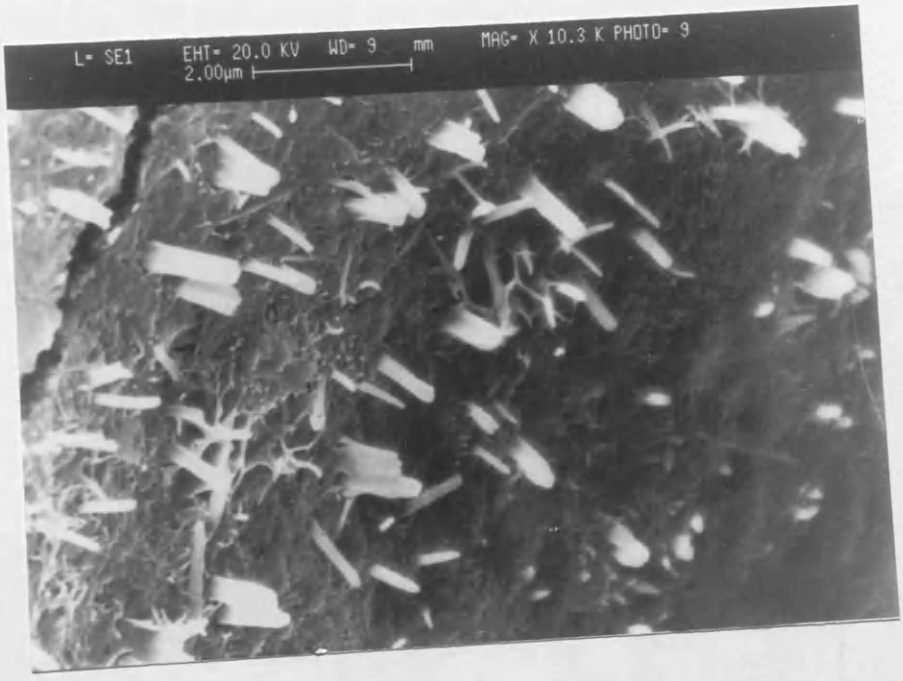

Figure. 3.

Table 1.

sample	n_w	n_e	optical sign	$n_w - n_e$
whiskers	1.468 ± 0.001	1.464 ± 0.01	uniaxial(-ve) length fast	0.004
natural ettringite	1.491	1.470	uniaxial(-ve) length fast	0.021

Chapter 5

Introduction and background

Chapter 5 (paper 4), is composed of an isotopic investigation of calcitic crusts and stalactites found growing on concrete structures in the Midland Valley of Scotland. Carbon and oxygen stable isotope ratios are used to determine the source and mechanism of carbonate mineral growth on concrete structures. The mechanisms are complex and previously not positively linked with concrete decay. The predominant reaction is the reaction of hyper-alkaline water with atmospheric carbon dioxide to produce calcite. This paper has been submitted to Isotope Geoscience for consideration for publication.

As previously discussed in Chapter 3, I felt that carbon and oxygen stable isotope analyses could be applied to carbonate mineral growth on concrete structures, and be used to more clearly define the mechanism. Previous to this research the mechanisms of carbonate crust (efflorescence) and stalactite growth on concrete structures was thought to be linked to the migration of moisture through the concrete transporting calcium hydroxide to the external surface of the structure.

Carbonate growth within and on the surface of concrete structures has been studied for many years. The research has allowed three different types of carbonation mechanisms of concrete to be defined (French, W.J., pers. comm.). The most common type of carbonation of concrete is the permeation of carbon dioxide into the concrete and the conversion of the paste phases into calcite. This reaction occurs in both structures open to the elements and interiors of buildings. Inside buildings the moderate

to low humidity accelerates the process. As the carbon dioxide permeates into the structure the pH of the system drops, portlandite and calcium silicates are taken into solution to restore a high pH. When the carbonation is complete then the concrete pH will be permanently changed from 12 to around 8.5 (Gray, 1983). The reaction progresses further into the structure. The rate of this type of carbonation can be related to the porosity of the structure, the relative humidity and the partial pressure of carbon dioxide (Grey, 1983).

The second effect of CO_2 on concrete is the corrosive effect produced by carbonic acid solutions. Many workers investigating this type of deterioration have produced indexes that can be used to determine whether a carbonic acid solution will corrode the structure or deposit calcite. A detailed survey of these indexes was carried out by Curtis, in 1984. The most common of these indexes is the Langelier Index (Rossun and Merrill, 1983). The index calculates the saturation of the fluid with respect to carbonate, taking into account simple speciation and pH. If the solution is undersaturated with respect to carbonate it is thought to be corrosive to concrete, if the solution is oversaturated with respect to carbonate the fluid will deposit calcite on the concrete. A detailed study of this type of alteration can be found in ASTM-STP691.

The third role of carbon dioxide, is that it reacts with efflorescent growths to produce surface crusts and stalactites. A short description of these types of growths can be found in the Cement and Concrete Association pamphlet, Appearance Matters No. 4 (Higgins, 1982). The mechanism of growth for efflorescence and

blooms has been related to the movement of moisture through the structure leaching portlandite and exuding it on the surface of the structure. Usually in the form of calcite. The following paper attempted to define and elucidate the mechanism of efflorescence growth by the use of carbon and oxygen stable isotopes.

The method used to analyse the calcites for their isotopic values was the phosphoric acid method (McCrea, 1950). The calcites were first plasma-ashed to remove any organic contaminants. The calcite was then assessed for purity and an amount weighed out dependent on this purity to allow a satisfactory yield of carbon dioxide. The sample is then placed in a reaction bottle and sealed. The bottle is turned on its side and a measured amount of 1 molar phosphoric acid in an attached finger pours on to the sample. The bottle is then attached to a vacuum line and the carbon dioxide produced by the reaction is pumped along the line. During this process the carbon dioxide is frozen in a "cold finger" to remove impurities. The clean carbon dioxide gas is then collected and analysed in a mass spectrometer for carbon and oxygen stable isotope values. The reproducability of the results is thought to be 0.1 per mill.

For the initial isotopic study of the carbonates from the structure investigated in Chapter 3, we drew a parallel with travertines formed in hyper-alkaline freshwaters. In order to verify this, a sequence of experiments was carried out. The first set of experiments involved the passing of carbon dioxide gas through three plastic containers. The first contained a cement block submerged below distilled water, the second a cement block only

and the third had a cement block suspended above water (Fig. 5a). Carbon dioxide was bubbled through the water in two of the containers, and passed through the other container. A similar suite of experiments was carried out using the same apparatus and crystals of $Ca(OH)_2$ (Fig. 5b). The calcite that formed on the cement blocks and $Ca(OH)_2$, was analysed for carbon and oxygen stable isotope values. The $\partial^{13}C$ and $\partial^{18}O$ value of the experimental gas was known, and the fractionation between the gas and the samples, was considerably different than that between the concrete hosted calcites and atmospheric carbon dioxide. Further consideration of the basis of these experiments led us to assume that they were not mimicking the natural concrete growth system.

Consideration of the mineralogical aspects of concrete decay led me to believe that water percolating through the structures was a major component in the decay of concrete. As this water interacted with the concrete it became hyper-alkaline. Thus we decided, that to isotopically model the carbonate mineral growth system in concrete systems, we had to expose similar hyper-alkaline solutions to carbon dioxide atmospheres. A series of experiments was carried out where $Ca(OH)_2$ rich solutions at varying pH values, were exposed to carbon dioxide atmospheres in sealed units in the laboratory. The calcitic scums formed were analysed for $\partial^{13}C$ and $\partial^{18}O$ values. Although the experiments proved to be indecisive on their own, when they were coupled with isotope analyses of numerous calcitic growths from concrete structures in the Midland Valley of Scotland, new detailed mechanisms for their growth could be produced. The following paper is the description of this study

and its results. I was senior author of the paper. Dr. Fallick and Dr. Hall contributed greatly to its production, in particular Dr. Fallick contributed greatly to the interpretation of the isotope results and our understanding of this new field of stable isotope geochemistry.

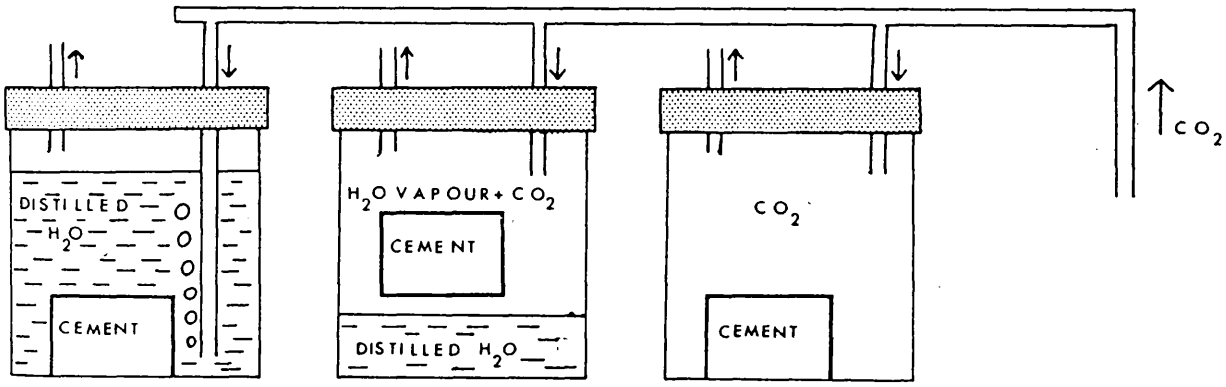

Figure 5a.

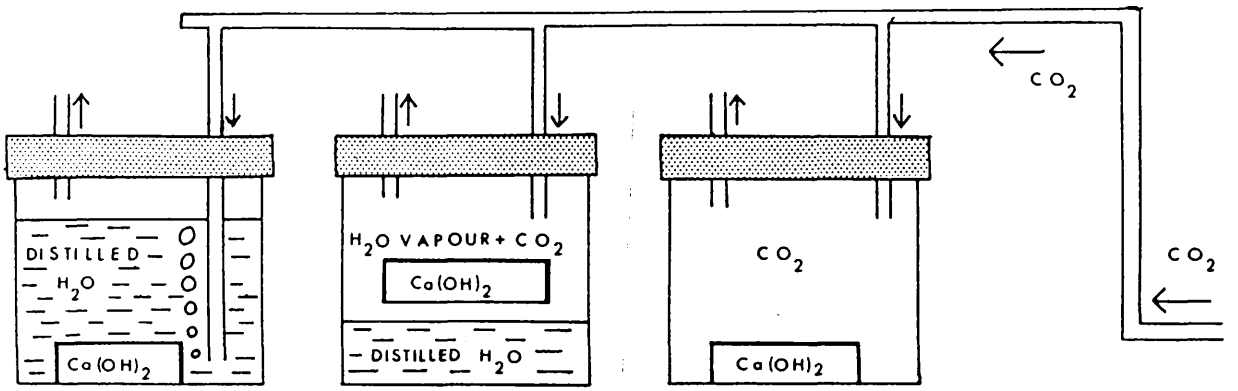

Figure 5b.

References

ASTM- STP691 Durability of building materials and components, Proceedings 1st International Conference, (Sereda and Litvan, 1980 Eds.).

Curtis, P. (1987) M. Sc Thesis, Queen Mary College, Dept. of Geomaterials.

Gray, M. J. (1983) Personal Communication.

Higgins, D. D. (1982) (Ed.) Efflorescence on concrete, Cement and Concrete Association , Appearance Matters No. 4.

McCrea, J. M. (1950) J. Chem. Phys (18), pp 849-857.

Rossun, J. R., Merrill, D. T. (1983) An evaluation of the calcium carbonate saturation indexes, Research and Technology Journal, AWWA, Feb 1983, pp 95-100..

5. The mechanism of carbonate mineral growth on concrete structures, as elucidated by carbon and oxygen isotope analyses.

(Draft of May 1990)

G. Macleod, A. E. Fallick* & A. J. Hall

Department of Geology and Applied Geology, Lilybank Gardens, University of Glasgow, Glasgow G12 8QQ, UK.

* Scottish Universities Research and Reactor Centre, East Kilbride, Glasgow G75 OQU, UK.

5.1 Abstract

Carbonate mineral growths on concrete structures are endemic throughout the world. The growths take the form of calcitic crusts and stalactites, the formation mechanism for which has not been clearly defined. We have applied carbon and oxygen isotope analyses to calcites collected from structures in the Midland Valley of Scotland. Carbonate $\partial^{13}C$ PDB values are in the range of -18.8‰ to -28.9‰ with $\partial^{18}O$ SMOW in the range of +8.5‰ to +16.5‰. These results indicate that the calcites are produced by the interaction of atmospheric carbon dioxide ($\partial^{13}C = -7$‰ PDB, $\partial^{18}O = +41$‰ SMOW) with hyper-alkaline water, in an isotopically open system. The water attains a high pH as it percolates through and interacts with the concrete, dissolving portlandite. Atmospheric carbon dioxide is fixed almost instantaneously

as calcite in the water. This reaction is more detailed than the mechanisms previously proposed. A large kinetic carbon isotope fractionation of -10‰ occurs as carbon dioxide molecules cross the gas to liquid interface. The final $\partial^{13}C$ value of the calcites produced on the surface of the concrete is also fractionated by another kinetic fractionation mechanism that may be pH controlled.

5.2 Carbonate growths

The British Department of Transport estimate that £101 million pounds will be required to repair concrete bridges in England in 1990/91 (Montague, 1989). One of the causes of concrete decay is carbonate mineral growth. Water flowing across and through concrete structures can cause both sulphate and carbonate mineral growth within and on the surface of the structures (Macleod *et al.*, 1990, Pye and Schiavon, 1989). The pH values of the pore waters of concrete are thought to be in the range 12-14 (Glasser, 1986), and the water flowing through and in prolonged contact with the external surface of the structures will also have pH values in this range. The high pH of the solutions is mainly caused by the amount of dissolved portlandite ($Ca(OH)_2$) which is a major component of the cement paste within concrete (Lea, 1970).

The concrete-hosted calcites sampled consist of crusts found growing on the top of bridge decks below the tar layer, and stalactites

found growing on the underside of major road and rail bridges in the Midland Valley of Scotland. The stalactites emerge immediately from the concrete itself, and from the mortar-bonds that seal the joints between concrete blocks.

Calcitic crusts have formed by the flowing of water across the top of the bridge decks below the tar layer (Macleod *et al.*, 1990). The surface of concrete is coated with portlandite crystals (Lea, 1970), some of which have been taken into solution. The fluid has then reacted with carbon dioxide and, with time, a calcite crust is deposited. It has previously been acknowledged that one of the carbonate growth mechanisms in concrete, consisted of a straight reaction between solid portlandite and paste components with diffusing carbon dioxide producing calcite (Eqn. 1)(Lea 1970). We wished to carry out a more detailed investigation on the surface carbonation of concrete, that produces efflorescence and "lime blooms".

Eqn. 1. $Ca(OH)_2\ (s) + CO_2\ (g) \longrightarrow CaCO_3\ (s) + H_2O\ (l)$

Stalactites found growing on the underside of concrete structures are probably formed by the formation of the outer shell first, and this shell is gradually infilled with successive calcite coatings (Fig. 1). Finally the central cavity is filled with fine grained calcite crystals (Fig. 2). The reactions are listed below (Eqns. 2,3,4).

Eqn. 2. $CO_2\ (g) + OH^-\ (aq) \longrightarrow HCO_3^-\ (aq)$

Eqn. 3. HCO_3^- (aq) $\longrightarrow$ CO_3^{2-} (aq) + H^+ (aq)

Eqn. 4. Ca^{2+} (aq) + CO_3^{2-} (aq) $\longrightarrow$ $CaCO_3$ (s)

The stalactites form in a manner different from that of speleothem stalactites formed in cave deposits (Hendy, 1971)(Eqn. 5).

Eqn. 5. Ca^{2+} (aq) + $2HCO_3^-$ (aq) $\longrightarrow$ $CaCO_3$ (s) + H_2O (l) + CO_2 (g)

5.3 Isotope analyses

A total of fifteen calcitic growths from concrete structures were analysed for $\partial^{13}C$ PDB and $\partial^{18}O$ SMOW values by the phosphoric acid method (McCrea, 1950). The assumption is made that the carbonate within the calcites is contributed to only by atmospheric carbon dioxide and not the small amount of particulate organic carbon in rainwater (Thurman, 1985). Thirteen of the samples analysed were stalactites, five of which had both the outer shell and the fine grained infilling material present. The other two specimens consisted of calcitic crusts that had grown on bridge decks below the tar road surface. The results of the analyses are listed in Table 1, along with the calculated formation temperature for the calcites, assuming equilibrium precipitation from a fluid of $\partial^{18}O$ SMOW = -8‰ (average value for local meteoric water). It is readily apparent that these temperatures

are unreasonably high, so that the assumption of equilibrium precipitation lacks validity.

The analyses of the calcite growths are plotted on a graph of $\partial^{18}O$ against $\partial^{13}C$ in Fig. 3. There is no apparent trend to the results. However, considering the five stalactites with both outer shell and inner pipe filling material analysed, it can be noted that the outer shell analyses for the stalactites have lower $\partial^{13}C$ values than the fine grained crystalline material from the interior pipe of the stalactite. This systematic difference in $\partial^{13}C$ values is not reflected in the $\partial^{18}O$ values of the samples.

To advance interpretation of the isotope results a comparison with a similar geological formation of calcites can be made. Freshwater travertines produced by the interaction of carbon dioxide with hyper-alkaline waters are geochemically comparable to the calcites produced in the concrete environment. The formation of calcites in alkaline freshwater solutions involves a kinetic carbon isotope fractionation between calcite and carbon dioxide involved in the reaction. By considering a kinetic process with an inverse square root of mass dependence, the fractionation has been calculated as being in the range of at least -10‰ to -11.3‰ (Turner,1982, Létolle *et al.*, 1988). The fractionation is essentially a diffusion velocity controlled process, and occurs as the carbon dioxide molecules cross the gas to liquid interface.

Assuming that the $\partial^{13}C$ value of atmospheric carbon dioxide to be on average -7‰ PDB (Bottinga and Craig, 1969), we would expect the

calcitic material formed on the surface of concrete to have $\partial^{13}C$ values in the range of -17‰ PDB to -18.3‰ PDB. However, all the calcites plot outside this minimum fractionation range (see Fig. 3), and have undergone a more severe fractionation than predicted by this simple model.

The oxygen isotope data for the calcite growths are more difficult to interpret. The calculated formation temperatures of the calcites using the $\partial^{18}O$ values are very high for atmospheric values (Table 1), and imply that the $\partial^{18}O$ values have been produced under non equilibrium conditions. In the case of freshwater travertines formed in alkaline solutions, it was suggested that the $\partial^{18}O$ value of the calcite is derived by a contribution of one third from the formation water and two-thirds from the carbon dioxide involved in the reaction (O'Neil and Barnes, 1971). The oxygen isotope values of the formation waters of the calcitic growths could not be measured to give an exact figure but we can assume that meteoric water is the main fluid involved in the calcite growth, and that it has a $\partial^{18}O$ value of around -8‰. Also, atmospheric carbon dioxide has a $\partial^{18}O$ value of +41‰ (Bottinga and Craig, 1969). On this model the calculated $\partial^{18}O$ value for the samples is therefore +10‰. A $\partial^{18}O$ value of +21‰ was calculated for calcite produced at equilibrium with water of $\partial^{18}O$= -8‰ at 20 ^{o}C. All of the calcitic growths have $\partial^{18}O$ values between +8‰ and +17‰, suggesting that they may be re-equilibrating after or during initial precipitation. This may also explain why all but two of the inner fine grained calcitic samples from the stalactites analysed have $\partial^{18}O$ values heavier than

the outer shell of the stalactite. Thus it can be seen that the bulk of the oxygen values of the samples lie between the calculated kinetic fractionation value and the equilibrium value (Table 1). However, it is also likely that the oxygen isotope value of carbonate hosted on the concrete structures is contributed to by other oxygen bearing soluble minerals that are found in the cement pastes and the aggregates within the concretes. These minerals may be taken into solution and oxygen isotopes exchanged.

5.4 Laboratory experiments

In order to investigate the fractionation of the carbon isotopes, and to elucidate the mechanism of the calcite formation on concrete structures, a suite of experiments was carried out in the laboratory. Five solutions of $Ca(OH)_2$ in petri dishes were placed in reaction chambers that had been flooded with carbon dioxide, and were left exposed to the carbon dioxide atmospheres in the sealed environments for twenty four hours. The pH of the solutions was measured before and after they were exposed to carbon dioxide and the calcitic precipitates produced were collected and analysed for $\partial^{13}C$ and $\partial^{18}O$ (Table. 2). Due to the attainment of a saturated solution of $Ca(OH)_2$ it was only possible to obtain solutions with maximum pH values in the range 11.7 to 12.1. This problem has been encountered by other workers trying to synthesise natural travertine waters (Létolle *et al.*, 1988). The $\partial^{13}C$ value of the carbon dioxide used in the experiments was -41‰ PDB.

The predicted fractionation of the carbon isotopes giving values of at least -51‰ were not obtained, the samples produced had values in the range -41‰ to -45‰ (Table. 2). We suggest that this is due to the solutions very rapidly returning to lower pH values; different thermodynamic and kinetic fractionations take place due to the mass of the different carbonate species present. Turner (1982), has carried out detailed studies of the fractionation processes that occur in the pH range of 4.5 to 9. At low pH values (6.4 to 10.3) the bicarbonate ion is dominant (Pourbaix, 1974) and thermodynamic fractionation processes affect the $\partial^{13}C$ value of the precipitated calcite.

At pH values up to 9 there is a kinetic fractionation of the various carbonate species on precipitation as they cross the liquid to crystal interface (Turner, 1982); this is due to the relative diffusivity of the light and heavy carbonate species (CO_3^{2-} and HCO_3^-). The fractionation occurs as the carbonate species diffuse to the crystal lattice incorporation site. Also at the liquid to crystal interface a thermodynamic equilibrium fractionation occurs; this is caused by the differing rotational vibrational energies of the isotopically light and heavy carbonate species (Turner, 1982) as they are incorporated at the lattice growth point. This thermodynamic fractionation is thought to enrich the solid phase in ^{13}C, whereas the kinetic fractionation depletes the solid phase with respect to ^{13}C.

At pH values greater than 12 the ionic strength of the solution is also thought to cause a fractionation (Létolle *et al.*, 1988), and it has been suggested that ^{13}C rich carbonate ions are more likely to stay in

solution as metal-carbonate complexes, such as the magnesium carbonate complex (Thode *et al.*, 1965).

The experiments were valuable in that they showed two important facts: when solutions of high pH are reacted, the carbon isotope fractionation between calcite and gas is not as large as expected, and indeed from the very high pH solutions is almost non existent; and secondly after the solutions have reacted with the carbon dioxide their pH values are always in the region of 7. It is the strong affinity of carbon dioxide for OH^- which results in rapid reactions to produce bicarbonate and carbonate species and lowering of the solution pH. This suggests that indeed, as observed by other workers (Létolle *et al.*, 1988), it is not easy to simulate the growth of calcite in the hyper-alkaline waters as the laboratory waters cannot be instantaneously chemically re-charged to their initial high pH.

5.5 Carbon isotope diffusion model

By plotting the $\partial^{13}C$ values for the natural samples in the form of a histogram (Fig. 4), it can be seen that that there is a strong grouping around -26‰ which represents outer shell values for the stalactites. It is has already been established that when carbon dioxide molecules interact with hyper-alkaline solutions to form calcitic scums a kinetic fractionation of around -10‰ is incurred (O'Neil and Barnes, 1971, Turner, 1982, Létolle *et al.*, 1988). Assuming the $\partial^{13}C$ value of atmospheric carbon dioxide to be around -7‰ (Bottinga and Craig, 1969), we can expect a value of around -18‰ , and this is the heaviest

value found in our samples. We have a lightest value of -29‰ and groupings at around -26‰ and -24‰ , requiring further fractionations of -11‰, -8‰ and -6‰ respectively. This could, of course, be a continuum of fractionations spanning -6 to -11‰. Other workers studying $\partial^{13}C$ of freshwater carbonates have encountered $\partial^{13}C$ values in the range of -25‰ PDB (Baertschi and Schweiz, 1957) to -10‰ PDB (Craig, 1953); Craig 1954, suggested that this further kinetic fractionation could possibly be due to a secondary diffusive process. Herczeg and Fairbanks 1987, studying carbonate scums on the surface of sea water suggest that carbon dioxide molecules undergo a fractionation as the molecules diffuse through the thin calcite scums. They also suggest that pH may enhance this fractionation, and indeed previous workers suggest that pH may have chemically enhanced the fractionation process (Siegenthaler and Münnich, 1981). Herczeg and Fairbanks 1987, suggest that at a pH of 10 and with a calcite film thickness of 50 microns a fractionation of -7‰ is incurred. If we add this to the known mass dependent diffusion velocity fractionation of -11‰ previously known for carbon dioxide crossing the gas to liquid interface, and take atmospheric carbon dioxide as -7‰ PDB we obtain an expected value of -25‰ PDB.

We have already noted that the external shell of the calcites is formed by the production of successive calcite films from the outside in (Fig. 1). The pH of the solutions involved in this formation is extremely high (12-14), and although the solution chemistry is different, we suggest that a similar diffusion through these calcite

films is taking place. Thus the very light $\partial^{13}C$ values of the shell of the stalactites can be explained.

The fine grained crystals of calcite in the interior of the stalactites have obviously had time to grow slowly following nucleation. We speculatively suggest that water trapped in the interior of the hollow pipe of the stalactite reacts slowly with carbon dioxide seeping up the interior of the pipe and with the small amount of carbon dioxide diffusing through the walls of the pipe to produce patches of calcite crystals (Fig. 5) with slightly heavier $\partial^{13}C$ values. This gives the grouping about -24‰ on Fig. 4

5.6 Conclusion

As hyper-alkaline bulbs of liquid emerge from the base of the concrete structure atmospheric carbon dioxide reacts immediately with the fluid and calcite is precipitated extremely rapidly in the form of calcitic scums. As carbon dioxide crosses the gas to water interface a kinetic isotope fractionation takes place, caused by the different diffusion velocities of the light and heavy carbon dioxide molecules. Lighter isotopes diffuse more quickly and are selectively taken into solution. The value of this fractionation has been calculated as -10‰ to -11.3‰ PDB (Turner, 1982; Létolle et.al., 1988). At high pH values (>10.3) the dominant carbonate species is the carbonate ion (Pourbaix, 1974), and deposition of calcite is essentially instantaneous. The calcite film produced is bonded to the concrete structure and the water drips away. A new chemically re-charged bulb of water appears

inside the semi spherical shell and the process is repeated as the bulb of calcite is infilled. The stem is gradually produced and diffusion of carbon dioxide through the calcite layers takes place. Finally, water in the interior of the pipe reacts slowly with any carbon dioxide to produce patches of fine grained calcite crystals. It is possible that evaporation of this pipe water may take place.

5.7 Discussion

By combining the previously reported fractionation mechanisms and our own experimental data, coupled with a knowledge of the mineralogical formation mechanism of the calcites we have attempted to explain the fractionation of carbon isotopes.

The analyses indicate that the growths are produced by the interaction of atmospheric carbon dioxide with hyper alkaline solutions, in a complex reaction system. The earlier models proposed for crust growth were based on the movement of portlandite to the surface of the structure by migrating moisture, where it was deposited as calcite. We feel that we have elucidated on the reaction and have proved that the dominant reaction that causes the growth of the calcite crusts on concrete surfaces is due to the interaction of hyper-basic fluids with carbon dioxide. No mechanism has been previously suggested for the growth of stalactites on the underside of concrete structures. The previous most plausible mechanism was that they were produced in a degassing mechanism similar to that of stalactitic cave growths (Hendy, 1971). This investigation has revealed that they

are deposited by a complex mechanism involving the interaction of hyper-alkaline waters that emerge on the underside of structures with atmospheric carbon dioxide.

Simulation of such mechanisms in the laboratory proved difficult. An analogy with freshwater travertine formation can be made, but it could not be proved. Previous workers (Létolle *et al.*, 1988), have suggested that the very light $\partial^{13}C$ values are approaching the value of -30‰, and that a biogenic reaction may be involved. Overall the calcites are extremely depleted in $\partial^{13}C$. There is as yet no evidence of a bacteria that can thrive in such alkaline conditions. But we do accept that a biogenic reaction could possibly be involved in the precipitation of concrete-hosted calcites. During the deposition of these calcites we have suggested that they have been fractionated by two separate diffusive mechanisms, one occurring at the gas to water interface and the other as carbon dioxide molecules permeate through the calcite films produced. We therefore suggest that the double diffusive fractionation satisfactorily explains the very low $\partial^{13}C$ values.

5.8 Acknowledgements

The SERC of Great Britain provide funding for Gordon Macleod. Sample analyses were carried out by T. Donnelly and staff at S.U.R.R.C, and they are thanked for their assistance. Strathclyde Region Roads Department are thanked for the provision of samples. The Isotope Geology Unit of S.U.R.R.C is funded by NERC and the Scottish Universities.

5.9 References Cited

Baertschi, P. Schweiz. Min Petr. Mitt., 37, 73-152, (1957).

Bottinga, Y. & Craig, H Earth. Planet. Sci. Lett., 5; 285-295, (1969).

Craig, H., Geochim. cosmochim. Acta Vol 3, 53-92, (1953).

Craig, H., J. Geology Vol 62, 115-149, (1954).

Glasser, F. P. Fortschr. Miner (64), 19-35, (1986).

Herczeg, A. L. & Fairbanks, R. G. Geochim. cosmochim. Acta Vol 51, 895-899, (1987).

Hendy, C. H. Geochim. cosmochim. Acta Vol 35, 801-824, (1971).

Lea, F.M. The Chemistry of Cement and Concrete, Edward Arnold Ltd., London (1970).

Létolle, R., Leroy, P. & Gegout, P. C. R. Acad Sci, Paris, t306, Serie2, 799-802, (1988).

McCrea, J. M. J. Chem. Phys (18), 849-857, (1950).

Macleod, G., Hall, A. J. & Fallick, A.E. Mineral Mag,(1990),(In Press).

Montague, S. New Civil Engineer, 2nd March, p.8, (1989).

O'Neil, J. R. & Barnes, I. Geochim. cosmochim. Acta Vol 35, 687-697, (1971).

Pourbaix , M. Atlas of electrochemical equilibria in aqueous solutions, Pergammon Press, (1974).

Pye, K. & Schiavon, N. Nature Vol. 342, 663-664,(1989)

Siegenthaler, U. & Münnich, K. O. Carbon Cycle Modelling (Scope 16), (B. Bolin) Ed., John Wiley & Sons, New York, 249-257, (1981).

Thode, H. G., Shima, M., Rees, C. E., Krishnamurty, K. V. Can. J. Chem, 43, 582-595, (1965).

Thurman, E. M. Organic geochemistry of natural waters, Dordrecht, Boston, USA. (1985).

Turner, J. V. Geochim. cosmochim. Acta Vol 46, 1183-1191, (1982).

5.10 Figure Captions

Fig. 1. Scanning electron photomicrograph of the cross section of a stalactite, showing apparent exfoliation of the numerous calcite layers of the outer shell.

Fig. 2. Scanning electron photomicrograph of the fine grained calcite crystals growing in the central pipe of the stalactite.

Fig. 3 Plot of $\partial^{13}C$ PDB against $\partial^{18}O$ SMOW for calcites collected from concrete structures. Inner and outer analyses for the stalactites are marked by 1 for outer and 2 for inner.

Fig. 4. Histogram of $\partial^{13}C$ analyses of natural samples.

Fig. 5. Scanning electron photomicrograph showing a patch of well formed calcite crystals growing in the central pipe of a stalactite.

Table 1. List of $\partial^{13}C$ and $\partial^{18}O$ values of the concrete hosted calcites, with calculated equilibrium formation temperatures assuming $\partial^{18}O$ meteoric water = -8‰ SMOW.

Table 2. List of $\partial^{13}C$ and $\partial^{18}O$ values for the laboratory synthesised samples, and the pH of the solutions in which they formed.

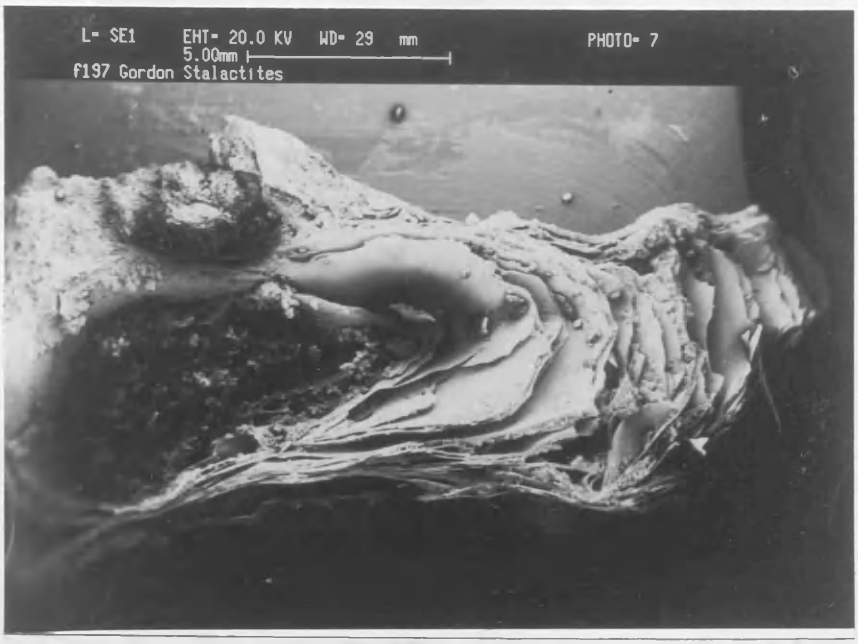

Figure 1.

Figure 2.

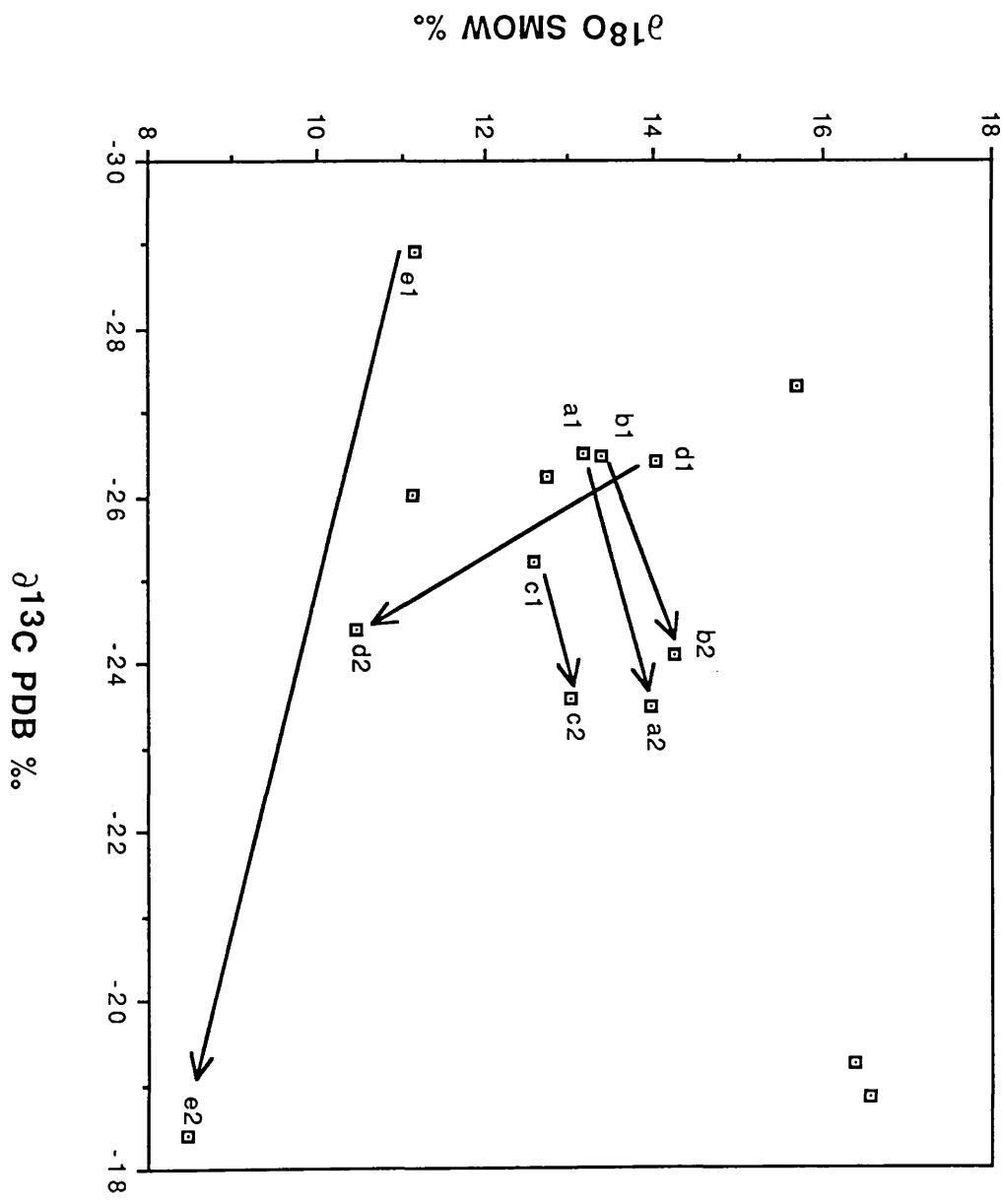
‰ SMOW δ18O
8
10
12
14
16
18
-30
-28
-26
-24
-22
-20
-18
δ13C PDB ‰
a1
b1
d1
c1
d2
b2
c2
a2
e1
e2

Figure. 3.

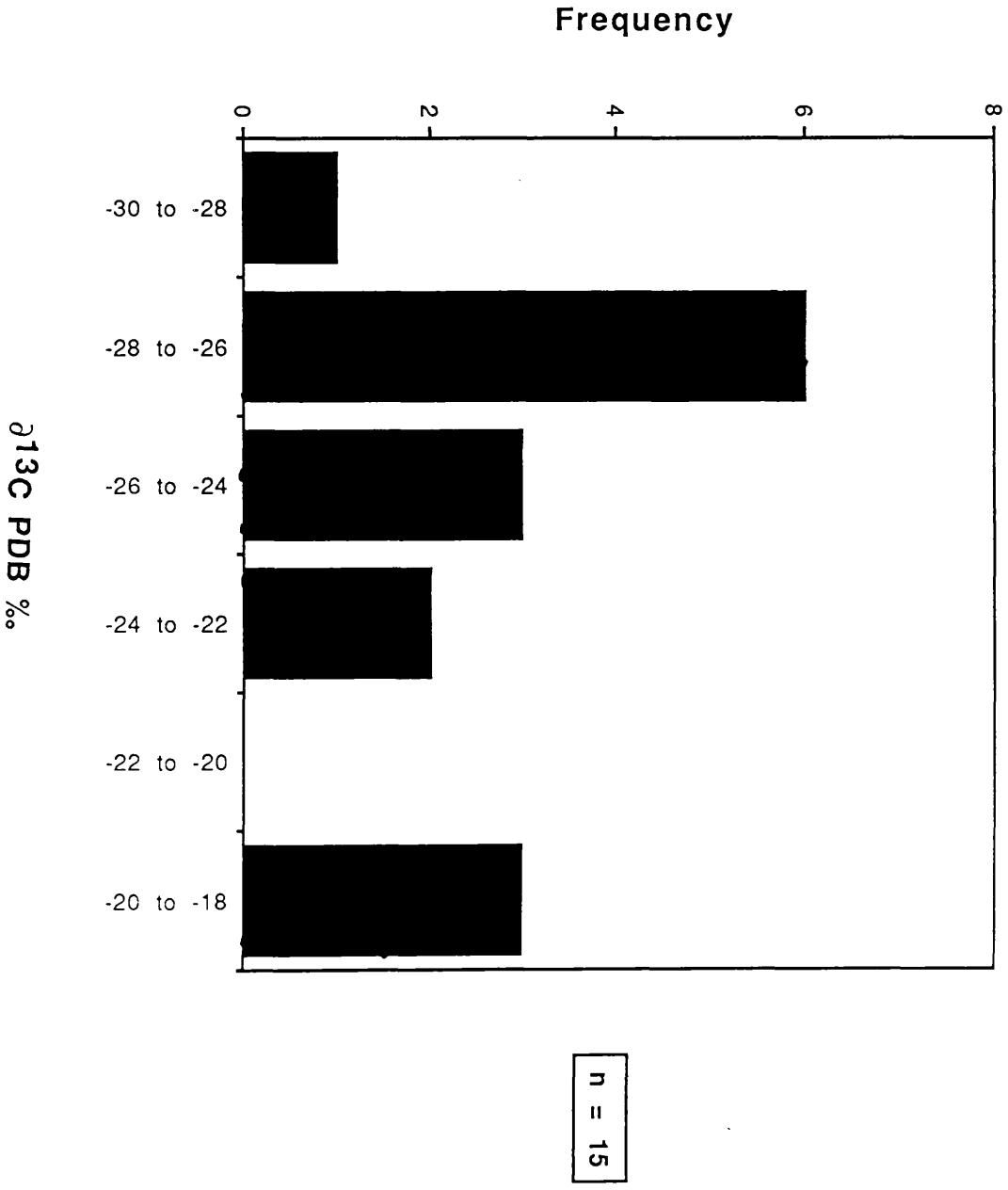
Frequency
0
2
4
6
8
-30 to -28
-28 to -26
-26 to -24
-24 to -22
-22 to -20
-20 to -18
∂13C PDB ‰
n = 15

Figure. 4.

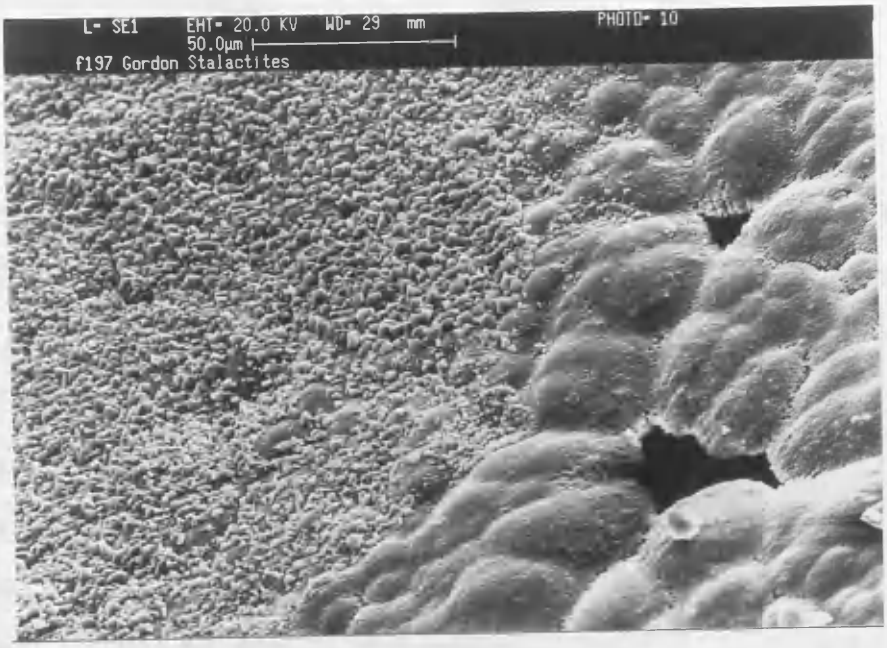
L- SE1
EHT- 20.0 KV
WD- 29 mm
PHOTO- 10
50.0µm
f197 Gordon Stalactites

Figure 5.

Table 1.

calcite growth	$\partial^{13}C$ ‰ PDB	$\partial^{18}O$ ‰ SMOW	calculated formation temperature °C, assuming $\partial^{18}O$ H_2O= -8‰
stalactite	-26.24	+12.75	70
stalactite	-26.03	+11.14	82
stalactite	-19.24	+16.36	46
stalactite (a)			
outer	-26.52	+13.17	67
inner	-23.50	+13.96	61
stalactite (b)			
outer	-26.49	+13.38	65
inner	-24.12	+14.25	61
stalactite (c)			
outer	-25.23	+12.59	71
inner	-23.57	+13.03	68
stalactite (d)			
outer	-26.14	+14.02	61
inner	-24.43	+10.46	88
stalactite (e)			
outer	-28.93	+11.17	82
inner	-18.63	+8.50	106
crust	-18.82	+16.56	45
crust	-27.31	+15.70	50

Table 2.

sample No.	$\partial^{13}C$‰ PDB	$\partial^{18}O$‰ SMOW	pH
1	-41	+8	11
2	-45	+2.7	12
3	-42.9	+2.8	11.5
4	-44	+3.7	11.8
5	-44	+2	12

Chapter 6

Introduction and background

Chapter 6 (paper 5), is a paper describing the modelling of concrete decay, due to the reaction of pyrite and pyrrhotine in aggregate fragments with rainwater, via the speciation/solubility/reaction path computer codes EQ3NR/EQ6. The paper also contains data on the modelling of rainwater reacting with cement paste itself. The models concur with the predictions made within other papers in the thesis and verify the proposed decay mechanisms. We suggest that the application of thermodynamics to concrete is speculative as many of the phases present in cement paste are meta-stable. Thus, it is only possible to take a simplistic view of the data produced by the code modelling. I was senior author of the following paper and Dr. Hall assisted in the interpretation of data and preparation of the paper.

6. EQ3NR/EQ6 geochemical speciation/solubility/reaction path computer codes, modelling of geochemical aspects of concrete decay systems.

(Draft of June 1990)

G. Macleod and A. J. Hall

Department of Geology and Applied Geology, University of Glasgow, Lilybank Gardens, Glasgow, G12 8QQ, Scotland, UK.

6.1 Abstract

Aqueous solutions have been modelled and synthesised by use of the aqueous geochemical speciation modelling code EQ3NR (Wolery, 1983), and the files produced are taken as representing an average chemical composition for a simple rainwater. The rain water files created on EQ3NR have been reacted with suites of solid materials via the EQ6 solubility and reaction path code (Wolery, 1989). The reaction of the fluids with different mineralogical phase composition solids is thought to be a reasonable simulation of concrete interaction with rainwater. The chemical composition of rainwater is taken as a simplistic model, as is the mineralogical composition of the concrete. We feel that a simple approach is necessary due to the extremely complex and variable mineralogy of concretes and cement pastes. The simulations are systematic in the fact that they predict the fluid left after reacting with the concrete

will have an extremely high pH (>12), and within the concrete the phases ettringite and calcite are produced within the different models. When the rainwater file is reacted with a simple cement paste, the remaining fluid has a pH of 13.9 and the minerals calcite and ettringite are produced. When the rainwater file is reacted with a paste containing pyrite and pyrrhotine the pH of the remaining fluid after reaction is 12.7, and the mineral ettringite is precipitated.

6.2 Introduction

The interaction of concrete and its constituent mineralogical phases and rainwater is of interest to civil engineers, mineralogists, waste disposal scientists, concrete technologists and environmental scientists. Applied mineralogical studies of concrete decay have revealed that a major factor in the decay of concrete structures is the percolation of water through that structure (Macleod *et al.*, 1990). Due to the complex mineralogy of concretes and the variability of aggregate composition and cement paste phase composition it has been almost impossible to verify the proposed decay mechanisms.

A lack of thermodynamic and reaction rate data has also hampered the geochemical modelling of cement paste and concrete decay. By taking a simplified mineralogical model of concrete and a simple chemical model of rainwater we have attempted to model the reactions involved in water induced concrete decay using the

computer codes EQ3NR/EQ6 (Wolery, 1983,1989). Other workers involved in radioactive waste disposal programmes in the United States, have carried out EQ3NR/EQ6 modelling of underground depositary concrete reacting with groundwaters (Gardener *et al.*, 1989). These workers also took a simplistic mineralogical view of concrete.

The modelling in this paper is concerned firstly with the reaction of rainwater with a simple cement paste, and secondly with the reaction of rainwater with a concrete that has the iron sulphides pyrite and pyrrhotine present in dolerite aggregate fragments. In the latter case which follows from a study of a concrete bridge undergoing active degradation (Macleod *et al.*, 1990a), some of the sulphides may have reacted to produce the secondary mineral ettringite. The bulk of the ettringite has been deposited by fluids in spherical cavities in the cement paste, the fluids moving sulphate already present in the cement paste to the ettringite growth points. On the surface of the concrete bridge deck calcitic crusts are found, and on the underside of the bridge deck calcitic stalactites are found. All of the alteration of the concrete to produce ettringite and calcite is related to the percolation of fluids (mainly rainwater), through the structure. Rainwater reacts with constituent phases of cement pastes leaching out portlandite to produce hyper-alkaline waters that react with atmospheric carbon dioxide to produce the calcitic growths (Macleod *et al.*, 1990b). The model represents complete thermodynamic equilibrium.

6.3 Rainwater composition file

A simplistic composition of rainwater was created via the EQ3NR aqueous geochemical speciation code (Wolery, 1983). The original data entered into the code was taken from numerous sources (Drever, 1982, Rankama and Sahama, 1950), and is no way representative of all rainwater. It is merely an attempt to create a simplified average rainwater composition for the U.K.. The chemical composition of the rainwater fed into the EQ3NR code is listed in Table 1. (Drever, 1982, Rankama and Sahama, 1950). The pH of the rainwater was taken as 5.8 and the redox potential of the water was set at an Eh of 0.70. The temperature of the rainwater was taken as 8°C, as an average temperature for rainwater. The $O_2(aq)$ value of rainwater was taken as an intermediate value between that of river water and sea water (Nordstrom, *et al.*, 1979), a value of 8 mg/l. The bicarbonate content of the rainwater was included in the code by inferring that its concentration in the rainwater was in equilibrium with atmospheric carbon dioxide gas. The chlorine ion was loaded into the code as the ion to be used for electrical balancing of the solution as recommended by the code handbook (Wolery, 1983).

The code processed the data and predicted the aqueous species present in the fluid and the fluids saturation state with respect to mineral phases. The code also calculated the pH, Eh and pe (-log a_{e^-}), of the solution, where e^-, is the hypothetical aqueous electron.

The solution was not supersaturated with respect to any minerals and thus no mineral precipitation is predicted for the rainwater.

The pH of the solution was predicted by the code as being 5.8 with an Eh of 0.703, and a log oxygen fugacity (at 8°C) of -15.142. This was checked by re-running the data through the code with the redox parameters set on log oxygen fugacity (Wolery, 1983); the results were identical, and thus verified the first runs predictions.

6.4 Cement paste file

A file was loaded into the EQ6 code to represent a simple Ordinary Portland Cement paste. The atomic % composition of the paste was taken as 50% C-S-H gel loaded as the 14 Å tobermorite type mineral $Ca_5Si_6O_{17}.10.5H_2O$, 24% porosity, 14% portlandite ($Ca(OH)_2$), 2% ettringite ($Ca_6Al_2(SO_4)_3.(OH)_{12}.26H_2O$) and 10% hydrogarnet $Ca_3Al_2O_6.6H_2O$. I felt that these values were a reasonable simulation of a cement paste, considering the phases present in the code database, and the variability in phase composition of cement pastes.

6.5 Cement paste and iron sulphide file

The phase composition of the cement was added into the EQ6 file in the form of moles per kg of solids that react with 1kg of water.. The calculation for preparing data for loading in the file, takes account of the density and porosity and equates the number of moles of each phase in the solid that will react with 1kg of the reacting fluid. It was noted in Chapter 3, that grains of pyrite and

pyrrhotine hosted in some of the aggregate fragments near the outer surface of the aggregate may have reacted with the percolating fluid, possibly contributing sulphur to the remobilised sulphur in the paste due to percolation of the fluid.

The cement paste of the studied concrete was found to be an OPC paste. Thus in order to simulate the reaction of that concrete with rainwater we decided to compose our solid phase of hydrous cementitious minerals similar to that modelled in the cement paste interaction, and a very small amount of pyrite and pyrrhotine. The solid composition loaded into the EQ6 code was of a composition 50% C-S-H gel, 12% portlandite, 10% hydrogarnet, 2% ettringite, 25% porosity and 0.5% pyrite (FeS_2) and 0.5% pyrrhotine ($Fe_{1-x}S$).

6.6 Results

The first set of simulations were carried out in order to simulate the interaction of rainwater with a simple cement paste. The model predicted the precipitation of the minerals andradite ($Ca_3Fe_2Si_3O_{12}$), portlandite $Ca(OH)_2$, calcite ($CaCO_3$), ettringite ($Ca_6Al_2(SO_4)_3.(OH)_{12}.26H_2O$), grossular ($Ca_3Al_2Si_3O_{12}$), monticellite ($CaMgSiO_4$), and wollastonite ($CaSiO_3$), with a residual fluid after reaction having a pH of 13.9. The reaction of the rainwater with the cement paste that had pyrite and pyrrhotine present predicted the precipitation of andradite ($Ca_3Fe_2Si_3O_{12}$), portlandite $Ca(OH)_2$, ettringite ($Ca_6Al_2(SO_4)_3.(OH)_{12}.26H_2O$), grossular ($Ca_3Al_2Si_3O_{12}$), monticellite ($CaMgSiO_4$), wollastonite ($CaSiO_3$), and pyrite ($FeS_2$). The residual fluid was predicted as

having a pH of 12.7. The reaction paths were modelled at the temperatures 8°C, 15°C and 20°C. In each simulation the results were mineralogically identical. In each case the residual fluids had calcium and other expected cations present, a high pH and no carbonate species or dissolved carbon dioxide present.

6.7 Discussion of results

In the first set of simulations where rainwater was reacting with a cement paste the code predicted the precipitation of andradite, grossular, monticellite, wollastonite, calcite, ettringite and $Ca(OH)_2$. However, the phases andradite, grossular, monticellite and wollastonite would not be precipitated in a real-life situation due to the fact that these are meta-stable under the required conditions. It is more probable to suggest that the silica may be incorporated in the C-S-H gel phase in the paste. The code assumes that equilibrium is attained instantaneously and makes no provisions for kinetic effects on the formation mechanisms. It is probable that calcite and ettringite would be deposited when rainwater reacts with a cement paste consisting of 50% C-S-H gel, 24% porosity, 14% portlandite, 2% ettringite and 10% hydrogarnet. Similarily, in the case of the rainwater interaction with the pseudo-concrete the only stable phase that would exist would be the pyrite (possibly due to a low oxygen fugacity input in the rain water file), and ettringite, which are in a pseudo-equilibrium state. In reality this would not occur, as chemically recharged fluids would be passing through the concrete causing disequilibrium and continually oxidising the iron

sulphide phases. The walls of the pores in cement paste may possibly be negatively charged (Hudec, P. P., 1989), and this coupled with diffusion mechanisms preferentially causes the precipitation of ettringite in spherical cavities in the cement paste (Macleod and Hall, 1990). We suggest that the results predicted by the EQ6 reaction path modelling code compare favourably to the predictions made in earlier studies of concrete decay (Macleod *et al.*, 1990, Macleod *et al.*,1990b).

6.8 Conclusion

The simulations modelled on the codes can only predict the possible solid products assuming instant equilibrium. Kinetics and time can not as yet be incorporated with ease and certainty into the codes. In a real life situation rainwater percolating through a concrete structure would have variable composition, and would undoubtedly on entry to the structure be in a state of redox equilibrium. Thus the prediction of the solid phases produced is tentative, but the equilibrium precipitation of ettringite and in certain cases calcite as previously proposed (Macleod *et al.*, 1990), has been verified by these computer geochemical simulations. It is almost impossible to imagine that a concrete structure reacting with rainwater would involve phases in equilibrium with the fluid; the constant re-charging of the fluid from the surrounding environment would cause a disequilibrium situation in thermodynamic and redox terms. Thus computer predictions of phase dissolution and

precipitation have to be combined with a knowledge of the more complex disequilibria geochemistry to allow predictions to be made. It is therefore possible to suggest that any silica dissolution from phases would be immediately matched by silica incorporation in the C-S-H gel phase, and iron sulphides such as pyrite and pyrrhotine would oxidise when in contact with the percolating rainwater, in turn, leading to the deposition of ettringite.

6.9 Acknowledgements

Thanks are given to Dr's G. Bowes, B. Bell, C. Farrow and A. Mullis, for their assistance in the loading of data into the codes and the interpretation of the results. Dr. T. J. Wolery is thanked for providing the computer codes for the use of Prof, M. J. Russell and the research Staff of the Department.

6.10 References Cited

Drever, J. I. The Geochemistry of natural waters, Prentice Hall, Englewood Cliffs, N. J., USA., 388.pp., (1982).

Gardener, M. A., Alcorn, S. R., Myers, J. and Givens C. A. Modelling simple cement-water systems using the speciation/solubility/reaction path computer codes EQ3NR/EQ6, with specific application to nuclear waste repositories., Water-Rock Interaction, Miles (Ed.), pp 235-238, Balkema, Rotterdam, (1989).

Hudec, P. P. Ionic control in deterioration of building materials, Water-Rock Interaction, Miles (Ed.), pp 305-308, Balkema, Rotterdam, (1989).

Macleod, G., Hall, A. J., Fallick, A. E.(a) An applied mineralogical investigation of concrete decay in a major concrete road bridge, Min. Mag., Dec, 1990 (In Press).

Macleod G., Fallick, A. E. Hall, A. J (b) The mechanism of carbonate mineral growth on concrete structures as elucidated by carbon and oxygen isotope analyses, This Thesis, (1990).

Macleod G. and Hall, A. J. Whisker crystals of the mineral ettringite., Mineralogy and Petrology, 1990 (In Press).

Nordstrom, D. K. A comparison of computerised chemical models for equilibrium calculations in aqueous systems, Chemical modelling in aqueous systems, ACS Syposium Series Vol. 93, Jeanne (Ed), American Chemical Society, p 857-892, (1979).

Rankama K., Sahama, T. G. Geochemistry, University of Chicago Press, Chicago, USA, (1950).

Wolery, T. J. EQ3NR, A computer program for speciation-solubility calculations: User's guide and documentation. Lawrence Livermore Nat. Lab., UCRL-53414,191 pp., (1983)

Wolery, T. J. EQ6 A computer program for reaction path modelling of aqueous geochemical systems: User's guide and documentation. Lawrence Livermore Nat. Lab., Draft Copy (1989).

6.11 Figure captions

Table.1 List of data for the species and their concentration, as loaded into EQ3NR for rainwater simulation.

Table 1.

species	concentration
O_2 (aq)	8 mg/l
NO_2^-	0.2 mg/l
Ca^{2+}	0.2 mg/l
Mg^{2+}	0.056 mg/l
Na^+	0.66 mg/l
K^+	0.66 mg/l
Cl^-	0.46 mg/l
SO_4^{2-}	2.64 mg/l
NH_4^+	0.66 mg/l
HCO_3^-	initially in equilibrium with CO_2 (g)

LIBRARY